



North Pacific Fisheries Commission

## Stock assessment report for chub mackerel

### EXECUTIVE SUMMARY

#### Background information

Chub mackerel (*Scomber japonicus*) in the Northwest Pacific Ocean (NWPO) is distributed from the coast of southern Japan to offshore waters of Kuril Islands. It is considered that both adults and juveniles are distributed as far east as the 170-degree East longitude line. The feeding migration of adults has expanded to the northeast recently, and since 2018 the distribution of adults during summer and fall has reached 47-degree North, 166-degree East, east offshore of Kuril Island. The spawning ground is known to be located within the range of the Japanese Exclusive Economic Zone (EEZ), with the main spawning ground located in Izu Island waters.

Chub mackerel are harvested by China, Japan and Russia (Figure E-1). Chinese light purse seine and pelagic trawl fisheries are operated in the NPFC Convention Area. Japanese chub mackerel fisheries consist mainly of purse seine and set net fisheries within the Japanese national waters. Russian chub mackerel fisheries mainly operated in the Russian national waters consist of mid-water trawl, purse seine and bottom trawl gears with operations in the Japanese national waters. The historical total landings have largely fluctuated and recently decreased from approximately 516,000 mt in 2018 to 151,000 mt in the most recent calendar year (CY) 2023. The Conservation and Management Measure for chub mackerel (CMM 2024-07) includes a catch limit of 100,000 mt set in the Convention Area for each of the 2024 and 2025 fishing seasons.

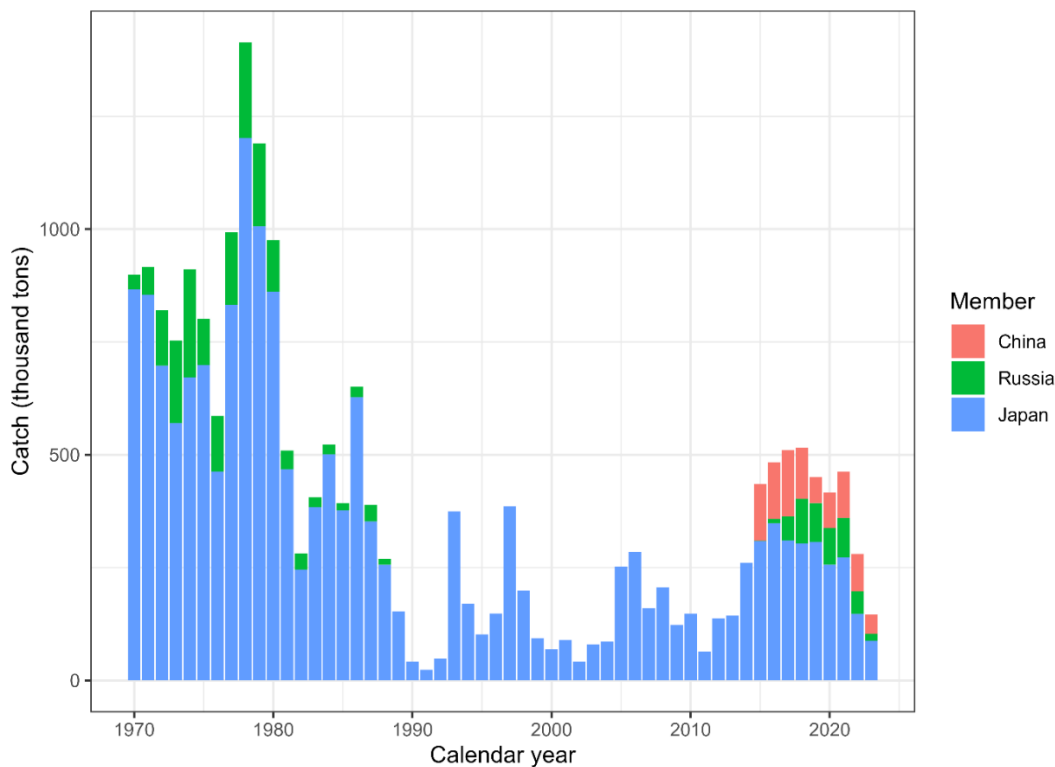


Figure E-1. Historical chub mackerel catch in weight by Member. The provisional Chinese catch for 2023 is estimated using the historical ratio for chub mackerel and blue mackerel.

## **Stock assessment model**

A state-space stock assessment model (SAM) was agreed to be used for the chub mackerel stock assessment by the Technical Working Group on Chub Mackerel Stock Assessment (TWG CMSA). SAM accounts for observation errors in catch-at-age data and abundance indices. It uses age-specific data on catch numbers, stock weight, and maturity rate in each year. Recruitment was defined as numbers at age 0, and spawning stock biomass (SSB) was calculated through multiplication of numbers-at-age by maturity-at-age and weight-at-age. SAM consists of two subparts: a population dynamics model and an observation model.

Age-structured population dynamics for chub mackerel estimated by SAM are driven through survival processes such as natural and fishing mortalities, and reproduction is calculated by a Beverton-Holt stock recruitment relationship. Fishing mortality coefficients by year and age group are assumed to follow a multivariate random walk, consequently allowing estimation of time-varying selectivity.

In the observation model of SAM, the catch-at-age is estimated through the fitting of the Baranov equation to the observed catch-at-age under a lognormal error distribution. SAM also fits to abundance indices with a lognormal error assumption. Non-linear relationships to population abundance estimates were estimated for abundance indices specific to ages 0 and 1, linear relationships were applied to the other abundance indices.

## **Data and biological parameters used in the assessment model**

Data are included from the NPFC Convention Area and Members' EEZs.

A fishing year (FY) starting from July and ending in June of the following year was applied in the stock assessment of chub mackerel. The TWG CMSA agreed for the stock assessment period to be FY1970 to FY2022. Seven age groups of ages 0 to 5 and 6+ were defined in the stock assessment. The historical catch-at-age, which was constructed from the quarterly data from each Member, is shown in Figure E-2. Time series of mean weight-at-age are illustrated in Figure E-3. Annual maturity-at-age with decadal time-varying changes is shown in Figure E-4. These data were available up to FY2022.

Although seven time series were available, only six time series of abundance indices were used during model development (Figure E-5): relative number of age 0 fish from the summer survey by Japan; relative number of age 0 fish from the autumn survey by Japan; relative number of age 1 fish from the autumn survey by Japan; relative SSB from the egg survey by Japan; relative SSB from the dip-net fishery by Japan; and relative vulnerable stock biomass from the light purse-seine fishery by China.

Russian CPUE data were not used for model development although the abundance indices from Japan and Russia were available until FY2023 and until FY2022 for China. While the FY2023 Japanese abundance indices were not used for the base case, as agreed in the TWG CMSA08, they were used for sensitivity runs.

An age-specific natural mortality ( $M$ ), corresponding to 0.80 for age 0, 0.60 for age 1, 0.51 for age 2, 0.46 for age 3, 0.43 for age 4, 0.41 for age 5, and 0.40 for age 6+, is applied for the stock assessment by the TWG CMSA.

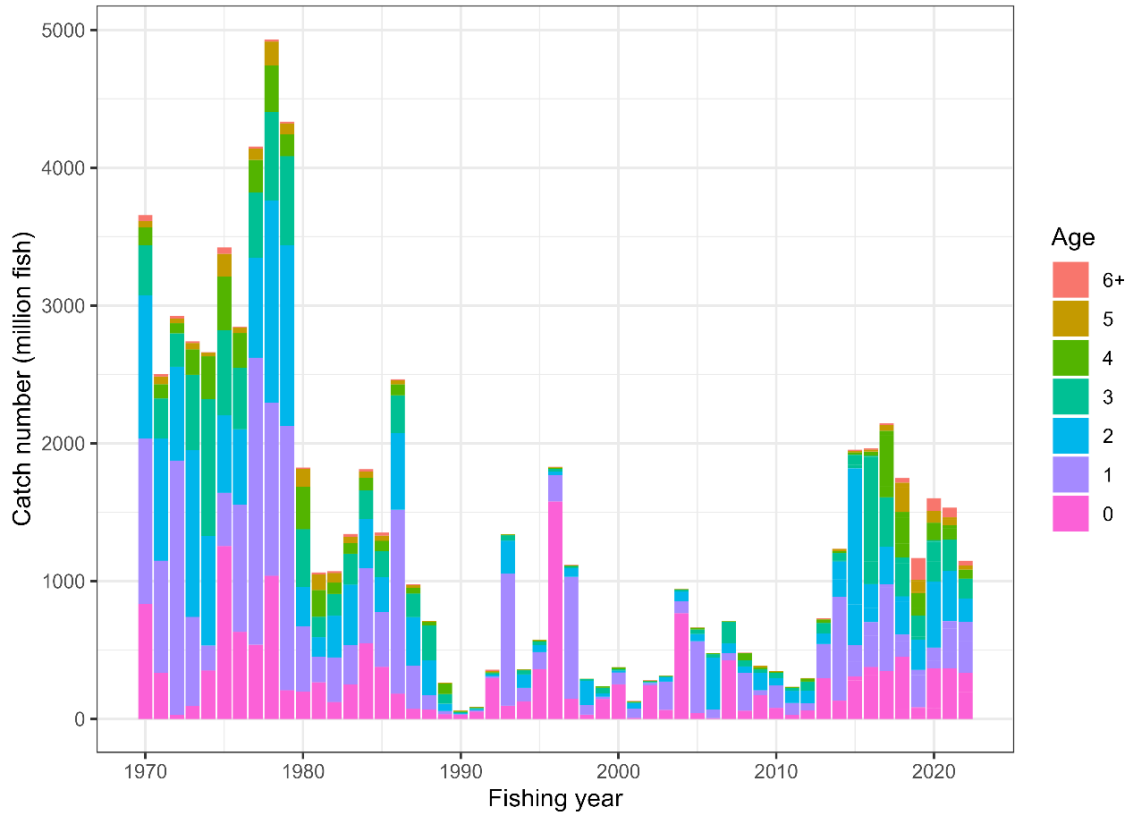


Figure E-2. Historical observed catch-at-age.

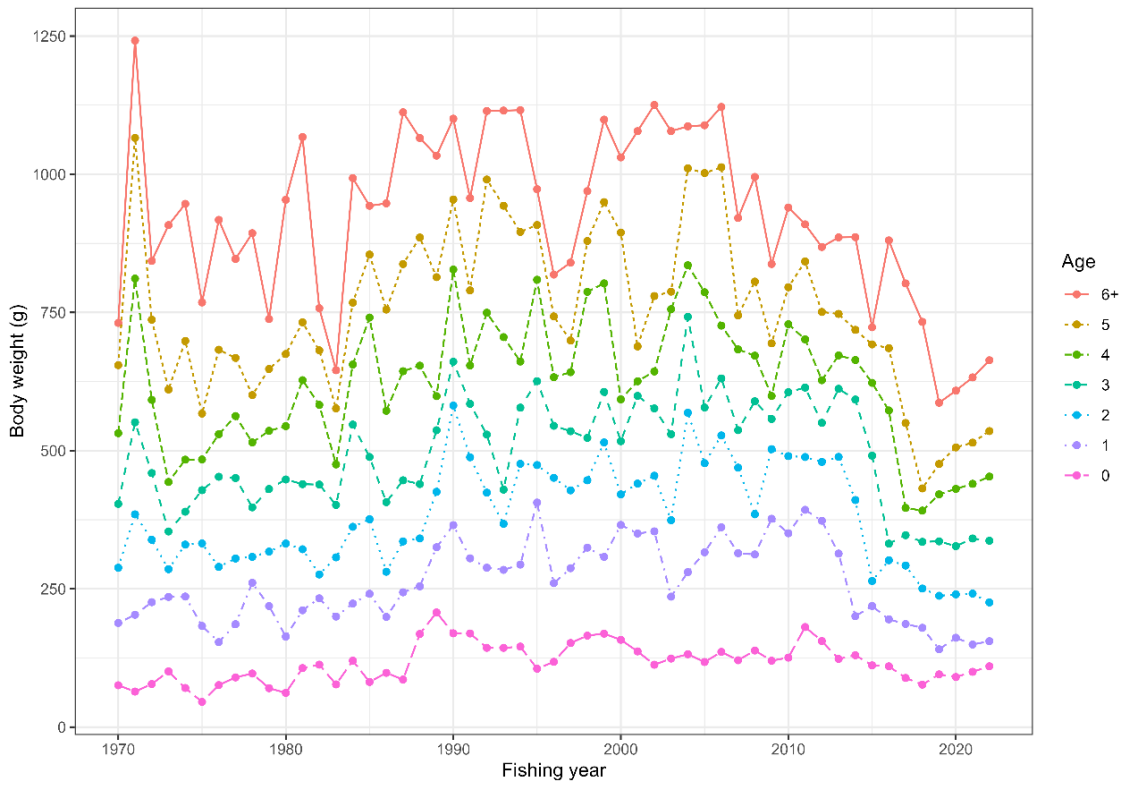


Figure E-3. Time series of weight-at-age.

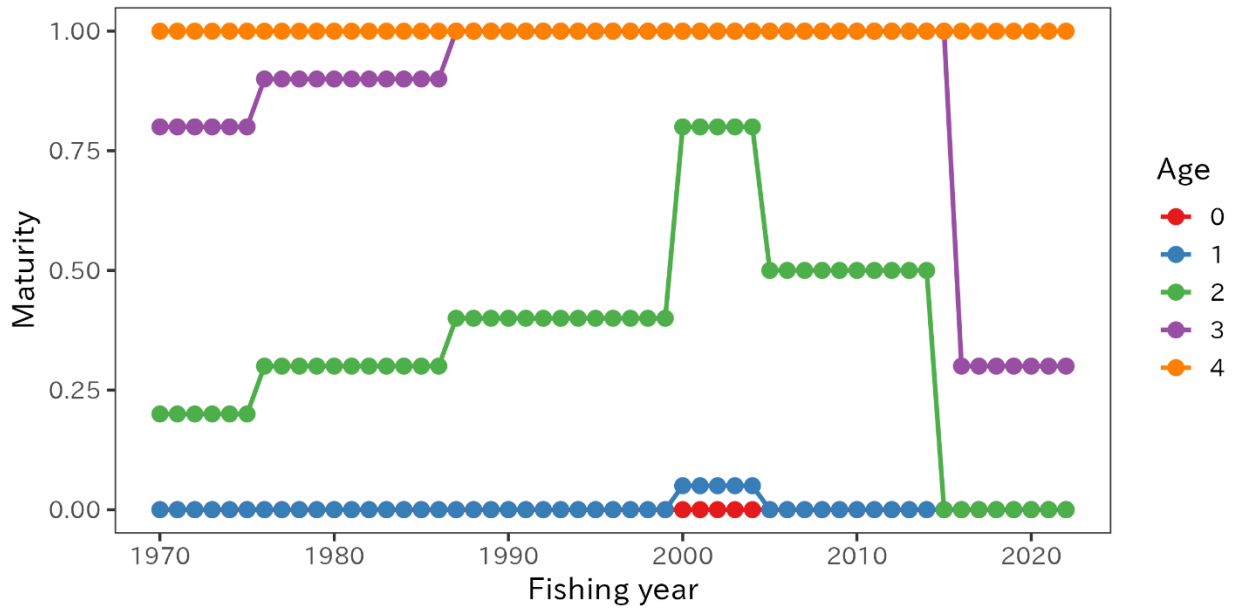


Figure E-4. Time series of maturity-at-age. Ages are simplified up to age 4 due to the similarity of maturity at age 4 and above.

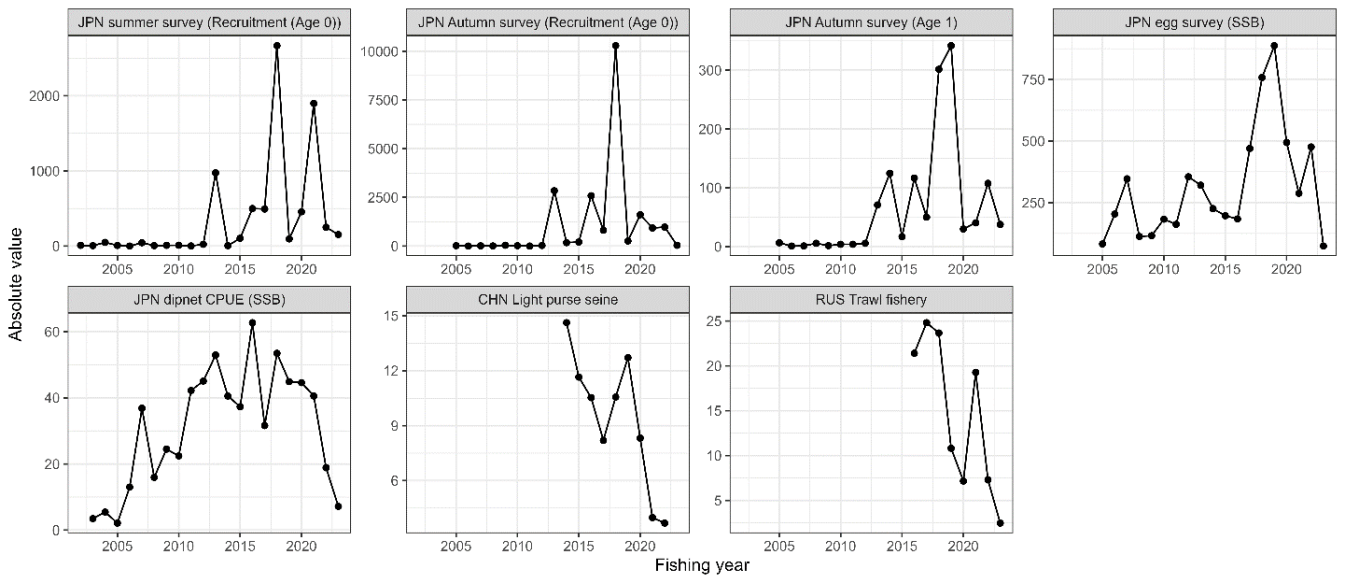


Figure E-5. Time series of abundance indices. The Russian CPUE data were not used in model estimation.

### **Stock assessment scenarios**

In order to improve the SAM fit to abundance indices and retrospective patterns, the TWG CMSA recognized the necessity of introduction of estimation of process error in survival of age groups older than age 0. The TWG CMSA also considered inclusion of FY2023 from the Japanese abundance indices, which had a large impact on the stock status of the most recent years. As a result, the following four scenarios were employed as representative cases:

- 1) B2, Estimate process error for only age 0 (recruitment);
- 2) S28-ProcEst, Estimate process error for all age groups;
- 3) S32-JP23, Estimate process error for only age 0 and use Japanese indices up to FY2023;  
and
- 4) S34-ProcEst23, Estimate process error for all age groups and use Japanese indices up to FY2023

TWG CMSA agreed to select S28-ProcEst as a base case scenario because of the better diagnostics than the model only with recruitment process error and agreement of data usage up to FY2022. The other three scenarios were employed to show possible range of uncertainty.

### **Reference points**

Using stock assessment results from the base case scenario, the TWG CMSA calculated commonly used biological reference points such as F%SPR (30%, 40%, 50%, 60% and 70%), F<sub>0.1</sub>, maximum sustainable yield (MSY)-based reference points, i.e. F<sub>MSY</sub> and SSB<sub>MSY</sub>, with mean biological parameters and selectivity of current F (mean F in FY2020 to FY2022). In particular, the biological parameters such as weight-at-age and maturity-at-age used for calculation of biological reference points are assumed as the average values during the most recent 7 years (FY2016 to FY2022), which represents the recent change in biological parameters. As a control, the average of the biological parameters was calculated over the stock assessment period. Reference points for the base case scenario are listed in Table E-1.

### **Description of specification of future projections**

The population dynamics model for stochastic future projections is the same as is used in SAM. The future harvesting scenario was predetermined as a total catch of 50, 100, 150, 200, 300 and 400 thousand tons after FY2023, compared with another future harvesting scenario under F<sub>cur</sub>.

Future biological parameters are assumed to equal the average of the recent seven years. Mean biological parameters for the entire model time period (FY1970-FY2022) are used as a control.

### **Stock status overview**

The chub mackerel stock in the NWPO has experienced large changes in biological parameters over the time period of the model. The main temporal changes are a recent decrease in maturity at age, along with a recent decrease in the weight at age, both of which were observed to change over the model time period to cause temporal changes of biological reference points. MSY-based reference points are highly variable over the time series of the assessment because the weight- and maturity-at age of chub mackerel has varied widely (Figures E-3 and E-4), which impacts the productivity of the stock. Unfished spawning biomass per recruit (SPR<sub>0</sub>) represents the theoretical equilibrium productivity per fish assuming no fishing. SPR<sub>0</sub> has varied remarkably over time (Figure E-6).

In addition, as there is little recruitment compensation in the stock-recruitment relationship within the range of historically observed SSB and recruitment (Figure E-8), estimates of biomass-based

MSY reference points are extreme explorations that are highly sensitive to model configuration.

Because of the above reasons, commonly used reference points such as MSY-related or SPR-related reference points vary over time and are uncertain, and they are potentially misleading with respect to stock status. For example, the MSY-based reference points have varied by the assumption of biological parameters to be used (Table E-1). The exploitation rates corresponding to the MSY was 10% when assuming biological parameters during the whole historical period, but it dropped to 5% when using the most recent 7 years biological parameters.

As such, at this time, the TWG CMSA does not recommend the use of MSY-based reference points for management advice. Instead, the TWG CMSA provides information of current estimates of chub mackerel SSB and F (average FY2020-FY2022) relative to the minimum, 25th, 50th, 75th and maximum value of the SSB and F values over the entire time period (FY1970-FY2022; Table E-2). Values relating to the most recent time period (FY2016-FY2022) are also shown in order to describe the current stock relative to recent conditions.

The abundance estimated by the Japanese egg survey and the CPUEs from the Japanese dipnet and Russian trawl decreased over recent years, showing that they were simultaneously reduced to about half the level of recent years in FY2023. The sensitivity run of the stock assessment model including Japanese CPUE for FY2023 shows substantial decline in biomass and SSB in FY2022 and further in FY2023 and higher fishing mortality in the last few years (Figure E-7).

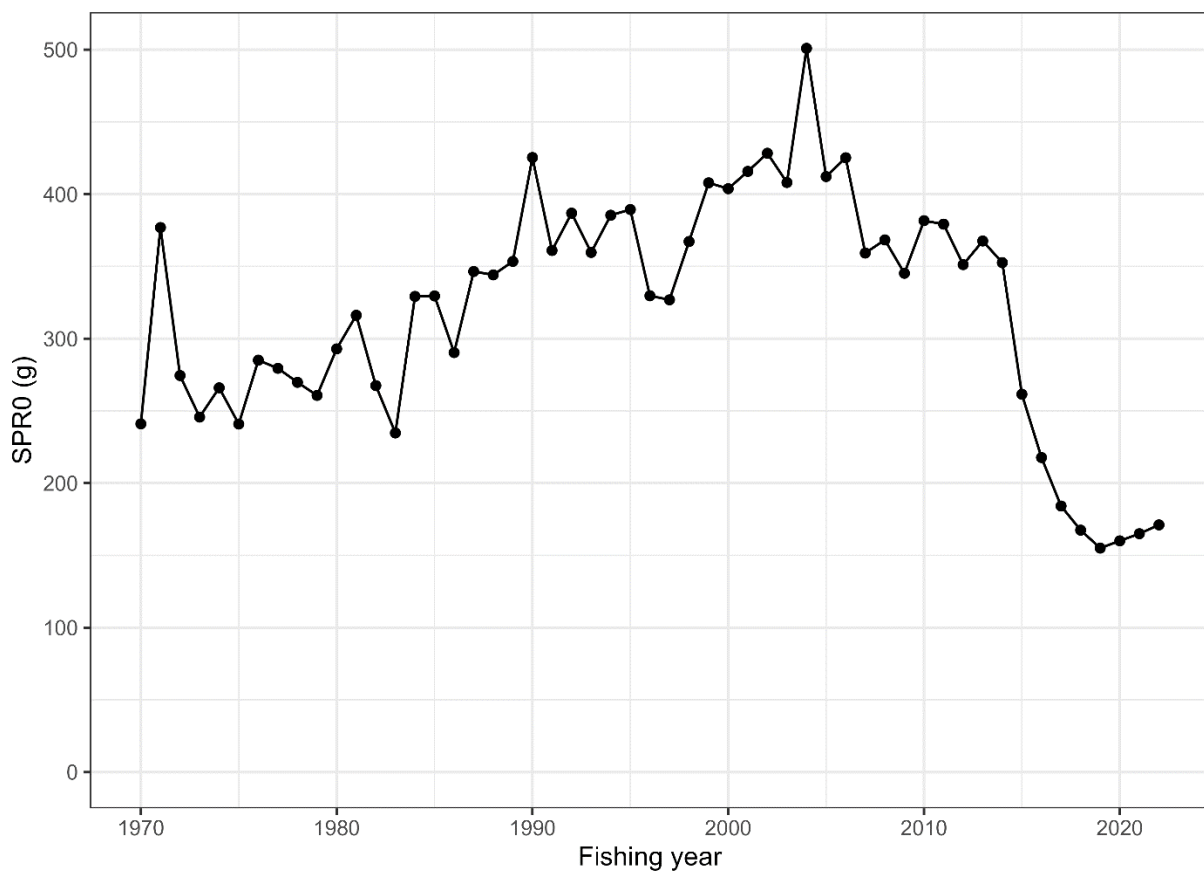


Figure E-6. Trajectories of spawners per recruit without fishing (SPR0).

Table E-1. Reference points for the base case scenario (S28-ProcEst). Reference point values in this table are calculated by holding  $F_{cur}$  the same for all calculations, but by varying the time period (either FY2016-FY2022 or FY1970-FY2022) over which the biological parameters are estimated. Refer to Glossary in the stock assessment report for the definitions.

Biological parameters used	FY2016- FY2022	FY1970-FY2022
	S28-ProcEst	S28-ProcEst
current%SPR	<b>28.3</b>	40.3
$F_{med}/F_{cur}$	<b>0.478</b>	1.629
$F_{0.1}/F_{cur}$	<b>1.344</b>	1.344
$F_{pSPR.30.SPR}/F_{cur}$	<b>0.942</b>	1.498
$F_{pSPR.40.SPR}/F_{cur}$	<b>0.673</b>	1.010
$F_{pSPR.50.SPR}/F_{cur}$	<b>0.484</b>	0.696
$F_{pSPR.60.SPR}/F_{cur}$	<b>0.342</b>	0.475
$F_{pSPR.70.SPR}/F_{cur}$	<b>0.230</b>	0.311
$F_{MSY}/F_{cur}$	<b>0.258</b>	0.668
$B_{MSY}$	<b>9396.157</b>	17179.502
$SSB_{MSY}$	<b>2904.704</b>	6084.597
h	<b>0.358</b>	0.501
$SSB_0$	<b>7123.476</b>	17441.919
$SSB_{MSY}/SSB_0$	<b>0.408</b>	0.349
$F_{MSYSPR}$	<b>0.673</b>	0.511
MSY	436.8467	1713.406
$MSY/B_{MSY}$ (exploitation rate at MSY)	0.046	0.10

Table E-2. Stock status summary from the base case scenario.

Stock Status Summary Table						
	SSB (Thousand MT)	Total Biomass (Thousand MT)	Recruitment (Million Individuals)	F	Exploitation	SPR_0
2022 Estimate	447	2,825	9,839	0.23	0.089	171.1
Current (Average 2020-2022)	526	2,888	11,097	0.28	0.119	165.4
<b>Values relative to the all years of the time series (i.e. 1970-2022)</b>						
	SSB (Thousand MT)	Total Biomass (Thousand MT)	Recruitment (million individuals)	F	Exploitation	SPR_0
Historical Minimum (Min)	45	172	365	0.23	0.071	155
Historical 25 percentile (25%)	97	634	1,308	0.36	0.136	266
Historical Median (Med)	335	1,566	4,353	0.61	0.185	344
Historical 75 percentile (75%)	744	3,177	9,839	0.71	0.25	379
Historical Maximum (Max)	1,394	6,050	23,579	1.11	0.422	501
<b>Ratios Relative to 1970-2022</b>						
	Stock Status Related to Biomass			Stock Status Related to Fishing Intensity		
Current / Historical Minimum	11.694	16.81	30.436	1.21	1.674	1.067
Current / 25%_Historical	5.418	4.554	8.483	0.79	0.874	0.622
Current / Med_Historical	1.569	1.844	2.55	0.47	0.643	0.481
Current / 75%_Historical	0.707	0.909	1.128	0.40	0.475	0.436
Current / Max_Historical	0.377	0.477	0.471	0.25	0.282	0.33
<b>Values relative to 2016-2022</b>						
	SSB (Thousand MT)	Total Biomass (Thousand MT)	Recruitment (million individuals)	F	Exploitation	SPR_0
Recent Minimum (Min)	447	2,825	6,043	0.23	0.089	155.0
Recent 25th percentile (25%)	486	2,919	10,154	0.26	0.112	162.5
Recent Median (Med)	620	3,018	11,077	0.29	0.123	167.5
Recent 75 percentile (75%)	748	3,605	12,622	0.30	0.130	177.6
Recent Maximum (Max)	774	4,108	22,898	0.31	0.143	217.7
<b>Ratios Relative to 2016-2022</b>						
	Stock Status Related to Biomass			Stock Status Related to Fishing Intensity		
Current / Recent Min	1.18	1.02	1.84	1.21	1.34	1.07
Current / 25%_Recent	1.08	0.99	1.09	1.10	1.06	1.02
Current / Med_Recent	0.85	0.96	1.00	0.98	0.97	0.99
Current / 75%_Recent	0.70	0.80	0.88	0.94	0.91	0.93
Current / Max_Recent	0.68	0.70	0.48	0.92	0.83	0.76

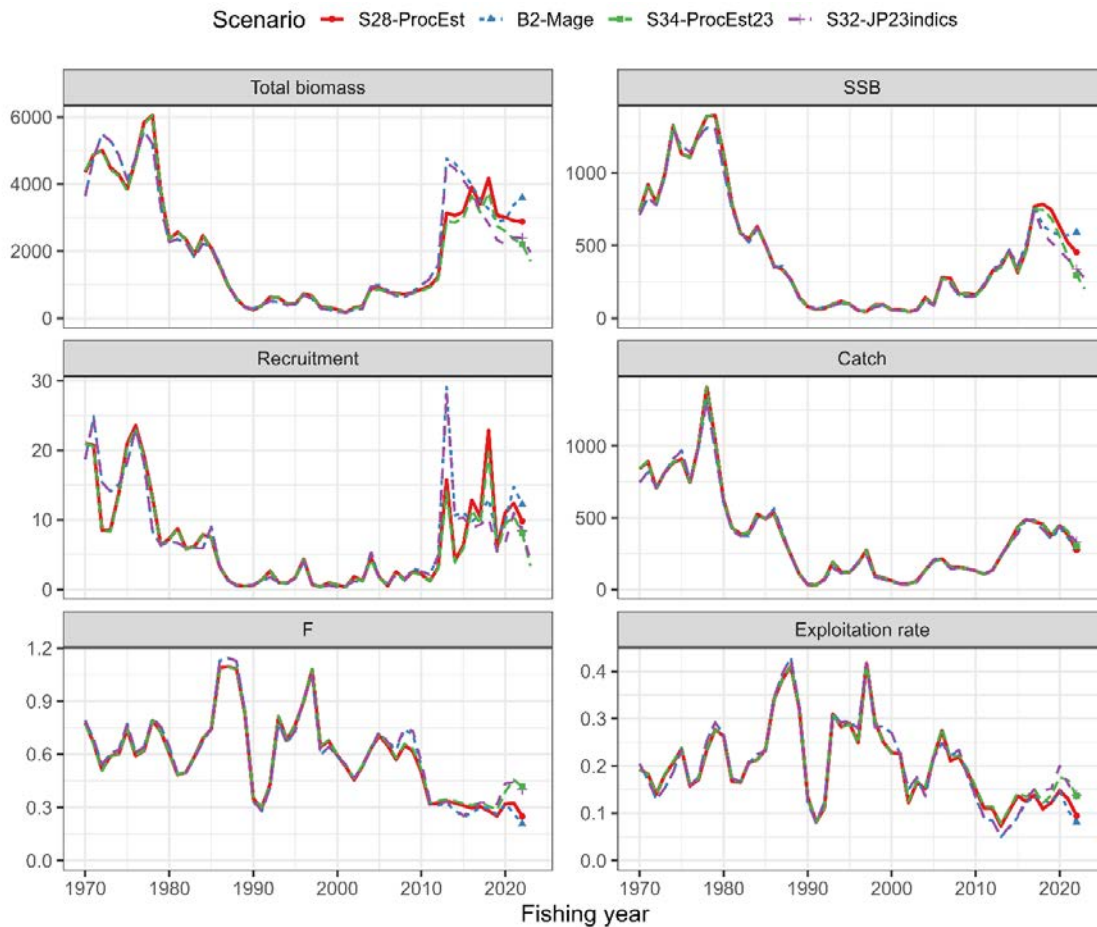


Figure E-7. Time series of estimates of total biomass (thousand mt), SSB (thousand mt), recruitment (billion fish), catch (thousand mt), mean fishing mortality (F) and exploitation rate (catch divided by total biomass) under the four representative scenarios. S28-ProcEst was selected as the base case scenario.

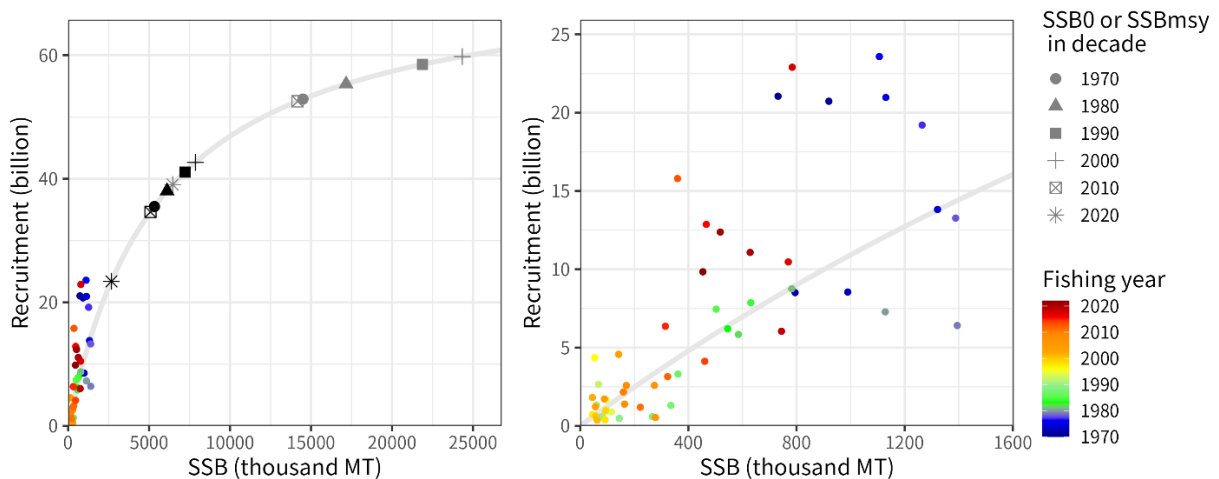


Figure E-8. Estimated stock-recruitment curve (gray lines) and estimated SSB and number of recruits (colored circles). Although both figures are same, in the left figure, estimated SSB<sub>0</sub> (equilibrium spawning biomass without fishing, gray symbols) and SSB<sub>MSY</sub> (black symbols) by decade are overlapped. The reference points are calculated using biological parameters averaged during the decades. The right panel also shows estimated recruitment and SSB by year along with the estimated stock recruitment curve.

## **Total biomass, Spawning Stock Biomass**

The time series of estimated chub mackerel total biomass and SSB from the base case model used to inform managers generally declined from the 1970s through the 1990s and the stock began to recover in the early 2000s, peaking in FY2018, after which it has generally declined over the last decade (total biomass and SSB are shown in Figure E-7 and Table E-2). The level of SSB in the 1970s was estimated to be approximately 1,104 thousand mt on average. SSB for FY2022 is estimated to be 450 thousand mt for the base case but varies from 300 thousand to 590 thousand mt among the sensitivity cases.

## **Recruitment**

Time series of estimated recruitment (age-0, billions of fish) abundance is presented in Figure E-7 and summary values in Table E-2 for the base model. The level of recruitment in the 1970s was estimated to be high (~16 billion individuals on average) and that in the most recent decade (FY2013-FY2022) was also high (=11 billion on average).

## **Stock-recruitment relationship**

Although the estimated stock recruitment relationship has not changed over time, the estimated average by decade of the SSB<sub>0</sub> (equilibrium spawning biomass without fishing, blue symbols) and SSB<sub>MSY</sub> (red symbols) are varied and decreased to the lowest points of the time series owing to the changes of biological parameters (Figure E-8).

## **Exploitation status**

Estimated rates of exploitation (fishing year catch/fishing year total biomass) time series generally fluctuated between 5 and 20% and followed the estimated  $F_t$  over time, with annual removal rates that ranged from roughly 10 to 30% over the modeled timeframe (Figure E-7), with some larger annual removals in excess of 40%.

## **Harvest Recommendations**

Given the uncertainty in biological parameters in future, which have a large impact on the projection results, the TWG CMSA considers it is not appropriate to provide long-term harvesting recommendations at this time. A short-term (towards FY2028) projection was undertaken to assess the effects of varying catch levels, ranging from 50 to 400 thousand tons, based on the most recent seven years' biological data (Figure E-9) and the entire time series of biological data (Figure E-10) for management considerations. Projections based on the most recent seven years' biological data showed that  $F_{cur}$  leads to future constant decline of SSB and it is necessary to reduce current fishing mortality (Table E-3).

## **Data and Research needs**

The assessment results, including projections, are dependent on biological parameters and processes which are uncertain. Therefore, future studies should be focused on collecting and analyzing biological information, e.g., maturity-at-age, weight-at-age, which would improve the assessment. Fisheries-dependent data, such as fleet-specific catch-at-age, are also critical to develop Member-specific fishing fleet and age-specific abundance indices.

A critically important recommendation that should be carried out in 2-3 years is to develop a harvest control rule (HCR) specific to this stock via a Management Strategy Evaluation (MSE) process. This HCR should be dynamic and able to adjust annual total catches depending on the stock abundance as well as the target and limit reference points. During the process of the development

of MSE, uncertainties in parameter estimates, time-varying or density-dependent biological parameters, and stock-recruitment assumptions should be considered.

Timely collection of biological information and further research on biological parameters and processes, including the effect of environment and climate change, are critically important to facilitate the accurate estimation of reference points.

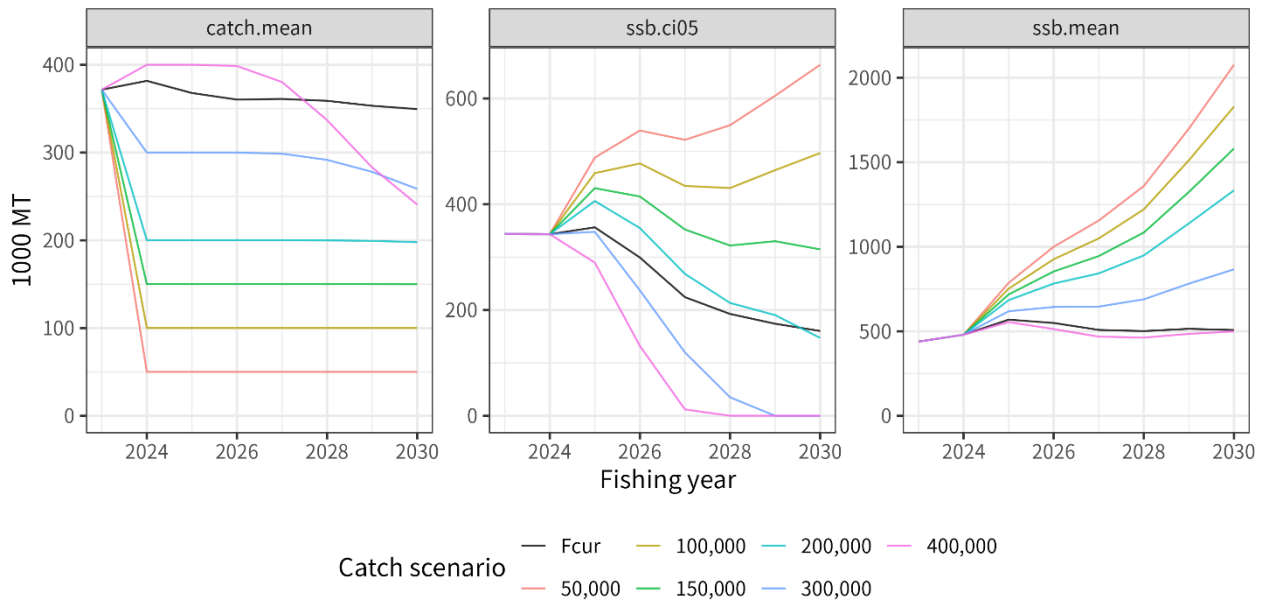


Figure E-9. Future trajectories of mean catch (left), 5% lower limit of predictive interval for SSB (middle) and mean SSB (right) with mean biological parameters in recent 7 years. Numbers and “Fcur” in “Catch scenarios” indicate total amount of catches (mt) in constant catch scenario and current fishing morality, respectively.

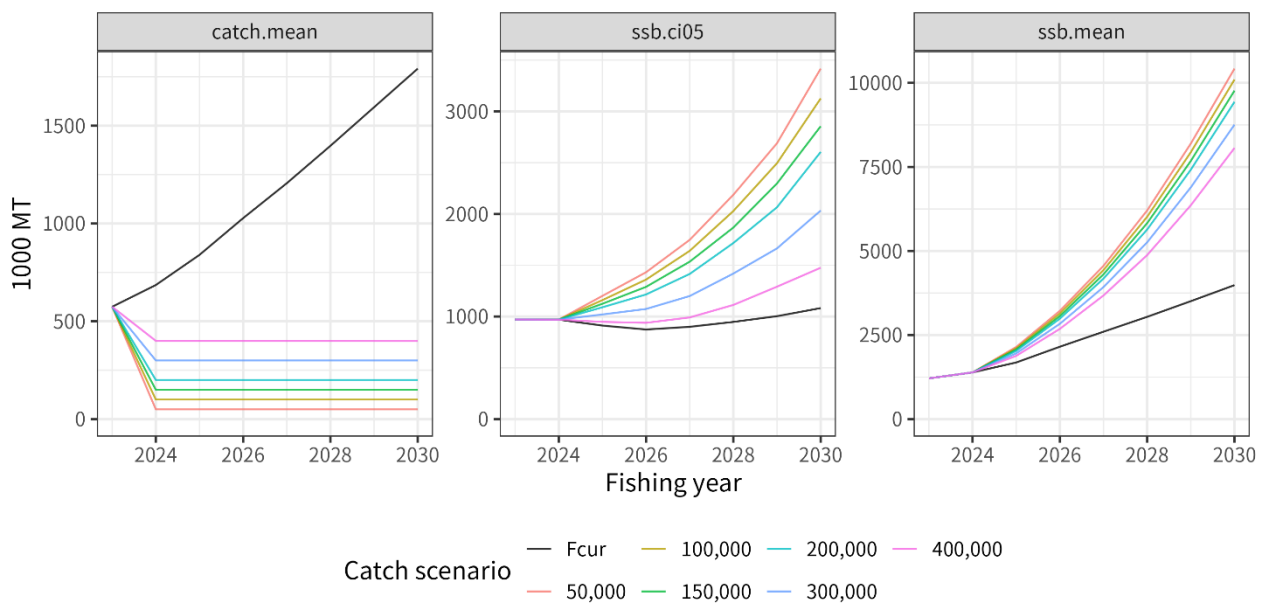


Figure E-10. Future trajectories of mean catch (left), 5% lower limit of predictive interval for SSB (middle) and mean SSB (right) with mean biological parameters for the entire time series. Numbers and “Fcur” in “Catch scenarios” indicate total amount of catches (mt) in constant catch scenario and current fishing morality, respectively.

Table E-3. Probability that future SSB on July 1, at the beginning of the fishing year, is above latest (FY2022) SSB under the base case scenario. The projection towards FY2028 is shown below.

Catch level	FY2025	FY2026	FY2027	FY2028
Fcur	76	64	48	44
50	97	99	98	98
100	96	96	94	94
150	93	92	88	88
200	89	87	80	78
300	79	70	58	56
400	66	49	38	36

# INTRODUCTION

## 1.1 Distribution and population structure

Chub mackerel (*Scomber japonicus*) is widely distributed throughout in the northwest Pacific, including in the waters of Japan, Korea, China, and Russia. The species exhibits highly migratory behavior, with distinct spawning, feeding, and wintering grounds. Spawning occurs primarily from spring to early summer in the subtropical waters, and the larvae and juveniles are often carried by ocean currents to feeding grounds further north. This migration pattern leads to a dynamic population structure that varies seasonally and spatially, reflecting the species' adaptation to environmental conditions.

In the northwest Pacific, two stocks of chub mackerel are recognized. Although there are no clear genetic differences between the two stocks, they are treated as different stocks due to their biological differences, distribution and spawning grounds. The first is the Tsushima Warm Current stock, which is distributed in the East China Sea and the Sea of Japan, and the latter is the Pacific stock, which can be defined as a straddling stock and is harvested in both national waters of Japan and Russia and the NPFC Convention Area. The Pacific stock, hereafter called chub mackerel in this report, is distributed from the coast of southern Japan to offshore waters of Kuril Islands (Figure 1). It is considered that both adults and juveniles are distributed as far east as 170°E longitude in periods of high abundance. During the low abundance period of 1990s-2000s, juvenile distributes from Japan to around 170°E, but adults were only found to 150°E due to the possible contraction of the feeding ground. The feeding migration of adult extends northeast, with the recent (since 2010) increase of stock abundance, the distribution of adult during the summer to fall season has expanded to 47° N, 166° E, east offshore of Kuril Island, after 2018. Adult fish spawn in Izu Islands waters in spring and then engage northward feeding migration to waters of Sanriku to east Hokkaido from summer to autumn.

## 1.2 Migration

Adult move to north (March to June) after spawning at Izu Islands area, which is the main spawning ground, and migrate to offshore area of Northeast of Japan (Sanriku and Hokkaido) from summer to fall for feeding (Meguro et al., 2002) (Figures 1 and 2). Larvae distribute broadly from the Pacific side of southern Japan to Kuroshio extension and Kuroshio-Oyashio transition area in spring. Larvae occurred at Kuroshio-Oyashio transition area and move to offshore of Kuril Island in summer and subadults migrate down south in fall to offshore of Chiba and Ibaraki prefecture for wintering (Kawasaki, 1968; Iizuka, 1974; Nishida et al., 2001; Kawasaki et al., 2006). Portion of adult and subadult migrate to Kii strait, Bungo strait and Seto inland sea, while the main spawning adults migrate to waters around Izu Islands area. Because of the occurrence of larvae originated upstream of Kuroshio current at the spawning ground of Izu Islands (Koizumi, 1992), spawning

ground extended from offshore of southern Japan to northern Japan (Kuroda, 1992).

### **1.3 Reproduction**

Chub mackerel mature at about age 2 or 3 and all fish at age 4 and above are supposed to be fully matured (Watanabe and Yatsu, 2006). One functional matured female produces 30–90 thousand eggs several times during a spawning season (Murayama et al., 1995; Watanabe et al., 1999; Yamada et al., 1999). The main spawning grounds are in the Japanese Exclusive Economic Zone (EEZ), in waters around the Izu Islands but also in areas off the Pacific coast of southern Japan, including the Kinan area, Cape Muroto and Cape Ashizuri (Figure 1). The waters around the Izu Islands are considered the main spawning ground (Watanabe, 1970; Usami, 1973). Although spawning occurs from offshore of southern Japan to northern Japan (Kuroda, 1992) and it has also been observed in the Tohoku waters (Kanamori et al., 1999).

The spawning season for chub mackerel is from January to June. In the main spawning ground of Izu Islands, spawning occurs in March and April, which historically are the peak spawning months. In the 2000s, the peak spawning timing has shifted to May and June because of the high fraction of younger adults, which tend to spawn eggs at later season (Watanabe, 2010). Additionally, the spawning ground is reported to exhibit northward shifting with extended spawning period associated with climate change (Kanamori et al., 2019).

The growth of chub mackerel is density dependent, and changes according to the recent recruitment and ocean environment (Watanabe and Yatsu, 2006). Maturity at age has changed depending on changes in growth (Watanabe and Yatsu, 2006). The maturity at age for chub mackerel has changed over time, for example the maturity rate of age 3 fish has decreased from 100% to 30% since 2015 (Figure 5).

### **1.4 Prey and predators**

Larvae feed on the eggs of copepods and nauplii, whereas juvenile prey on small zooplankton such as small copepods, noctilucines, cercariae, and salpae (Kato and Watanabe, 2002). The feeding behaviors of immature and adult fish differ depending on the waters and lifecycle, but they mainly prey on other fishes (e.g., anchovies and lantern fish), crustaceans (e.g., krill and copepods) and salpae. In the Sanriku waters, the main prey are mysid shrimp and anchovies.

Before the 1980s, when stock abundances were high, chub mackerel were often observed to be eaten by large fishes such as the mackerel shark, blue shark, pomfret, albacore, and skipjack tuna (Kawasaki, 1965; Nagasawa, 1999), as well as the minke whale (Kasamatsu and Tanaka, 1992). In the 1990s, the lower abundance period, predation of minke whales was not reported (Tamura et al., 1998). From the research report of baleen whale predations, composition of anchovy decreased in

the stomach contents after 2012, but mackerels and sardine increased. Especially in the case of sei whale, the main prey item shifted from anchovy in early 2000s to mackerel and sardine in late 2000s and after 2010 (Tamura et al., 2016; Konishi et al., 2016). When the abundance of mackerels is high, they appear to be main prey items for whales.

### **1.5 Age and growth**

Longevity of chub mackerel is estimated to be approximately 8 years, based on age determination of sampled catch, and maximum age was recorded at 11-year-old (Iizuka, 2002). Fish at age 6 and above are very rare in the catches in recent years. There is no significant difference in growth between sex. Growth of chub mackerel is density dependent, and the parameters of growth function are variable among the year classes. According to Kamimura et al. (2021), the asymptotic body length  $L_{inf}$  and growth coefficient  $k$  of von Bertalanffy growth function varied between 339.9 to 440.5 mm and 0.25 to 0.55 (/year), respectively, for each year class of 2006-2016.

Average size (fork length) and weight of catch in 2018 are shown in Figure 3, with comparison of those at 2011-2014 which did not show any slow growth. Average weight of 2018 was low comparing with those of 2011-2014 and 1970s, especially for age 5 (extremely high recruitment in the 2013 year class). It is considered that density dependence may be the cause for this change. (Kamimura et al., 2021). However, slower growth has been observed at periods of high abundance, this may be due to poor environmental conditions (i.e. lower temperatures due to range expansion), or feeding competition with Japanese sardine, or other factors (Kamimura et al., 2021).

## **FISHERIES AND SCIENTIFIC SURVEYS**

### **2.1 Overview of fisheries**

Chub mackerel are harvested by China, Japan and Russia (Figure 4). Chinese light purse seine and pelagic trawl fisheries are operated in the NPFC Convention Area. Japanese chub mackerel fisheries consist mainly of purse seine and set net fisheries within the Japanese national waters. Russian chub mackerel fisheries mainly operate in the Russian national waters, consist of mid-water trawl, purse seine and bottom trawl gears with operations in the Japanese national waters. The historical total landings have largely fluctuated. In last decade, the total catch was stable at higher level and subsequently decreased from approximately 498 thousand mt in 2021 to 151 thousand mt in the most recent calendar year (CY) 2023. The Conservation and Management Measure for chub mackerel (CMM 2024-07) includes a catch limit of 100,000 mt set in the Convention Area for each of the 2024 and 2025 fishing seasons (1 June to 31 May).

China harvests this species dominantly by light purse seine fishery in the NPFC Convention Area. A smaller component of the catch is taken by pelagic trawl. Chinese catch statistics on mackerels

in the NPFC Convention Area are available from 2015. The Chinese mackerel fisheries in the NPFC Convention Area initiated in 2014 mainly caught the three fish species such as chub mackerel, blue mackerel, and Japanese sardine (Zhang et al., 2023). The fishing seasons of Chinese fleet is from April to December.

The major Japanese fisheries for chub mackerel are purse seine, set net and dip-net fishing, and stick-held dip-net fishing. Large-scale purse seiners, accounting for more than 50% of total catch in Japan, operate all the year over during the main fishing season from September to February in the offshore waters off Joban and Sanriku coasts on the Pacific side of Japanese main island. Small-scale purse seiners operate year-round in the coastal waters south of Chiba Prefecture. Set net fisheries are deployed extensively along the Japanese coast and yield a large catch from Sanriku coast. Dip-net and stick-held dip-net fisheries which target adult fish in spawning season (age 2 to 4 fish) are mainly operated from January to June in the Izu Islands waters. Chub mackerel is also caught by angling all over Japan.

Russian fisheries targeting mackerel species and sardine operate in the NW area of the NPFC Convention area and operate both purse seine vessels and pelagic trawl vessels. Russian fisheries first exploited mackerel in the Far East in the early 1960s and harvested it until the late 1980s, when its stocks in areas accessible to the domestic fleet were completely depleted (Baryshko, 2009). Out of 26 years of mackerel fishery for 13 years more than 50 thousand tonnes per year was harvested, including 9 years when the catch was more than 100 thousand mt. Commercial fishing of mackerel in the North-West Pacific Ocean by vessels under the Russian (Soviet) flag began in 1968. Since the second half of the 1980s, due to a sharp decline in mackerel abundance, its commercial fishing for mackerel in the Russian EEZ has been rare. Until recently, there has been no target fishing for mackerel by Russia in the Northwest Pacific. Russian fisheries resumed fishing in 2015. In 2021, the chub mackerel catch by the Russian fleet totaled to 87 thousand mt.

## **2.2 Overview of scientific surveys**

China has been conducting a scientific survey program using its fishery research vessel "Song Hang" in the NPFC convention area since 2021 (Ma et al., 2023). The survey is conducted during June-August, with methods of mid-trawling, acoustic and squid jigging, covering about 70 stations per year. The results indicated that Chub mackerel is one of the dominant species in the four years survey.

In Japan, monthly egg surveys have been intensively conducted off the Pacific coast of Japan in the western North Pacific since 1978 by a historical cooperative system among many national and regional fisheries research bodies (Nishijima et al., 2024a). The survey protocol can be found at Oozeki et al. (2007). The objective of this egg survey is to monitor egg abundance of major small

pelagic fish species such as Japanese sardine, Japanese anchovy, chub mackerel, etc. The survey area roughly covered the major spawning grounds of small pelagic fish off the Pacific coast, mainly inshore waters but also offshore waters related to the warm Kuroshio and cold Oyashio currents. In addition, Japan has conducted the surface trawl net surveys in summer (June to July) and autumn (September to October) to monitor abundance of ages 0 and 1 (Nishijima et al., 2024b; 2024c; Yukami et al., 2024). The summer survey has been initiated in 2001 and annually carried out, covering the waters approximately from 141.5° E to 170.0° W and from 32.0° to 45.0° N. It provides information on abundance of age 0 fish. The autumn survey was started in 2005 and has been conducted annually, covering the area approximately of 141.5°–175° E and 37.0°–50.0° N. This survey provides abundance information on ages 0 and 1.

Russia has conducted a summertime acoustic-trawl survey since 2010 that examines mid-water and upper epipelagic species including chub mackerel. This survey completes 60-80 stations per year and aims to assess changes in abundance and migration patterns. Data collected include catch and effort, catch at length, and data for ageing.

## **DATA**

### **3.1 Data preparation for stock assessment model**

The Technical Working Group on Chub Mackerel Stock Assessment (TWG CMSA) agreed to apply a State-space Stock Assessment Model (SAM; Nielsen and Berg, 2014) for its stock assessment (TWG CMSA, 2023). It requires age-specific input data such as catch-at-age, maturity-at-age and weigh-at-age and abundance indices. A fishing year (FY) starting from July and ending in June of the following year was applied in the stock assessment of chub mackerel. The TWG CMSA agreed for the stock assessment period to be FY1970 (CY1970/quarter 3 (Q3)) to FY2022 (CY2023/Q2). Seven age groups of ages 0 to 5 and 6+ were defined in the stock assessment. The Members submitted their data on quarter basis and then, they were compiled for construction the input data based on the fishing year. Manabe et al., (2024a; 2024b) comprehended the age-specific input data.

China has collected length frequency data of commercial catch through onboard and port samplings since CY2016, and aging of the samples has been started since CY2017. Japan also collects length, weight, maturity and age data from the survey and fishery to support their stock assessment. Russian length frequency and aging data of commercial catch are available since CY2016. The length frequency data obtained through research surveys are available since CY2010.

### **3.2 Catch-at-age**

The catch-at-age is prepared for each Member on quarterly-basis for China and Russia. Japanese catch-at-age is prepared for Eastern Japan and Western Japan due to its difference in catch, size, and season in which the border of two regions is located at Mie-Shizuoka prefectural border.

The Members provided their quarterly catch-at-length data on calendar year basis as follows:

- 1) China, CY2016 to CY2022/Q2 ;
- 2) Eastern and Western Japan, CY2014 to CY2023/Q2;
- 3) Russia, CY2016 to CY2022.

The Members provided their quarterly age-length key (ALK) on calendar year basis as follows:

- 1) China, CY2018 to CY2022;
- 2) Eastern and Western Japan, CY2014 to CY2023/Q2.

For the catch-at-age prior to CY2014, Japan provided fishing year-based catch-at-age data for FY1970-FY2013 from the Japanese domestic stock assessment (Yukami et al. 2024). The data contains Russian catch in FY1967-1988 however due to the difficulty of separation into two Members, the catch is incorporated as Japanese catch. For the period of CY2014-2023/Q2, the TWG CMSA has agreed to calculate catch-at-age based on the catch-at-length data and corresponding ALK data of each quarter and region, which the detailed procedures are described in Manabe et al. (2024b). The ALK of Russia is substituted by the Eastern Japanese ALK due to the similarity in the area of catch.

For the period with missing catch-at-length, the procedures to supplement the data are as follows:

- 1) For China CY2015, use mean catch-at-length of China of CY2016-2018 for equivalent quarter;
- 2) For Russia CY2014-2015, use mean catch-at-length of Russia of CY2016-2018 for equivalent quarter;
- 3) For Russia CY2022-2023/Q2, use Eastern Japanese catch-at-length of the equivalent quarter/year.

For the period with missing ALK, Eastern Japanese ALK of the equivalent quarter/year is applied to calculate catch-at-length. The calculated catch-at-length from each quarter is converted to fishing year basis by setting the data of age incrementation as July 1st. Ages are subtracted by 1 for the first and second quarters and early caught age 0 fish in those quarters, which are calculated as age -1, are incorporated into the third quarter as age 0. The detailed procedures are described in Manabe et al. (2024b).

Through the procedures described above, catch-at-age data had been prepared for the stock assessment (Figure 5a). Chub mackerel catch was historically composed mainly of fish younger than age 3. In the periods of FY1970s, FY1980s and late-FY2010s to beginning of FY2020s, the catch of fish older than age 3 was prominent. There were differences in age compositions in catch by year and by member from FY2014 to FY2022 (Figure 6). Catches of ages 1 to 3 were prominent in FY2014 to FY2016, respectively. In addition, dominant age classes of catch were different among China and Japan.

### **3.3 Weight-at-age**

The Members provided their quarterly weight-at-age data on calendar year basis as follows:

- 1) China, CY2018 to CY2023/Q2;
- 2) Eastern and Western Japan, CY2014 to CY2023/Q2;
- 3) Russia, CY2016 to CY2022.

The TWG CMSA has agreed to calculate a single weight value for each age to convert stock number into biomass (NPFC, 2024). The single weight-at-age were calculated through the following procedure, as described in Manabe et al. (2024b). The proportion of catch number for each quarter is calculated for four regions: China, Eastern Japan, Western Japan, and Russia, using the following equation, where  $P$  is proportion of catch number,  $N_{a,t,r}$  represents the catch number of age  $a$  at year  $t$ , and region  $r$ .

$$P_{a,t,r} = \frac{N_{a,t,r}}{\sum N_{a,t,r}}$$

The yearly catch number ratio for each region is then averaged between FY2014-2022 to calculate the constant ratio of catch number across the members.

$$P_{a,r} = \frac{\sum_{t=2014}^{2022} P_{a,t,r}}{9}$$

The weighted mean of weight  $W$  at age  $a$  at quarter  $q$  of year  $t$  is then calculated as:

$$W_{a,q,t} = \frac{P_{china}W_{a,q,t,china} + P_{japan}W_{a,q,t,japan} + P_{russia}W_{a,q,t,russia}}{3}$$

The quarterly weight-at-age within a single fishing year is taken an arithmetic mean to calculate the annual weight-at-age, which is used for the stock assessment.

$$W_{a,t} = \frac{\sum W_{a,q,t}}{4}$$

Through this procedure, annual weight-at-age were calculated for FY2014 to FY2022 (Figure 5b). Since the weight-at-age prior to FY2014 was not reported by other members, the weight-at-age of CM in FY1970 to FY2013 was sourced from the Japanese domestic stock assessment of the Pacific stock of chub mackerel. Historical weight-at-age showed time-varying attributes and decreased obviously in last decade in age groups older than age 0.

### 3.4 Maturity-at-age

The TWG CMSA has agreed to use the annual maturity-at-age data from Japanese domestic stock assessment (NPFC, 2024) (Figure 5c). The Japanese maturity-at-age data is derived from the observation of catch from the spawning area, and based on previous studies (Watanabe and Yatsu, 2006; Watanabe, 2010). Chinese maturity-at-age data submitted on a quarterly basis were not included in the base-case maturity-at-age however the alternative maturity-at-age data are prepared for the sensitivity analysis, which the data preparation and data are described in NPFC-2024-TWG CMSA9-WP02.

Annual maturity-at-age used for base case showed decadal time-varying changes from FY1970 to FY2022 (Figure 5c). The maturity rate of age 2 and 3 fish is expected to be lower after FY2015 than in the period before FY2014, due to the slow growth of the 2013-year class. In the recent years, maturity rate of age 2 is zero, and that of age 3 is 0.3 in the Japanese national waters.

### **3.5 Natural mortality**

Initially the assessment investigated set two cases of natural mortality (TWG CMSA, 2024). One is  $M = 0.5$  for all age classes while the other is age-specific  $M$  (0.80 for age 0, 0.60 for age 1, 0.51 for age 2, 0.46 for age 3, 0.43 for age 4, 0.41 for age 5, and 0.40 for age 6+) (Figure 7). These natural mortality coefficients have been determined according to different natural mortality estimators with biological parameters from various samples (Ma et al., 2024; Nishijima et al., 2021). It is assumed that the natural mortalities are time-invariant throughout all years. The TWG CMSA agreed to use the age specific natural mortality estimates for all models at its 9th meeting.

### **3.6 Abundance indices**

The inventory of abundance indices time series shown in Figure 6d was as follows.

- 1) Relative number of age 0 fish from the summer survey by Japan from FY2002 to FY2023 (Nishijima et al., 2024a (NPFC-2024-TWG CMSA08-WP06 (Rev. 1)))
- 2) Relative number of age 0 fish from the autumn survey by Japan from FY2005 to FY 2023 (Nishijima et al., 2024c (NPFC-2024-TWG CMSA09-WP06))
- 3) Relative number of age 1 fish from the autumn survey by Japan from FY2005 to FY 2023 (Nishijima et al., 2024c (NPFC-2024-TWG CMSA09-WP06))
- 4) Relative spawning stock biomass (SSB) from the egg survey by Japan from FY2005 to FY2023 (Ishida et al., 2024 (NPFC-2024-TWG CMSA09-WP07))
- 5) Relative SSB from the dip-net fishery by Japan from FY2003 to FY2023 (Nishijima et al. 2024b (NPFC-2024-TWG CMSA08-WP03))
- 6) Relative vulnerable stock biomass from the light purse seine fishery by China from FY2014 to FY2022 (Shi et al., 2024 (NPFC-2024-TWG CMSA09-WP13 (Rev. 1)))
- 7) Relative vulnerable stock biomass from the trawl fishery by Russia from FY2016 to FY2023 (Chernienko and Chernienko, 2024 (NPFC-2024-TWG CMSA09-WP11))

Six time series except for the Russian abundance indices were used during model development and applied for the base case. The Russian ones were used for a sensitivity run. The abundance indices from Japan and Russia were available until FY2023 and until FY2022 for China. The FY2023 Japanese abundance indices were applied in two of the representative runs.

## **SPECIFICATION OF STOCK ASSESSMENT**

### **4.1 State-space Stock Assessment Model (SAM)**

SAM is a statistical catch-at-age model that accounts for observation errors in catch at age, which was originally developed by Nielsen and Berg (2014). Furthermore, in order to match the nature of data of this stock, improvements have been made to allow more flexible settings (Nishijima and Ichinokawa, 2023), and this assessment used the modified version. The detailed settings are described as follows. SAM consists of two subparts: population dynamics model and observation model.

#### 4.1.1 Population dynamics model

The population dynamics of chub mackerel in SAM basically follows an age-structured model:

$$\log(N_{0,y}) = \log[f(SSB_y)] + \eta_{0,y}, \quad a = 0 \quad (1)$$

$$\log(N_{a,y}) = \log(N_{a-1,y-1}) - F_{a-1,y-1} - M_{a-1,y-1} + \eta_{a,y}, \quad 1 \leq a \leq 5 \quad (2)$$

$$\log(N_{6+,y}) = \log(N_{5,y-1}e^{-F_{5,y-1}-M_{5,y-1}} + N_{6+,y-1}e^{-F_{6+,y-1}-M_{6+,y-1}}) + \eta_{6+,y}, \quad a = 6+ \quad (3)$$

where  $\eta_{a,y}$  is the process error at age  $a$  in year  $y$  following  $\eta_{a,y} \sim N(0, \omega_a^2)$ . The recruitment of chub mackerel occurs at age 0, described by a function of SSB and process errors (Eqn. 1). We use a Beverton-Holt stock-recruitment relationship (Beverton and Holt, 1957):

$$f(SSB_y) = \frac{\alpha \times SSB_y}{1 + \beta \times SSB_y}, \quad (4)$$

where  $SSB_y$  is the sum-product of number ( $N$ ), weight ( $w$ ), and maturity ( $g$ ) at age:

$$SSB_y = \sum_{a=0}^{6+} g_{a,y} w_{a,y} N_{a,y}. \quad (5)$$

For fish older than age 0, the number of each cohort decreases by fishing mortality coefficient ( $F_{a,y}$ ) and natural mortality coefficient ( $M_{a,y}$ ) from the previous year and also be affected by process errors  $\eta_{a,y}$  (Eqn. 2). For the plus-age group (6+), the number is described as the sum of surviving numbers of age 5 and age 6+ from the previous year (Eqn. 3).

In SAM, fishing mortality coefficients are assumed to follow a multivariate random walk:

$$\log(\mathbf{F}_y) = \log(\mathbf{F}_{y-1}) + \boldsymbol{\xi}_y, \quad (6)$$

where  $\mathbf{F}_y = (F_{1,y}, \dots, F_{A+,y})^T$ ,  $\boldsymbol{\xi}_y \sim \text{MVN}(0, \boldsymbol{\Sigma})$ , and  $\boldsymbol{\Sigma}$  is the variance-covariance matrix of multivariate normal distribution (MVN). The diagonal elements of matrix  $\boldsymbol{\Sigma}$  were  $\sigma_a^2$ , while off-diagonal elements represent covariance of  $F$  process errors between age classes. This assumption of  $F$  random walk allows us to estimate time-varying selectivity (Nielsen and Berg 2014). For the covariance of MVN, we assume that the correlation coefficient of  $F$  between ages  $a$  and  $a'$  decreases

along with their age differences:  $\rho^{|a-a'|} \sigma_a \sigma_{a'}$  ( $a \neq a'$ ).

#### 4.1.2 Observation model

SAM is fitted to the data of catch-at-age and abundance indices. SAM uses the Baranov equation for estimates in catch-at-age:

$$\hat{C}_{a,y} = \frac{F_{a,y}}{F_{a,y} + M_{a,y}} (1 - \exp(-F_{a,y} - M_{a,y})) N_{a,y} . \quad (7)$$

In this equation,  $F_{a,y}$  and  $N_{a,y}$  are estimated parameters by random effects, while  $M_{a,y}$  is the natural mortality coefficient. That is, the predicted catch at age in number ( $\hat{C}_{a,y}$ ) is a derived parameter. SAM then fit to observed catch-at-age in a lognormal assumption:

$$\log(C_{a,y}) = \log(\hat{C}_{a,y}) + \varepsilon_{a,y} , \quad (8)$$

where  $\varepsilon_{a,y} \sim N(0, \tau_a^2)$ .

We have agreed to use six abundance indices (Figure 5d) which represent, respectively,

1. Relative number of age 0 fish from the summer survey by Japan,
2. Relative number of age 0 fish from the autumn survey by Japan,
3. Relative number of age 1 fish from the autumn survey by Japan,
4. Relative spawning stock biomass (SSB) from the egg survey by Japan,
5. Relative SSB from the dip-net fishery by Japan, and
6. Relative vulnerable stock biomass to Chinese fleet from the light purse-seine fishery by China.

The predicted values of these abundance indices can be expressed in the following general equation:

$$\hat{I}_{k,y} = q_k \left[ \sum_{a=0}^{6+} (\chi_{a,y,k} N_{a,y}) \right]^{b_k} . \quad (9)$$

The subscripts  $k$ ,  $y$ ,  $a$  represent index, year, and age, respectively.  $q_k$  and  $b_k$  are the proportionality constant and the nonlinear coefficient, respectively, for index  $k$ . Note that this equation does not mean that all the abundance indices are all nonlinear against abundance but includes a linear case ( $b_k = 1$ ). The parameter  $\chi_{a,y,k}$  is a multiplier on the number of fish in age  $a$  and year  $y$  ( $N_{a,y}$ ) for index  $k$ . For the abundance indices for age 0 fish number ( $k=1,2$ ),

$$\chi_{a,y,k} = \begin{cases} 1, & a = 0 \\ 0, & \text{otherwise} \end{cases} . \quad (10)$$

For the abundance index for age 1 fish number ( $k=3$ ),

$$\chi_{a,y,k} = \begin{cases} 1, & a = 1 \\ 0, & \text{otherwise} \end{cases} . \quad (11)$$

For the abundance indices for SSB ( $k=4,5$ ),

$$\chi_{a,y,k} = g_{a,y} w_{a,y} . \quad (12)$$

The abundance indices for vulnerable stock biomass to Chinese fleet ( $k=6$ ) would represent a part of the stock for each fleet or each member's fishery. For the abundance indices for vulnerable stock biomass ( $k=6$ ), therefore,

$$\chi_{a,y,k} = \hat{s}_{a,y,k} w_{a,y,k}, \quad (13)$$

where  $\hat{s}_{a,y,k}$  is the estimated fishery selectivity in age  $a$  and year  $y$  for index (or fleet)  $k$ . We cannot estimate fleet-specific  $F$  in the current setting of SAM or, therefore, derive fleet-specific predicted catch at age (see Eqn. 1). Since the fleet-specific catch-at-age data is available (Figure 5a), however, we can approximate the fleet-specific  $F$  as follows:

$$F_{a,y,k} \doteq \frac{C_{a,y,k}}{\sum_f C_{a,y,f}} F_{a,y}, \quad (14)$$

where  $C_{a,y,k}$  are the observed catch number in age  $a$  and year  $y$  for fleet  $k$ . This approximation assumes that the fleet-specific  $F$  is proportional to fleet-specific "observed" catch at age in number. We then obtain the fleet-specific selectivity:

$$\hat{s}_{a,y,k} = \frac{F_{a,y,k}}{\max[\mathbf{F}_{y,k}]}, \quad (15)$$

where  $\mathbf{F}_{y,k} = (F_{0,y,k}, F_{1,y,k}, \dots, F_{6+,y,k})^T$ . It is important to note that  $\chi_{k,a,y}$  for  $k=6$  include the estimated parameters ( $F_{a,y,k}$ ), whereas  $\chi_{k,a,y}$  for  $k=1-5$  are provided from input data. We used the ratios of catch numbers of China to the total catch numbers as input data to fit the CPUE of Chinese light purse seine fishery. In calculating the vulnerable biomass, fleet- and age- specific weight ( $w_{a,y,k}$  in Eqn. 12) is needed. However, since there are no agreed data of fleet- and age- specific weights in fishing year by Chinese fishery, we took a simp approach to using the stock weights for biomass calculation:  $w_{a,y,k} = w_{a,y}$  (Figure 5b).

The list of fixed-effect and random-effect parameters is shown in Table 1. The parameters are estimated to maximize the marginal likelihood of summing process-error components and observation error components. The marginal likelihood is computed by the numerical integration using the Laplace approximation via Template Model Builder (TMB: Kristensen et al., 2016). We applied a generic bias-correction estimator for derived quantities calculated as a nonlinear function of random effects (e.g.,  $N_{a,y}$  is a derived quantity calculated from the random effect of  $\log(N_{a,y})$ ), which is implemented in TMB (Thorson and Kristensen, 2016). Estimation uncertainties including standard errors (SEs) and confidence intervals were computed from the delta method in TMB. In this stock of chub mackerel, the period from July to the following June is treated as a fishing year (Manabe et al., 2024a (NPFC-2024-TWG CMSA08-WP15)), and the estimated abundance is that at the beginning of the fishing year (i.e., July).

#### 4.2 Model settings of process and observation errors and nonlinearity of abundance indices

SAM estimates multiple fixed-effect parameters of process and observation errors (Table 1). Estimating these parameters by age may cause the failure to converge or over-parameterization.

Furthermore, CPUE does not always respond linearly to the stock abundance, and the presence of these indices can lead to overestimation or underestimation of resources (Nishijima et al., 2019; Rose and Kulka, 1999). One way to solve this problem is to estimate nonlinearity parameters, which may improve model performance such as the fit to the abundance index and retrospective analysis (Hashimoto et al., 2018). We therefore conduct model selection for process and observation errors and nonlinearity of abundance indices based on AIC (see Nishijima et al. 2024d for details).

The following model settings were chosen for the base case scenario:

- (1) all the six abundance indices have difference standard deviations (SDs) for observation errors,
- (2) the nonlinear coefficients are estimated for the age-0 index from the Japanese summer survey, the age-0 index from the Japanese autumn survey, and the age-1 index from the Japanese autumn survey, while they are fixed at 1 (i.e., linear) for the other indices,
- (3) SDs of catch-at-age observation errors differ for ages 0-1, ages 2-3, ages 4-5, and ages 6+,
- (4) SDs of F random walk process errors differ between ages 0-1 and ages 2-6+, and
- (5) SDs of N process errors differ for age 0, age 1, ages 2-4, and ages 5-6+.

Regarding N process errors, we set two cases depending on whether the SDs for age 1 and older are fixed at

a very small value (0.01) or estimated. The former case means that process errors occur only for age 0 recruitment (i.e., recruitment variability, while the latter means that the population size in a cohort fluctuates after recruitment by unknown factors other than fishery and pre-determined natural mortality.

### 4.3 Model diagnostics

For the selected models, we applied several model diagnostics to check the reliability from a statistical view. Firstly, we performed a jitter analysis in which the initial values of the parameters were varied and re-estimated to confirm that the estimated parameters reach the global optimum. We checked whether the final gradients of the fixed effect parameters are close to zero, which is a necessary condition for model convergence.

We then plotted residuals in the catch number by age and in abundance indices to examine whether the residuals have temporal patterns. We also examined residuals in process errors for numbers by age ( $\eta_{a,y}$  in Eqns. 1-3) and F by age (diagonal components of  $\xi_y$  in Eqn. 6). to show the stock abundance historically changed by these process errors.

A five-year retrospective analysis was performed to examine if the estimates had systematic bias for the removal (updating) of data. Mohn's rho was calculated for total biomass, SSB, recruitment, and mean F. We also performed a retrospective forecasting, which excludes the stock index values and catch number by age from the latest year and compares the results of a one-year-ahead

forecasting from the terminal year of those data (in which age-specific weight and maturity rates were used) with estimates from the model using all data.

The leave-one-out (LOO) index analysis was next conducted by excluding the six abundance indices one by one and comparing the estimates with the results obtained when all indices were used. This analysis allows us to examine the impact of each index on abundance estimates and check their robustness.

To evaluate systematic under or over fitting One Step Ahead (OSA, Trijoulet et al., 2023) residuals were used. OSA residuals can assess how well a model fits the data, while not relying on assumptions of normality in the underlying data. These residuals represent the difference between the observed value at a particular time step and the value predicted by the model based on all prior information. OSA residuals were calculated for the indices of abundance and age composition data.

#### **4.4 Agreed base case scenario**

In order to improve the SAM fit to abundance indices and retrospective patterns, the TWG CMSA recognized the necessity of introduction of estimation of process error in survival of age groups older than age 0. The TWG CMSA also considered inclusion of FY2023 from the Japanese abundance indices, which had a large impact on the stock status of the most recent years. As a result, the following four scenarios were employed as representative cases:

- 1) B2, Estimate process error for only age 0 (recruitment) ;
- 2) S28-ProcEst, Estimate process error for all age groups;
- 3) S32-JP23, Estimate process error for only age 0 and use Japanese indices up to FY2023;  
and
- 4) S34-ProcEst23, Estimate process error for all age groups and use Japanese indices up to FY2023

TWG CMSA agreed to select S28-ProcEst as a base case scenario because of the better diagnostics than the model only with recruitment process error and agreement of data usage up to FY2022. The other three scenarios were employed to show possible range of uncertainty.

#### **4.5 Setting and equations for future projection and biological reference points**

Projections were carried out using parameter estimates from the models of B2-Mage (B2), S28-ProcEst, S32-JP23, and S34-PRocEst23. The model S28-ProcEst was agreed to be used as the base case, while the settings of the other models are found to be the most other plausible representations of current stock status. Biological parameters such as weight-at-age and maturity-at-age used for

calculation of biological reference points are assumed as the average values during the most recent 7 years (FY2016 to FY2022), which represents the recent change in biological parameters. As a control, the average of the biological parameters was calculated over the stock assessment period.

The future harvesting scenario was predetermined as a total catch (CC) of 50, 100, 150, 200, 300 and 400 thousand tons after FY2023, compared with another future harvesting scenario under  $F_{CUR}$  (average of  $F$  values from FY2020-2022).

#### **4.5.1 Biological reference points and evaluation of spawning potential**

We calculated commonly used biological reference points such as  $F\%SPR$  (20%, 30%, 40%, and 50%),  $F_{0.1}$ ,  $F_{MSY}$ , and  $SSB_{MSY}$  with the biological parameters described above (bio2020 and bio2010) and selectivity of  $F_{CUR}$ . As for the  $F$ -based reference points, relative values to  $F_{CUR}$  are shown in the results (e.g.  $F_{MSY}/F_{CUR}$ ). The equations to derive these reference points are described in Annex D in the past report for developing an operating model for this stock (<https://www.npfc.int/summary-2nd-meeting-small-working-group-operating-model-chub-mackerel-stock-assessment>) and definitions of these performance measures are same as the working paper for the sensitivity analysis (NPFC-2024-TWG CMSA09-WP04).

We also calculated annual spawner per recruit (SPR) with historically changing weight and maturity rate at age of this stock (Figures 5b and 5c) to evaluate the historically changing spawning potential of this species. SPR is the cumulative weight of equilibrium spawning biomass (g) along its life history (growth, maturity, and natural mortality) of a recruit of fish under a certain fishing mortality coefficient of  $F$ . Usually,  $SPR(F)$  is defined as

$$SPR(F) = \sum_{a=0}^{\infty} \exp(-M_a - F_a) g_a w_a$$

where  $M_a$ ,  $g_a$  and  $w_a$  is natural mortality rate, maturity rate, and weight at age  $a$ . With this equation, we defined annually changing SPR without fishing as  $SPR_{0y}$  where  $F_a = 0$ ,  $g_a = g_{a,y}$ , and  $w_a = w_{a,y}$  ( $y = \text{FY1970, FY1971, ..., FY2022}$ ). Similarly, we also calculated  $MSY$  reference points under the selectivity of  $F_{CUR}$  and  $SSB_{0y}$  with biological parameters averaged during each decade ( $y = \text{FY1970-1979, 1980-1989, etc....}$ ) to evaluate the effect of the changes in biological parameters on  $MSY$  reference points.

#### **4.5.2 Equations for calculating and population dynamics in future projection**

The population dynamics model for future projections is the same as that used in SAM. The calculation was conducted by an R package named `frasyr` (<https://github.com/ichimomo/frasyr>), which has been developed for the stock assessment of Japanese domestic fisheries resources. In particular, we used the functions for future projection and the calculation of biological reference points in `frasyr`. The general equations of the forward calculation of the population dynamics are

$$N_{a,y}^i = \begin{cases} \frac{\hat{\alpha}SSB_y^i}{1 + \hat{\beta}SSB_y^i} \exp(\eta_{0,y}^i) & (a = 0) \\ N_{a-1,y-1}^i \exp(-M_{a-1} - F_{a-1,y-1}^i) \exp(\eta_{a,y}^i) & (0 < a < 6) \\ N_{a-1,y-1}^i \exp(-M_{a-1} - F_{a-1,y-1}^i) \exp(\eta_{a,y}^i) + N_{a,y}^i \exp(-M_a - F_{a,y}^i) \exp(\eta_{a,y}^i) & (a = 6+) \end{cases}$$

where  $\hat{\alpha}$  and  $\hat{\beta}$  are stock recruitment parameters estimated by SAM,  $N_{a,y}^i$  is the number of fish in year  $y$  and age  $a$  at  $i$ th iteration,  $F_{a,y}^i$  is fishing mortality coefficient in year  $y$  and age  $a$  at  $i$ th iteration,  $\eta_{a,y}^i \sim N(0, \hat{\omega}^2)$  where  $\hat{\omega}^2$  is the variance of process error at recruitment estimated by SAM, and  $SSB_y^i$  is SSB defined as  $\sum_{a=0}^6 N_{a,y}^i w_{a,y} g_{a,y}$ . The equations are generally applied from the end year of the stock assessment period with the initial conditions of  $N_{a,2022}^i = \hat{N}_{a,2022}$  in B1 and B2 and  $N_{a,2023}^i = \hat{N}_{a,2023}$  in S7 and S8, where  $\hat{N}_{a,y}$  is the point estimates by SAM. The fishing mortality in the initial and future years is assumed as  $F_{a,2022}^i = \hat{F}_{a,2022}$  ( $\hat{F}_{a,y}$  is point estimates by SAM),  $F_{a,2023}^i = F_{cur}$ , and  $F_{a,y}$  ( $y > \text{FY2023}$ ) is determined by future harvesting scenarios. The future biological parameters of  $w_{a,y}$  and  $m_{a,y}$  are given according to the scenarios described above (bio2020 or bio2010) for  $y \geq \text{FY2023}$ .

The future harvesting scenario was predetermined as a total catch ( $CC$ ) ranging from 50 to 400 thousand tons (along with a  $CC=0$  scenario, Table 5). When catch number at age  $C_{a,y}^i$  in year  $y$  and age  $a$  is calculated with the Baranov catch equation as  $C_{a,y}^i = \frac{F_{a,y}^i}{F_{a,y}^i + M_a} (1 - \exp(-F_{a,y}^i - M_a)) N_{a,y}^i$ ,  $F_{a,y}^i$  is equal to be  $x_y^i F_{cur}$  with the same selectivity as  $F_{cur}$  and adjustment factor of  $x_y^i$  that is determined to satisfy the equation of  $\sum_{a=0}^{6+} w_a C_{a,y}^i = CC$ . If we cannot find  $x_y^i$  to satisfy the equation because of too small number of fishes, we took the smaller of the two numbers,  $x_i = \exp(10)$  or fishing mortality corresponding to 99% of total catches when  $x_i = \exp(100)$ . The stochastic simulations were conducted 5,000 times for each model and scenario.

## STOCK ASSESSMENT RESULTS

### 5.1 Base case model results

TWG CMSA agreed to select S28-ProcEst as a base case scenario because of the better diagnostics than the model only with recruitment process error and agreement of data usage up to FY2022. The chub mackerel stock in the NWPO has experienced large changes in biological parameters over the time period of the model. The main temporal changes are a recent decrease in maturity at age, along with a recent decrease in the weight at age, both of which were observed to change over the model time period to cause temporal changes of biological reference points. Fixed Effects parameter estimates are shown in Table 2, and the management related quantities are listed in Table 3.

### **5.1.1 Parameter estimates**

The estimated fixed effects parameters are shown in Tables 2 for S28-ProcEst (the other representative runs B2-Mage (B2), S32-JP23, and S34-PRocEst23 are shown in Appendix 2.). For all parameters, the final gradient values were very close to 0 and the SE values were less than 3. Correlation coefficients from the covariance matrices of the fixed effects parameters showed that  $q_k$  and  $b_k$  for age-0 and age-1 fish in the Japanese trawl surveys were highly negatively correlated (Figure 8). In addition, the parameters  $\alpha$  and  $\beta$  of the Beverton-Holt stock-recruitment relationship were highly positively correlated, however since  $\beta$  can affect the estimation of  $\alpha$  and vice versa, this is to be expected (Beverton and Holt 1957). These strong correlations are explained by the scales of abundance and SSB (see Discussion for details), and there were no problems with model convergence, as indicated by the absolute values of the final gradients approaching zero and sufficiently small SEs for these parameters (Table 2 and Appendix 1). The nonlinear coefficients in the Japanese trawl survey indices were estimated in the range of 1.6-2.4 (Table 2), suggesting that they have a tendency toward hyperdepletion (Figure 9).

### **5.1.2 Time-series estimates for abundances and fishing impacts**

Since 1970, total biomass, SSB, and recruitment of chub mackerel have fluctuated widely from high to low to high (Table 4 and Figure 10). Specifically, stock levels were high in the 1970s, but declined in the 1980s, and stock levels were maintained at fairly low levels from the 1990s to the early 2000s; stock levels gradually recovered in the late 2000s and increased rapidly after the occurrence of the strong year class in FY2013. However, total biomass and SSB during the most recent 10-year period (FY2013-2022) did not reach the same high level as in the 1970s. In SAM, the estimated catch (sum product of estimated age-specific catch and age-specific weight) and the observed catch (sum product of observed age-specific catch and age-specific weight) do not match because of the assumption of observational error in the age-specific catch numbers, but the difference between these values was small, except in some years. Exploitation rate (estimated catch biomass / total biomass) and mean F remained constant, with some fluctuations, until the 2000s, but decreased thereafter. The overall trajectory, scale and trend of the runs were quite similar across all representative scenarios. The inclusion of the FY2023 data in the scenarios S32-JP23, and S34-PRocEst23 led to lower estimated SSB in the terminal years and higher F and exploitation rate since approximately 2019. Recruitment was higher in these scenarios as well over the years of FY2013-2015. In recent years, SSB had been increasing since the beginning of the 2010s, but after peaking in FY2017 it declined, slightly for the B2-Mage scenario, and significantly for the other three scenarios.

### **5.1.3 Stock-recruitment relationship**

The estimated Beverton-Holt stock-recruitment relationship is shown in Figure 11. In the final base case scenario (S28-PRocEst), recruitment tended to increase in proportion to the increase in SSB,

suggesting that the density-dependent effect in the stock-recruitment relationship is little found in the historical range of estimated SSB for chub mackerel. SD of recruitment variability was 0.8 S28-Proc-Est, 0.75 for B2-Mage (B2), 0.74 for S32-JP23, and 0.79 for S34-PRocEst23.

## **5.2 Model diagnostics**

### **5.2.1 Residual plots**

Observation errors in catch number by age were largest for young and old age groups and smallest for intermediate age group 3 fish (Figures 12 and 13, see also Table 2). The time-series trend of the residuals was weak.

For abundance index values, observation error was largest for the Japanese trawl survey indices and smallest for the spawning egg index (Figure 14). The summer and autumn age-0 indices tended to have positive residuals in recent years (Figure 15).

Process errors in  $\log(N)$  for age-0 fish (deviation from the stock-recruitment relationship) were highly variable, but those for age-1 fish and older were reasonably variable (Figure 16, left). Since the occurrence of the strong year class in 2013, process errors for age-0 fish have been positive, except for 2014 and 2019. After the 2018 class, the process errors for age-1 fish and older were mostly negative.

Process errors for  $\log(F)$  (deviation from random walk) were larger in ages 0 and 1 than in the other ages (Figure 16, right). The pattern of random walks for each age was very similar, as evidenced by the very high correlation coefficient of 0.97 between the closely adjacent ages (Table 2).

### **5.2.2 Retrospective analysis**

In the retrospective analysis, recruitment was slightly positively biased for 2018 and, as a result, total biomass also tended to be overbiased (i.e., revised downward as the data were updated) (Figure 17). Mohn's rho values for SSB were close to zero, and had small positive biases for the last three years; the mean F in 2017 tended to be higher.

In the retrospective forecasting, the retrospective bias for recruitment was reduced due to the loss of positive bias for the 2018 and 2020 year-classes (since they are predicted from the stock-recruitment relationship and therefore no longer takes extreme values), but retrospective patterns for other state variables were similar to those when no future forecasting was done (Figure 18).

### **5.2.3 Leave-one-out index analysis**

The LOO index analysis showed that the abundance and exploitation rate did not change much regardless of which index was removed, indicating that the stock estimates are very robust (Figure

19). A closer look shows that the SSB estimates increased slightly in recent years when the dipnet fishery CPUE and spawning egg indices were excluded, and the SSB estimates decreased slightly when the age-0 and age-1 fish indices were excluded. This may be because the age-0 and age-1 fish indices have had high values in many years since 2013 and have a role in increasing SSB, whereas the two SSB indices have tended to decrease slowly in recent years and thus decrease SSB (Figure 19). Although there were conflicting trends in the indices for age 0-1 fish and the indices for SSB, the effect of a single index was small because there were multiple indices for young and old fish, respectively. The influence of the Chinese purse seine CPUE was small.

#### ***5.2.4 Evaluation of the One Step Ahead residuals***

OSA residuals were calculated for the age composition data the indices of abundance (Figures 20 and 21). The largest age composition residual was in the first year of the model for age 2 fish. In general, the age composition OSA residuals tended to be small and lacked any consistent patterning. The OSA residuals from the fits to the indices of abundance showed a similar lack of patterning and did not suggest systematic model deficiencies such as underfitting or overfitting. Overall, the OSA residuals indicate no issues with the model's performance. The residuals are appropriately centered around zero and show no significant persistent patterning, the quantile plot (Figure 22) indicates a good fit.

### **5.3 Reference points**

#### ***5.3.1 Historical change in spawning potential of SPR<sub>0</sub>***

SPR<sub>0</sub> has changed annually according to the biological parameters that changed each year (Figure 23). In particular, SPR<sub>0</sub> decreased significantly from FY2015 onwards, reaching a minimum in 2019 and remaining low during the FY2020-2023 period. The average SPR<sub>0</sub> for the 2020s (FY2020-2022) was 165 g in scenario S28-ProcEst which is about half of the SPR<sub>0</sub> averaged for other decades.

#### ***5.3.2 MSY-based reference points***

In the stock-recruitment relationship estimated by the base case model (S28-ProcEst), there was almost no density dependence effect within the range of spawning stock biomass and recruitment numbers observed in past, so the SSB<sub>0</sub> and SSB<sub>MSY</sub> calculated based on this stock-recruitment relationship are extrapolated values that greatly exceed the past recruitment and spawning stock biomass (Fig. 10). Furthermore, since the productivity of this stock, represented by SPR<sub>0</sub>, has changed significantly over the years as seen in Fig. 6, the estimated values of SSB<sub>0</sub> and SSB<sub>MSY</sub> (even under the single stock-recruitment relationship) varied greatly depending on which year's biological parameters were used. For example, the SSB<sub>MSY</sub> estimated using the biological parameters from 2016-2022 was about half of the estimate by using the biological parameters from all of the years (Table 3). In addition, the MSY reference points differed greatly among the different

model specifications owing to the extreme extrapolation (Table ANNEX 2).

#### **5.4 Future projections**

The future projection under a constant catch scenario has a much wider prediction interval for future spawning biomass than the projection with a constant  $F_{cur}$  (Figure 24). Because there is a trade-off between fluctuations in stock abundance and catch, it is impossible to avoid these high fluctuations in stock abundance under the scenario of constant catches. Therefore, in future projections, it is necessary to focus not only on the average values of SSB but also on the lower confidence interval (e.g. lower 5%) of SSB to evaluate the probability of the future SSB falling below a level below which we do not want to fall.

The future projection under a constant catch scenario has a very different outlook depending on whether the biological parameters are based on the recent years (FY2016-2022) or all years (FY1970-2022) (Figures 25 and 26).

The 5th percentile of the future SSB and average catch and SSB were compared among various harvesting scenarios (Figures 25 and 26). The results of the projections from the base case differed greatly based on choice of the biological parameters. These results suggest that the future projection of the stock depends greatly on the assumption of future biological parameters, whether or not the delay in growth and maturation will continue in the future. In detail, Table 5 shows the probabilities that future SSB is above the estimated SSB in FY2022 based on the results of 5000 times stochastic projections.

## **DISCUSSION**

In this working paper, a stock assessment of Northwestern Pacific chub mackerel was conducted using SAM with existing agreed data. SSB gradually decreased from the high period in the 1970s to the 1980s, and SSB remained at a low level from the 1990s to the early 2000s; the beginning of the decreasing trend in SSB in the 1980s can be explained by a reversal from the positive recruitment residuals that often appeared until FY1977 to negative residuals that often appeared thereafter, shown in the plot for process errors (Figure 18). High fishing mortalities were found since FY1986 through the 1990s, causing the extremely low levels of SSB for this time period. In the late 2000s, SSB gradually recovered as fishing pressure slowly decreased, and after the occurrence of the strong year class in FY2013. Although SSB recovered in the 2010s, it was still lower than in the late 1970s.

In SAM, it is possible to account for process errors for age-specific stock numbers, but we assumed that process errors after recruitment (for age-1 fish and older) would be much smaller. This is due to the difficulty of interpreting process errors for age-1 and older fish and the complexity of

population dynamics, which makes it difficult to predict the future. The results of relaxing this assumption are presented in a separate working paper (NPFC-2024-TWG CMSA09-WP04).

SAM requires estimating the process error in age-specific  $F$  and the observation error in age-specific catch number. Since attempting to calculate these standard deviations (SDs) by age may lead to the failure of model convergence and overfitting, model selection based on AIC was performed. As a result, the observation errors in age-specific catch numbers were common for age-5 fish in the selected model, showing high SD for young and old age groups and low SD for intermediate age groups (minimum for 3-year-old fish). On the other hand, the process error for  $F$  was estimated to be larger for 0-1 year old fish than for older fish, suggesting that the change in fishing pressure is greater for younger age groups.

Because it is known that estimating nonlinearities in stock abundance index in an age-structured model improves model performance, such as reducing retrospective bias (Hashimoto et al. 2018), we examined whether to estimate nonlinear coefficients. We showed that AICs were significantly reduced in models with nonlinear coefficients estimated for age-0 and age-1 fish indices from the Japanese trawl surveys. AIC was only slightly reduced in the model with estimated nonlinear coefficients for the spawning egg index, but since the estimation of nonlinear coefficients can make the model estimation unstable, a simpler model assuming linearity for spawning egg was chosen here as the model for the base case scenarios. Nonlinear coefficients were estimated larger than 1 for the Japanese trawl survey indices and had a tendency toward hyperdepletion. The reason for this is not clear, but it may be because the survey was conducted at a particular time of year, and thus the variation in the index values is larger than the actual variation in recruitment. In addition, there was a strong negative correlation between this nonlinear coefficient and the proportionality constant, which can be explained by the relationship between the intercept and slope in the simple regression. The relationship between the index value and the number of stock tails is expressed as  $\log_{10}(I_{(k,y)}) = \log_{10}(q_k) + b_k \log_{10}[(N_{(a,y)})] + \varepsilon_{(k,y)}$ . In this equation  $\log_{10}(q_k)$  and  $b_k$  correspond to the intercept and slope, respectively, in the linear regression model having  $\log_{10}(I_{(k,y)})$  as the response variable and  $\log_{10}[(N_{(a,y)})]$  as the explanatory variable. In the current specification,  $N_{a,y}$  has very large values (in millions) and is far from zero in the range of  $\log_{10}[(N_{(a,y)})]$ . Therefore, a small difference in slope  $b_k$  can greatly change the value of intercept  $\log_{10}(q_k)$ , resulting in a high correlation between these parameters, and relatively large estimation errors and confidence intervals for  $\log_{10}(q_k)$ . As a test, when the unit of  $N_{a,y}$  was made larger (1 billion fish) and  $\log_{10}[(N_{(a,y)})]$  was made closer to zero, the correlation became weaker and the estimation error smaller, but the estimated parameters remained the same except for  $\log_{10}(q_k)$ . Thus, the high correlation between the nonlinear coefficients and the proportionality constant and the relatively larger SE of the proportionality constant are considered to be a matter of abundance scale and not a threat to estimability or identifiability for these

parameters.

Retrospective analysis revealed a positive bias in recruitment and total biomass. This is because recent high recruitment (especially for the 2018 and 2020 classes), elevated by high recruitment index values, has been revised downward by low catch numbers and low SSB index values. In other words, there is a conflict between the age-0 and age-1 fish indices, which have been high since FY2013, and the SSB indices, which have been declining in recent years. The LOO index analysis showed that the effect of excluding one index was small, suggesting that the age-0 and age-1 fish indices have similar information to each other and the two SSB have similar information to each other. In a nutshell, this situation means that the high recruitment expected in the survey has disappeared, never showing up as catch or SSB. Unfortunately, the reason for this curious phenomenon is unknown at this moment.

In this stock, the choice of the stock-recruitment relationship is a difficult issue. In this case, we used the Beverton-Holt model, which is the simplest model and fits well with chub mackerel, but recruitment shows almost proportional relationship with SSB and the density-dependent effect is very small. Therefore, the uncertainty of the parameters related to the density dependence was large. Such low density-dependent effects and large uncertainties greatly affect the calculation of biological reference points and future projections (NPFC-2024-TWG CMSA09-WP05). Estimating stock recruitment relationships in an assessment model is inherently challenging due to the complex interplay of biological and environmental factors that influence fish population dynamics. Variability in recruitment can result from factors such as fluctuating environmental conditions, changes in predator-prey interactions, and genetic diversity within the stock (Myers, 1998). Additionally, data limitations, such as insufficient time series data, measurement errors, and biases in sampling methods, further complicate the estimation process (Maunder & Deriso, 2013). These difficulties are exacerbated by the non-linear and often unpredictable nature of recruitment, making it hard to develop reliable models that accurately capture the true dynamics of fish populations (Hilborn & Walters, 1992). Another possible stock-recruitment relationship is the use of the hockey-stick model, but it cannot be applied as is in SAM using TMB, where optimization is performed by automatic differentiation. From the viewpoint of stock assessment and management for chub mackerel, it will be necessary to consider how the stock-recruitment relationship should be characterized in the future.

This is the first chub mackerel stock assessment in NPFC since the TWG CMSA was established in 2017. Although it has taken a very long time to select the stock assessment model by simulation, the data and model to be used this time have been determined with the agreement of all Members. The stock of chub mackerel was increasing in the 2010s, but the situation has changed since the beginning of the 2020s, and at least the period of increase is considered to have passed. Furthermore,

the abundance indices for SSB in 2023 for Japan, which was not used in the base case analysis, is significantly reduced (Figure 1), and a sensitivity analysis using these indices would reduce SSB more recently than in the base case (NPFC-2024-TWG CMSA09-WP04), so this SSB in this working paper may also be an overestimate. Although there are still issues to be resolved, such as retrospective bias and highly uncertain parameters, it is hoped that the results of the stock assessment in the base case scenario while taking into account the results of sensitivity analysis will provide effective scientific advice for the sustainable use of chub mackerel in the Northwestern Pacific Ocean.

The chub mackerel stock in the NWPO has experienced large changes in biological parameters over the time period of the model. The main temporal changes are a recent decrease in maturity at age, along with a recent decrease in the weight at age, both of which were observed to change over the model time period to cause temporal changes of biological reference points. Maximum sustainable yield (MSY)-based reference points are highly variable over the time series of the assessment because the weight- and maturity- at age of chub mackerel has varied widely (Figures 3 and 4), which impacts the productivity of the stock. Unfished spawning biomass per recruit (SPR0) represents the theoretical equilibrium productivity per fish assuming no fishing. SPR0 has varied remarkably over time (Figure 5).

In addition, as there is little recruitment compensation in the stock-recruitment relationship within the range of historically observed SSB and recruitment (Figure 8), estimates of biomass-based MSY reference points are extreme explorations that are highly sensitive to model configuration.

Because of the above reasons, commonly used reference points such as MSY-related or SPR-related reference points vary over time and are uncertain, and are potentially misleading with respect to stock status. For example, the MSY based reference points have varied by the assumption of biological parameters to be used (Table 31). The exploitation rates corresponding to the MSY as 10% when assuming biological parameters during the whole historical period, but it dropped to 5% when using the most recent 7 years biological parameters.

As such, at this time, the TWG CMSA does not recommend the use of MSY-based reference points for management advice. Instead, the TWG CMSA provides information of current estimates of chub mackerel SSB and F (average FY2020-2022) relative to the minimum, 25th, 50th, 75th and maximum value of the SSB and F values over the entire time period (FY1970-2022; Table 6). Values relating to the most recent time period (FY2016-2022) are also shown in order to describe the current stock relative to recent conditions.

The abundance estimated by the Japanese egg survey and the CPUEs from the Japanese dipnet and

Russian trawl decreased over recent years, showing that they were simultaneously reduced to about half the level of recent years in 2023. The run of the stock assessment model including Japanese CPUE for FY2023 shows substantial decline in biomass and SSB in FY2022 and further in FY2023 and higher fishing mortality in the last few years (Figure 7).

## **SUMMARY**

### **Exploitation status**

Estimated rates of exploitation (fishing year catch/fishing year total biomass) time series generally fluctuated between 5 and 20% and followed the estimated  $F_s$  over time, with annual removal rates that ranged from roughly 10 to 30% over the modeled timeframe (Figure 9), with some larger annual removals in excess of 40%.

### **Harvest Recommendations**

Given the uncertainty in biological parameters in future, which have a large impact on the projection results, the TWG CMSA considers it is not appropriate to provide long-term harvesting recommendations at this time. A short-term (towards 2028) projection was undertaken to assess the effects of varying catch levels, ranging from 50 to 400 thousand tons, based on the most recent seven years' biological data (Figure 9) and the entire time series of biological data (Figure 10) for management considerations. Projections based on the most recent seven years' biological data showed that  $F_{cur}$  leads to future constant decline of SSB and it is necessary to reduce current fishing mortality (Table 3).

### **Data and Research needs**

The assessment results, including projections, are dependent on biological parameters and processes which are uncertain. Therefore, future studies should be focused on collecting and analyzing biological information, e.g., maturity-at-age, weight-at-age, which would improve the assessment. Fisheries-dependent data, such as fleet-specific catch-at-age, are also critical to develop Member-specific fishing fleet and age-specific abundance indices.

A critically important recommendation that should be carried out in 2-3 years is to develop a harvest control rule specific to this stock via an MSE process. This HCR should be dynamic and able to adjust annual total catches depending on the stock abundance as well as the target and limit reference points. During the process of the development of MSE, uncertainties in parameter estimates, time-varying or density-dependent biological parameters, and stock-recruitment assumptions should be considered.

Timely collection of biological information and further research on biological parameters and processes, including the effect of environment and climate change, are critically important to facilitate the accurate estimation of reference points.

## REREFENCES

- Beverton, R. J. H., & Holt, S. J. (1957). On the dynamics of exploited fish populations. Chapman and Hall, London, Fish and Fisheries Series No. 11, fascimile reprint 1993.
- Chernienko, I. and Chernienko E. (2024). Standardized CPUE of Chub mackerel (*Scomber japonicus*) caught by the Russia's trawls fishery up to 2023. NPFC-2024-TWG CMSA09-WP11.
- Hashimoto, M., Okamura, H., Ichinokawa, M., Hiramatsu, K., and Yamakawa, T. (2018). Impacts of the nonlinear relationship between abundance and its index in a tuned virtual population analysis. *Fisheries Science*, 84(2), 335–347. <https://doi.org/10.1007/s12562-017-1159-0>
- Hilborn, R., & Walters, C. J. (1992). *Quantitative Fisheries Stock Assessment: Choice, Dynamics, and Uncertainty*. Springer.
- Ichinokawa M., Nishijima S., Oshima K., and Rice J. (2024) Biological reference points and future projections with the results of stock assessment for the Pacific chub mackerel. NPFC-2024-TWG CMSA09-WP05.
- Iizuka, K. (2002). Stock and fishing grounds of chub mackerel in 1960s and 1970s. *Gekkan Kaiyo*, 34, 273–279 (in Japanese).
- Ishida, K., Nishijima, S., Ichinokawa, M. and Yukami, R. (2024). Standardizing monthly egg survey data as an abundance index for spawning stock biomass of chub mackerel in the Northwest Pacific. NPFC-2024-TWG CMSA09-WP07.
- Kamimura, Y., Taga, M., Yukami, R., Watanabe C. and Furuichi S. (2021). Intra- and inter specific density dependence of body condition, growth, and habitat temperature in chub mackerel (*Scomber japonicus*). *ICES J. Mar. Sci.*, 78, 3254-3264.
- Kanamori, Y., Takasuka, A., Nishijima, S., and Okamura, H. (2019). Climate change shifts the spawning ground northward and extends the spawning period of chub mackerel in the western North Pacific. *Marine Ecology Progress Series*. 624, 155-166. <https://doi.org/10.3354/meps13037>
- Kato, M. and Watanabe, C., (2002). Maturation, spawning and feeding habitat of chub and blue mackerels. *Gekkan Kaiyo*, 34, 366–272 (in Japanese).
- Kristensen, K., Nielsen, A., Berg, C. W., Skaug, H., and Bell, B. M. (2016). TMB: Automatic differentiation and laplace approximation. *Journal of Statistical Software*, 70(5), 1–21. <https://doi.org/10.18637/jss.v070.i05>
- Liu, Z. and Ma, Q. (2024). Abundance and distribution estimation for chub mackerel and blue mackerel in the Northwest Pacific based on scientific research surveys. NPFC-2024-TWG CMSA08-IP03.
- Ma Q., Liu Z., Zhang H., and Tian S. (2024) Growth and mortality estimation for chub mackerel based on Chinese data in the Convention Area of NPFC. NPFC-2024-TWG CMSA08-WP12.
- Ma, Q., Liu, B. and Dai, L. (2023) Overview surveys from 2021 to 2023 by Chinese research

- vessel "Song Hang" in the NPFC convention area. NPFC-2023-SC08-WP12. 10pp.  
<https://www.npfc.int/system/files/2023-12/NPFC-2023-SC08-WP12%20Chinese%20surveys%202021-2023%20by%20Song%20Hang%20in%20NWP.pdf>
- Manabe, A., Higashiguchi, K., Yukami, R. and Oshima, K. (2024a). The data description for the base case stock assessment of chub mackerel *Scomber japonicus* in the northwestern Pacific Ocean. NPFC-2024-TWG CMSA09-WP01.
- Manabe, A., Yukami, R., Ichinokawa, M., Zhang, H., Chernienko, I., & Chernienko, E. (2024b). Catch at length, age-length key, and catch at age of chub mackerels (*Scomber japonicus*) caught in the northwestern Pacific Ocean by China, Japan, and Russia. NPFC-2024-TWG CMSA08-WP15.
- Maunder, M. N., & Deriso, R. B. (2013). A stock–recruitment model for highly fecund species based on temporal and spatial extent of spawning. *Fisheries Research*, 146, 96-101.
- Murayama, T., Mitani, I., Aoki, I. (1995) Estimation of the spawning period of the Pacific mackerel *Scomber japonicus* based on the changes in gonad index and the ovarian histology. *Bull .Jpn. Soc. Fish. Oceanogr.* 59, 11-17 (in Japanese, with English abstract).
- Myers, R. A. (1998). When do environment-recruitment correlations work? *Reviews in Fish Biology and Fisheries*, 8(3), 285-305.
- Nielsen, A., and Berg, C. W. (2014). Estimation of time-varying selectivity in stock assessments using state-space models. *Fisheries Research*, 158, 96–101.  
<https://doi.org/10.1016/j.fishres.2014.01.014>
- Nishijima, S., Kamimura, Y., Yukami, R., Manabe, A., Oshima, K., and Ichinokawa, M. (2021). Update on natural mortality estimators for chub mackerel in the Northwest Pacific Ocean. NPFC-2021-TWG CMSA04-WP05.
- Nishijima, S., Suzuki, S., Ichinokawa, M., and Okamura, H. (2019). Integrated multi-timescale modeling untangles anthropogenic, environmental, and biological effects on catchability. *Canadian Journal of Fisheries and Aquatic Sciences*, 76(11), 2045–2056.  
<https://doi.org/https://doi.org/10.1139/cjfas-2018-0114>.
- Nishijima, S., and Ichinokawa, M. (2023). On the description and flexibility of state-space assessment model. NPFC-2023-TWG CMSA07-WP07.
- Nishijima, S., Kamimura, Y., Ichinokawa, M. and Yukami, R. (2024a). Standardized abundance index for recruitment of chub mackerel from Northwest Pacific summer surveys up to 2023. NPFC-2024-TWG CMSA08-WP06 (Rev. 1).
- Nishijima, S., Yukami, R. and Ichinokawa, M. (2024b). Standardized CPUE of Japanese commercial dip-net fishery targeting spawners of chub mackerel in the Northwest Pacific up to 2023. NPFC-2024-TWG CMSA08-WP03.
- Nishijima, S., Ichinokawa, M. and Yukami, R. (2024c). Revised Standardized Abundance Indices for Ages 0 and 1 Fish of Chub Mackerel from Northwest Pacific Autumn Surveys up to

2023. NPFC-2024-TWG CMSA09-WP06.

- Nishijima, S., Ichinokawa, M., Manabe A., Oshima K., and J. Rice (2024d) Base case stock assessment for chub mackerel in Northwest Pacific Ocean in 2024. NPFC-2024-TWG CMSA09-WP03 (Rev. 1).
- Oozeki, Y., A. Takasuka, H. Kubota and M. Barange (2007) Characterizing spawning habitats of Japanese sardine (*Sardinops melanostictus*), Japanese anchovy (*Engraulis japonicus*), and Pacific round herring (*Etrumeus teres*) in the northwestern Pacific. CalCOFI Reports, 48, 191-203.
- Pozdnyakov S. E., Vasilenko A.V. 1994. Distribution, migration routes and helminth fauna of the Japanese mackerel *Scomber japonicus* in the north-western part of the Pacific Ocean // Vopr. ichthyol. T. 34. №1, C. 22-34.
- Pyrkov V.N., Solodilov A.V., Degaj A.Yu. Sozdanie i vnedrenie novyh sputnikovyh tekhnologij v sisteme monitoringa rybolovstva // Sovremennye problemy distancionnogo zondirovaniya Zemli iz kosmosa. — 2015. — T. 12, No 5. — S. 251–262.
- Rose, G., and Kulka, D. (1999). Hyperaggregation of fish and fisheries: how catch-per-unit-effort increased as the northern cod (*Gadus morhua*) declined. Canadian Journal of Fisheries and Aquatic Sciences, 56(S1), 118–127. <https://doi.org/10.1139/cjfas-56-S1-118>
- Shi, Y., Zhang, H. and Han, H. (2024). Standardized CPUE of Chub mackerel (*Scomber japonicus*) caught by the China's lighting purse seine fishery up to 2022. NPFC-2024-TWG CMSA09-WP13 (Rev. 1).
- Thorson, J. T., and Kristensen, K. (2016). Implementing a generic method for bias correction in statistical models using random effects, with spatial and population dynamics examples. Fisheries Research, 175, 66–74. <https://doi.org/10.1016/j.fishres.2015.11.016>
- Technical Working Group on Chub Mackerel Stock Assessment (2023) 7th Meeting Report. NPFC-2023-TWG CMSA07-Final Report. 53 pp. (Available at [www.npfc.int](http://www.npfc.int))
- Technical Working Group on Chub Mackerel Stock Assessment. (2024) 8th Meeting Report. NPFC-2023-TWG CMSA08-Final Report. 32 pp. (Available at [www.npfc.int](http://www.npfc.int))
- Trijoulet, V., Albertsen, C. M., Legault, C. M., Miller, T. J., Kristensen, K., & Nielsen, A. (2023). Model validation for compositional data in stock assessment models: Calculating residuals with correct properties. Fisheries Research. 257, 106487
- Usami, S. (1973) Ecological studies of life patten of the Japanese mackerel *Scomber japonicus* HOUTTUYN on the adult of the Pacific subpopulation. Bull. Tokai. Reg. Fish. Res. Lab., 76, 71-178 (in Japanese, with English abstract).
- Vasilenko A.V. Intraspecific structure and commercial value of Japanese mackerel populations. 1990. Avtoref. diss.... candidate of biological sciences. Vladivostok, 24 p.
- Watanabe, T. (1970) Morphology and ecology of early stages of life in Japanese common mackerel, *Scomber japonicus* HOUTTUYN, with special reference to fluctuation of population. Bull. Tokai. Reg. Fish. Res. Lab., 62, 1-283 (in Japanese, with English abstract).

- Watanabe, C., Hanai, T., Meguro, K., Ogino, R., Kimura, R. (1999) Spawning biomass estimates of chub mackerel *Scomber japonicus* of Pacific subpopulation off central Japan by a daily egg production method. Bull. Jpn. Soc. Sci. Fish., 65(4),695-702 (in Japanese, with English abstract).
- Watanabe, C. and A. Yatsu (2004) Effects of density-dependence and sea surface temperature on inter-annual variation in length-at-age of chub mackerel (*Scomber japonicus*) in the Kuroshio-Oyashio area during 1970–1997. Fish. Bull., 102, 196-206.
- Watanabe, C. and A. Yatsu (2006) Long-term changes in maturity at age of chub mackerel (*Scomber japonicus*) in relation to population declines in the waters off northeastern Japan. Fish. Res., 78, 323-332.
- Watanabe, C. (2010). Changes in the reproductive traits of the Pacific stock of chub mackerel *Scomber japonicus* and their effects on the population dynamics. Bull. Jpn. Soc. Fish. Oceanogr., 76, 46-50.
- Yamada, T., Aoki, I., Mitani, I. (1999) Spawning time, spawning frequency and fecundity of Japanese chub mackerel, *Scomber japonicus* in the waters around the Izu Islands, Japan. Fisheries Reserch., 38, 83-89.
- Yukami, R., Nishijima, S., Kamimura, Y., Isu, S., Furuichi, S., Watanabe, R., Higashiguchi, K., Saito, R. and Ishikawa, K. (2024). Stock assessment and evaluation for Chub Mackerel Pacific stock (fiscal year 2023). FRA-SA2024-AC005. In Marine fisheries stock assessment and evaluation for Japanese waters (fiscal year 2023/2024). Japan Fisheries Agency and Fisheries Research and Education Agency of Japan. Tokyo, 71pp. [https://abchan.fra.go.jp/wpt/wp-content/uploads/2024/03/details\\_2023\\_05.pdf](https://abchan.fra.go.jp/wpt/wp-content/uploads/2024/03/details_2023_05.pdf)
- Zhang, H., Han, H., Sun, Y., Xiang, X., Li, Y. and Shi, Y. (2023) Data description on fisheries bycatch in the chub mackerel fisheries in China. NPFC-2023-TWG CMSA07-WP12 (Rev. 1). 3pp. <https://www.npfc.int/system/files/2023-09/NPFC-2023-TWG%20CMSA07-WP12%28Rev%201%29%20Data%20description%20on%20fisheries%20bycatch%20in%20CM%20fisheries%20in%20China.pdf>

## TABLES

Table 1

The list of mathematical notations for SAM, including the symbol used, its type (Index, Data, random effects: RE, fixed effects: FE, and derived quantities: DQ, and its description).

Symbol	Type	Description
$a$	Index	Age class (from 0 to 6+)
$y$	Index	Fishing year (from 1970 to 2022)
$k$	Index	Fleet ID for abundance index (from 1 to 6)
$C_{a,y}$	Data	Observed catch number at age $a$ in a year $y$
$w_{a,y}$	Data	Stock weight at age $a$ in a year $y$ (also used as catch weight for simplicity)
$g_{a,y}$	Data	Maturity at age $a$ in a year $y$
$M_{a,y}$	Data	Natural mortality coefficient at age $a$ in a year $y$
$N_{a,y}$	RE	Number at age $a$ in a year $y$
$F_{a,y}$	RE	Fishing mortality coefficient at age $a$ in a year $y$
$\omega_a$	FE	SD for the process error in number at age $a$
$\sigma_a$	FE	SD for the process error in F at age $a$
$\rho$	FE	Correlation coefficient in MVN of F random walk between adjacent age classes
$\tau_a$	FE	SD for the measurement error in catch at age $a$
$q_k$	FE	Catchability coefficient for abundance index $k$
$v_k$	FE	SD for the measurement error in abundance index $k$
$b_k$	FE	Nonlinear coefficient for abundance index $k$
$\alpha$	FE	Slope of stock-recruitment relationship at the origin
$\beta$	FE	Strength of density dependence in stock-recruitment relationship
$\hat{C}_{a,y}$	DQ	Predicted catch number at age $a$ in a year $y$
$\hat{s}_{a,y}$	DQ	Selectivity at age $a$ in a year $y$

Table 2

Fixed-effect parameters (FE), their maximum likelihood estimates (MLE), their standard errors (SE), their final gradients, symbols including the information on age class and index fleet, and unlinked value (inverse link function of MLE) in the selected model (see Table 4) under Scenario S28-ProcEst.

FE	MLE	SE	Gradient	Unlinked value	Symbol
logQ	-14.65	2.15	0.0000	4.36E-07	$q_1$
logQ	-15.54	2.25	0.0001	1.79E-07	$q_2$
logQ	-10.10	1.68	0.0000	4.12E-05	$q_3$
logQ	-0.23	0.14	-0.0001	0.7926	$q_4$
logQ	-2.50	0.17	-0.0001	0.0818	$q_5$
logQ	-4.85	0.24	0.0000	0.0078	$q_6$
logB	0.80	0.12	0.0001	2.2251	$b_1$
logB	0.89	0.11	0.0025	2.4281	$b_2$
logB	0.54	0.13	0.0003	1.7182	$b_3$
logSdLogFsta	-0.89	0.18	0.0000	0.4101	$\sigma_{0-1}$
logSdLogFsta	-1.24	0.17	0.0000	0.2894	$\sigma_{2-6+}$
logSdLogN	-0.22	0.13	0.0001	0.7993	$\omega_0$
logSdLogN	-1.06	0.29	0.0000	0.3475	$\omega_1$
logSdLogN	-1.31	0.22	-0.0001	0.2698	$\omega_{2-4}$
logSdLogN	-1.27	0.60	0.0000	0.2814	$\omega_{5-6+}$
logSdLogObs	-0.41	0.11	0.0001	0.6624	$\tau_{0-1}$
logSdLogObs	-1.31	0.19	0.0000	0.2695	$\tau_{2-3}$
logSdLogObs	-0.90	0.17	0.0000	0.4067	$\tau_{4-5}$
logSdLogObs	-0.12	0.14	-0.0001	0.8842	$\tau_{6+}$
logSdLogObs	-0.27	0.23	0.0000	0.7603	$\nu_1$
logSdLogObs	-0.58	0.39	0.0000	0.5595	$\nu_2$
logSdLogObs	-0.33	0.23	0.0000	0.7166	$\nu_3$

logSdLogObs	-1.06	0.20	0.0000	0.3455	$v_4$
logSdLogObs	-0.56	0.17	0.0000	0.5721	$v_5$
logSdLogObs	-0.51	0.25	0.0000	0.5987	$v_{6+}$
rec_loga	-4.36	0.20	0.0001	0.0128	$\alpha$
rec_logb	-8.66	2.17	0.0000	0.0002	$\beta$
logit_rho	3.65	0.80	0.0000	0.9747	$\rho$

---

Table 3

Reference points for the base case scenario. Reference point values in this table are calculated by holding  $F_{current}$  the same for all calculations, but by varying the time period (either FY1970-FY2022 or FY2016-FY2022) over which the biological parameters are estimated. Refer to Glossary in the body of the assessment for the definitions. For the description of the biological parameters, see Table ANNEX 3.

Biological parameters used	FY2016- FY2022	FY1970-FY2022
	S28-ProcEst	S28-ProcEst
current%SPR	<b>28.3</b>	40.3
Fmed/Fcur	<b>0.478</b>	1.629
F0.1/Fcur	<b>1.344</b>	1.344
FpSPR.30.SPR/Fcur	<b>0.942</b>	1.498
FpSPR.40.SPR/Fcur	<b>0.673</b>	1.010
FpSPR.50.SPR/Fcur	<b>0.484</b>	0.696
FpSPR.60.SPR/Fcur	<b>0.342</b>	0.475
FpSPR.70.SPR/Fcur	<b>0.230</b>	0.311
$F_{MSY}/F_{cur}$	<b>0.258</b>	0.668
$B_{MSY}$	<b>9396.157</b>	17179.502
$SSB_{MSY}$	<b>2904.704</b>	6084.597
h	<b>0.358</b>	0.501
$SSB_0$	<b>7123.476</b>	17441.919
$SSB_{MSY}/SSB_0$	<b>0.408</b>	0.349
$F_{MSY}SPR$	<b>0.673</b>	0.511
MSY	436.8467	1713.406
$MSY/B_{MSY}$ (exploitation rate at MSY)	0.046	0.10

Table 4

Time series of estimates of total biomass, spawning stock biomass, recruitment, catch, and exploitation rate (catch/biomass) and their standard error (SE) under Scenario S28-ProcEst. The SEs were derived using the delta method.

Fishing year	Biomass (1000 MT)		SSB (1000 MT)		Recruitment (billion)		Catch (1000 MT)		Exploitation rate	
	Estimate	SE	MLE	SE	MLE	SE	MLE	SE	MLE	SE
1970	4,019	749	678.8	99.3	18.991	7.573	782.6	133.2	0.195	0.040
1971	4,547	771	863.4	124.8	18.903	7.061	842.6	123.2	0.185	0.033
1972	4,700	830	749.4	113.0	7.774	3.115	668.9	107.6	0.142	0.026
1973	4,224	659	937.1	137.5	7.824	2.953	780.2	110.7	0.185	0.030
1974	4,026	590	1253.2	191.4	12.672	4.621	846.4	115.6	0.210	0.034
1975	3,616	534	1070.1	158.5	19.237	6.994	867.6	119.3	0.240	0.037
1976	4,417	765	1046.2	147.7	21.643	7.800	708.0	98.0	0.160	0.029
1977	5,481	887	1200.8	163.1	17.649	6.316	947.0	139.1	0.173	0.029
1978	5,700	868	1322.2	171.6	12.187	4.505	1345.9	208.5	0.236	0.036
1979	3,563	485	1327.6	184.9	5.883	2.137	996.9	138.1	0.280	0.038
1980	2,228	302	1068.2	160.1	6.684	2.414	594.3	81.6	0.267	0.039
1981	2,392	409	734.4	116.7	8.037	2.880	404.5	58.2	0.169	0.032
1982	2,203	357	551.1	82.2	5.372	1.916	365.5	52.2	0.166	0.028
1983	1,795	261	517.9	71.7	5.721	2.020	374.6	51.4	0.209	0.032
1984	2,322	379	601.2	80.3	7.272	2.565	498.0	69.2	0.214	0.035

1985	1,978	299	480.7	62.3	6.889	2.416	468.5	70.6	0.237	0.036
1986	1,486	218	347.0	45.0	3.056	1.075	509.2	86.8	0.343	0.043
1987	937	124	322.3	41.3	1.206	0.431	362.0	55.8	0.386	0.041
1988	554	71	256.0	37.6	0.549	0.208	230.7	34.1	0.416	0.045
1989	313	48	137.0	20.5	0.446	0.166	102.9	15.1	0.329	0.051
1990	237	48	75.3	13.8	0.548	0.209	32.4	4.9	0.137	0.030
1991	342	83	56.5	10.5	1.230	0.448	28.2	4.7	0.082	0.020
1992	589	139	63.4	10.1	2.436	0.910	65.8	13.1	0.112	0.025
1993	581	105	92.5	14.9	0.923	0.322	181.2	45.1	0.312	0.051
1994	407	61	110.4	15.4	0.825	0.294	116.1	19.0	0.285	0.041
1995	395	69	92.2	12.5	1.544	0.544	115.6	21.7	0.292	0.045
1996	677	183	51.2	6.6	4.024	1.507	169.6	46.8	0.250	0.048
1997	621	139	43.7	5.8	0.671	0.233	262.1	80.0	0.422	0.062
1998	316	47	87.9	15.1	0.358	0.129	94.6	17.0	0.300	0.041
1999	298	58	89.3	14.0	0.883	0.313	75.8	12.6	0.255	0.042
2000	248	49	54.0	7.3	0.574	0.225	57.2	12.7	0.230	0.044
2001	161	27	59.4	9.3	0.336	0.128	36.9	6.3	0.229	0.039
2002	299	56	42.5	6.3	1.743	0.469	36.2	7.2	0.121	0.025
2003	345	61	53.6	7.2	1.183	0.332	56.6	12.4	0.164	0.032

2004	854	160	137.3	20.9	4.418	1.147	128.3	24.0	0.150	0.028
2005	894	153	86.4	11.5	1.692	0.395	194.4	45.4	0.217	0.038
2006	759	106	272.3	44.2	0.525	0.142	209.2	36.2	0.275	0.039
2007	728	104	268.2	44.5	2.545	0.644	153.1	22.6	0.210	0.033
2008	692	99	158.8	25.4	1.367	0.290	150.6	25.8	0.218	0.035
2009	754	104	165.7	26.4	2.539	0.535	139.5	21.4	0.185	0.032
2010	846	127	155.0	27.6	2.130	0.438	124.3	21.6	0.147	0.029
2011	941	143	217.8	39.1	1.176	0.271	102.0	16.4	0.108	0.021
2012	1,206	176	317.3	54.3	3.103	0.712	129.2	18.2	0.107	0.020
2013	3,093	541	352.9	59.5	15.566	3.718	220.4	37.7	0.071	0.015
2014	3,004	570	453.2	75.4	4.067	1.092	309.9	60.5	0.103	0.021
2015	3,126	484	309.9	58.3	6.271	1.404	420.0	67.9	0.134	0.023
2016	3,850	574	459.8	84.3	12.688	3.016	471.9	68.8	0.123	0.022
2017	3,360	464	762.4	145.3	10.329	2.364	457.1	62.4	0.136	0.022
2018	4,108	666	774.4	151.4	22.590	5.807	435.8	59.7	0.106	0.020
2019	3,018	462	734.2	154.9	5.963	1.257	358.4	51.4	0.119	0.022
2020	2,971	445	619.7	125.0	10.933	2.537	423.9	55.9	0.143	0.026
2021	2,868	516	512.0	106.9	12.216	3.355	357.4	48.7	0.125	0.026
2022	2,825	555	446.9	109.5	9.695	2.397	252.3	39.6	0.089	0.022

Table 5

Probability that future SSB is above 2022 SSB in each model.

Name	HCR_name	2023	2024	2025	2026	2027	2028	2029	2030
B2-Mage	Catch000	0	100	100	90	44	43	45	43
B2-Mage	Catch050	0	100	100	100	100	100	100	100
B2-Mage	Catch100	0	100	100	100	100	100	100	100
B2-Mage	Catch150	0	100	100	100	100	98	98	98
B2-Mage	Catch200	0	100	100	100	98	92	93	94
B2-Mage	Catch300	0	100	100	100	72	68	69	70
B2-Mage	Catch400	0	100	100	66	42	43	42	40
S32-JP23indics	Catch000	0	0	0	0	1	3	3	2
S32-JP23indics	Catch050	0	0	100	100	100	100	100	100
S32-JP23indics	Catch100	0	0	100	100	100	97	95	96
S32-JP23indics	Catch150	0	0	100	100	92	67	71	73
S32-JP23indics	Catch200	0	0	100	100	31	35	41	42
S32-JP23indics	Catch300	0	0	5	1	4	8	8	6
S32-JP23indics	Catch400	0	0	0	0	1	2	1	1
S28-ProcEst	Catch000	38	57	76	64	48	44	46	43
S28-ProcEst	Catch050	38	57	97	99	98	98	98	99
S28-ProcEst	Catch100	38	57	96	96	94	94	95	96
S28-ProcEst	Catch150	38	57	93	92	88	88	89	90
S28-ProcEst	Catch200	38	57	89	87	80	78	79	80
S28-ProcEst	Catch300	38	57	79	70	58	56	56	56
S28-ProcEst	Catch400	38	57	66	49	38	36	34	32
S34-ProcEst23	Catch000	0	7	47	26	10	12	14	12
S34-ProcEst23	Catch050	0	7	95	98	97	96	97	98
S34-ProcEst23	Catch100	0	7	89	93	88	84	86	88
S34-ProcEst23	Catch150	0	7	80	81	69	64	67	68
S34-ProcEst23	Catch200	0	7	70	63	45	42	44	45
S34-ProcEst23	Catch300	0	7	45	25	13	14	14	12
S34-ProcEst23	Catch400	0	7	24	7	3	5	4	3

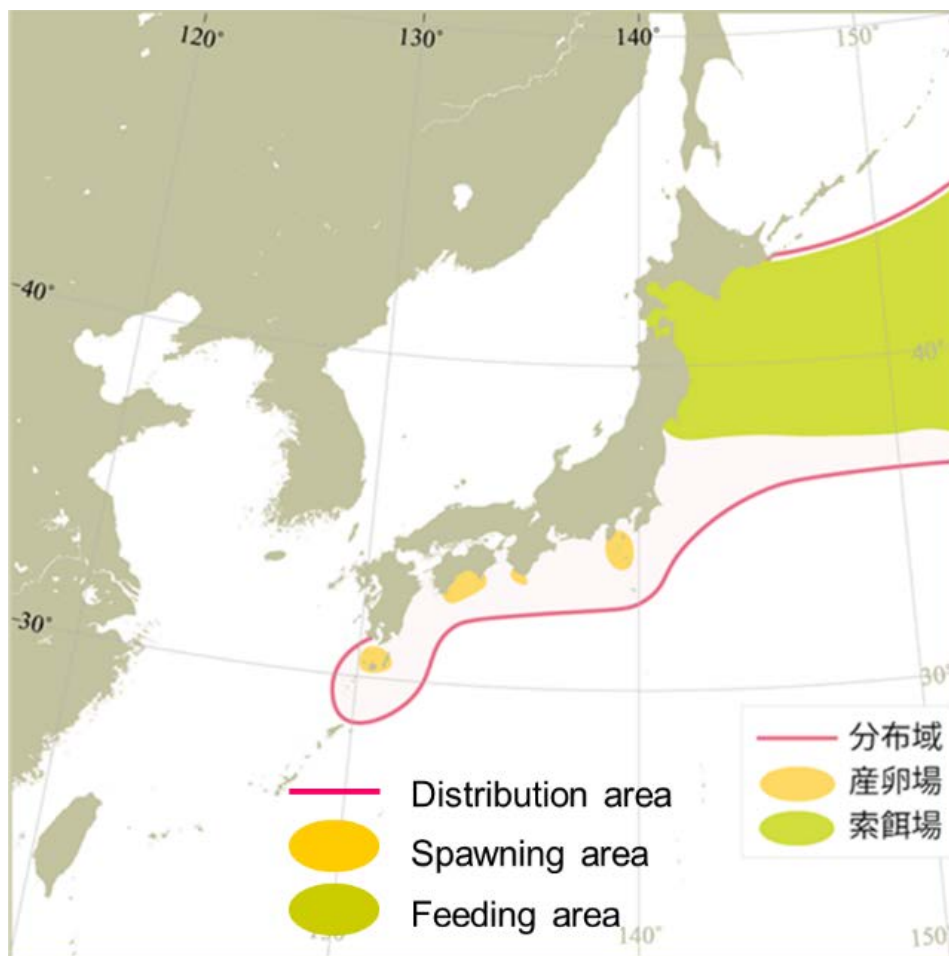
Table 6

Stock status summary from the base case scenario.

Stock Status Summary Table						
	SSB (Thousand MT)	Total Biomass (Thousand MT)	Recruitment (Million Individuals)	F	Exploitation	SPR_0
2022 Estimate	447	2,825	9,839	0.23	0.089	171.1
Current (Average 2020-2022)	526	2,888	11,097	0.28	0.119	165.4
<b>Values relative to the all years of the time series (i.e. 1970-2022)</b>						
	SSB (Thousand MT)	Total Biomass (Thousand MT)	Recruitment (million individuals)	F	Exploitation	SPR_0
Historical Minimum (Min)	45	172	365	0.23	0.071	155
Historical 25 percentile (25%)	97	634	1,308	0.36	0.136	266
Historical Median (Med)	335	1,566	4,353	0.61	0.185	344
Historical 75 percentile (75%)	744	3,177	9,839	0.71	0.25	379
Historical Maximum (Max)	1,394	6,050	23,579	1.11	0.422	501
<b>Ratios Relative to 1970-2022</b>						
	Stock Status Related to Biomass			Stock Status Related to Fishing Intensity		
Current / Historical Minimum	11.694	16.81	30.436	1.21	1.674	1.067
Current / 25%_Historical	5.418	4.554	8.483	0.79	0.874	0.622
Current / Med_Historical	1.569	1.844	2.55	0.47	0.643	0.481
Current / 75%_Historical	0.707	0.909	1.128	0.40	0.475	0.436
Current / Max_Historical	0.377	0.477	0.471	0.25	0.282	0.33
<b>Values relative to 2016-2022</b>						
	SSB (Thousand MT)	Total Biomass (Thousand MT)	Recruitment (million individuals)	F	Exploitation	SPR_0
Recent Minimum (Min)	447	2,825	6,043	0.23	0.089	155.0
Recent 25th percentile (25%)	486	2,919	10,154	0.26	0.112	162.5
Recent Median (Med)	620	3,018	11,077	0.29	0.123	167.5
Recent 75 percentile (75%)	748	3,605	12,622	0.30	0.130	177.6
Recent Maximum (Max)	774	4,108	22,898	0.31	0.143	217.7
<b>Ratios Relative to 2016-2022</b>						
	Stock Status Related to Biomass			Stock Status Related to Fishing Intensity		
Current / Recent Min	1.18	1.02	1.84	1.21	1.34	1.07
Current / 25%_Recent	1.08	0.99	1.09	1.10	1.06	1.02
Current / Med_Recent	0.85	0.96	1.00	0.98	0.97	0.99
Current / 75%_Recent	0.70	0.80	0.88	0.94	0.91	0.93
Current / Max_Recent	0.68	0.70	0.48	0.92	0.83	0.76

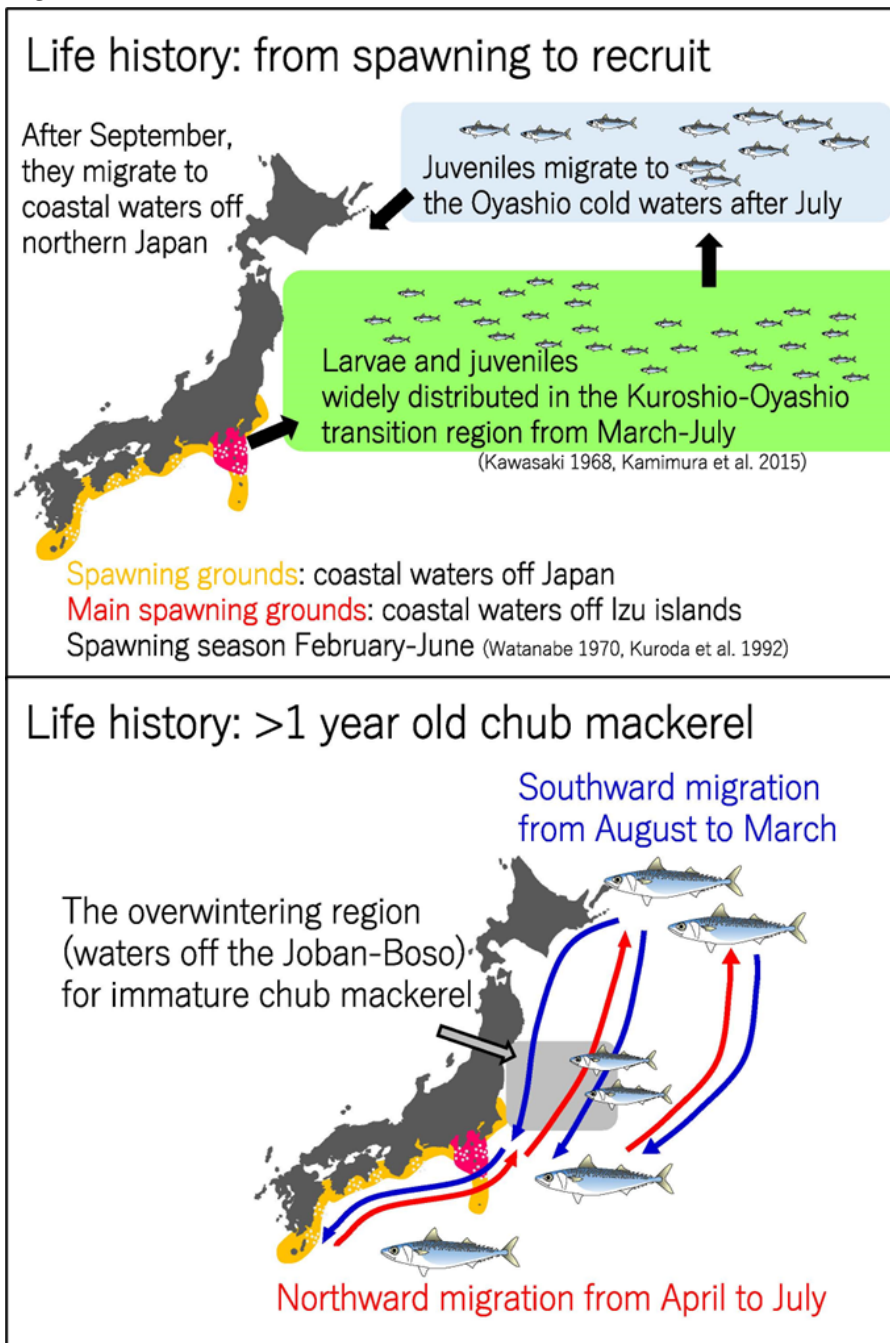
## FIGURES

Figure 1



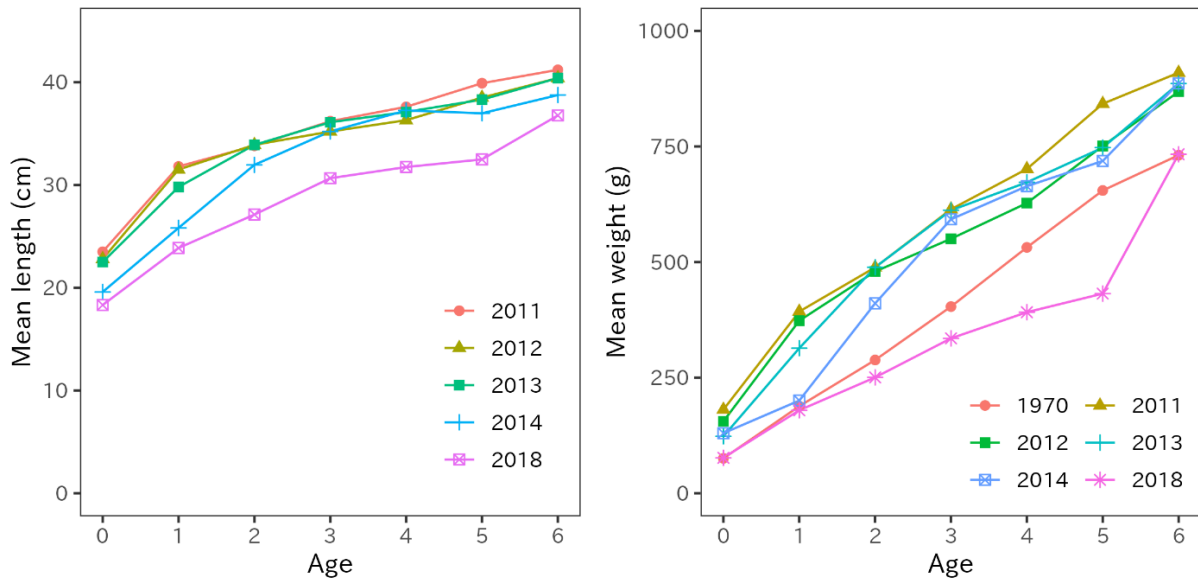
Map of distribution of chub mackerel in the North Pacific (Yukami et al. 2024).

Figure 2



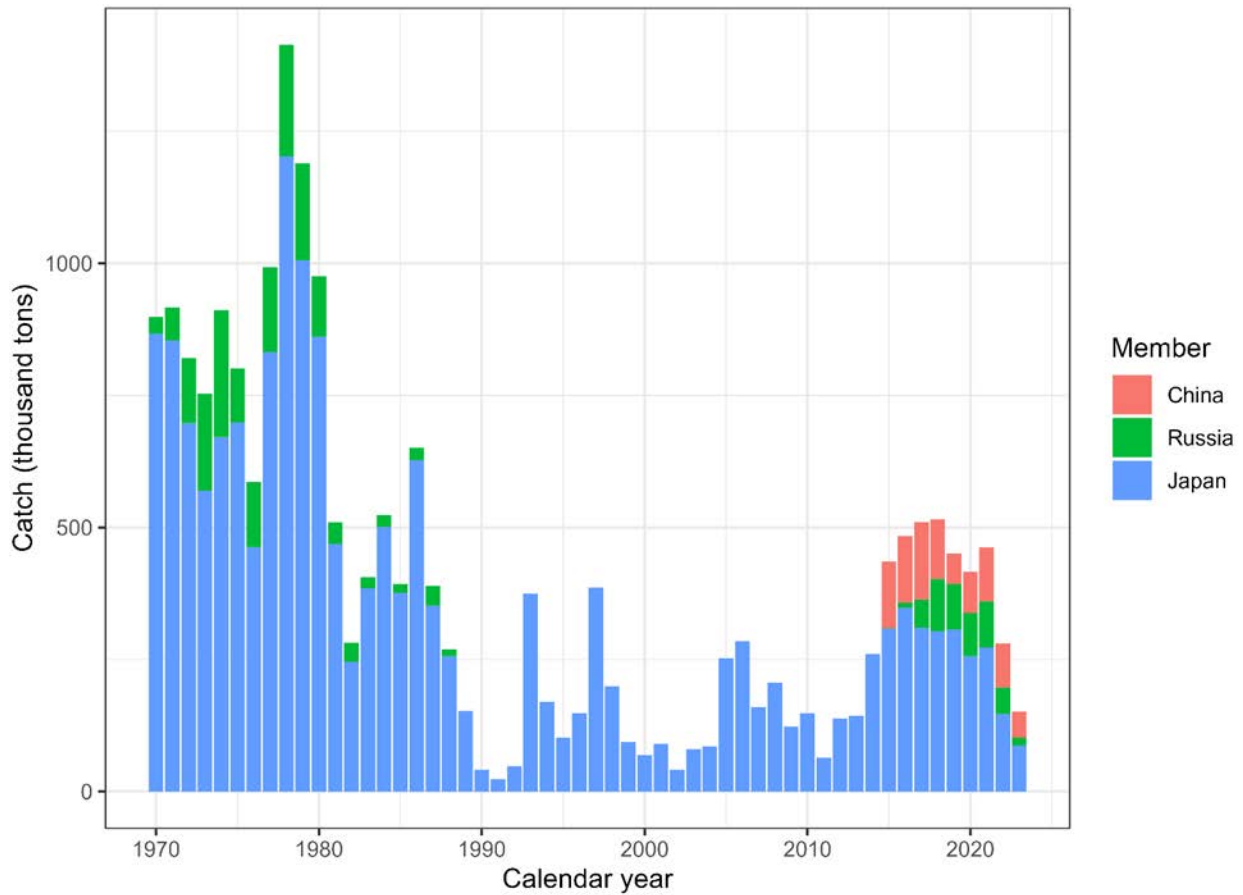
Migration pattern of chub mackerel by growth stage. The upper and bottom panels show seasonal movement of age 0 fish from spawning to recruitment and fish at age 1 and older, respectively (Kamimura, 2017).

Figure 3



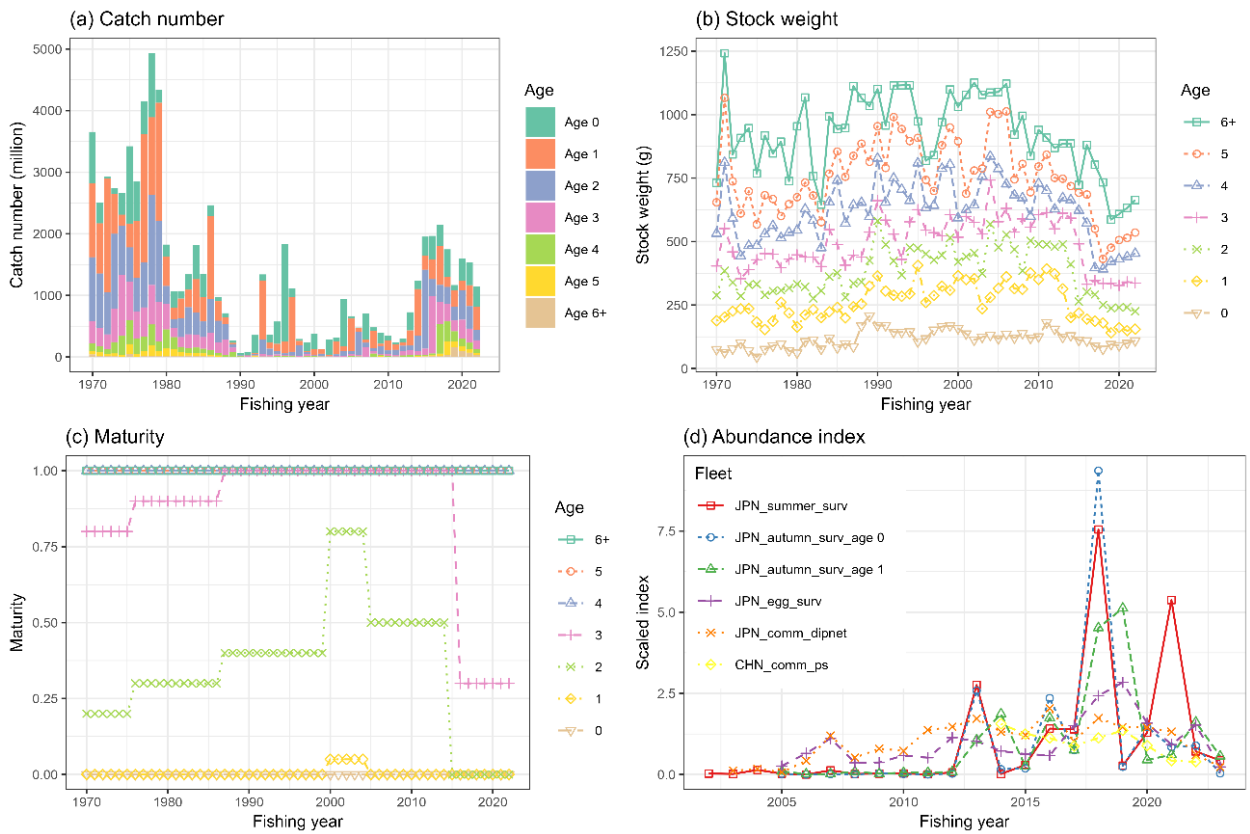
Mean fork lengths of chub mackerel at ages 0 to 6 in FY2011-2014 and FY2018 (left panel). Mean weight at age in FY1970s, FY2011-2014 and FY2018 (right panel).

Figure 4



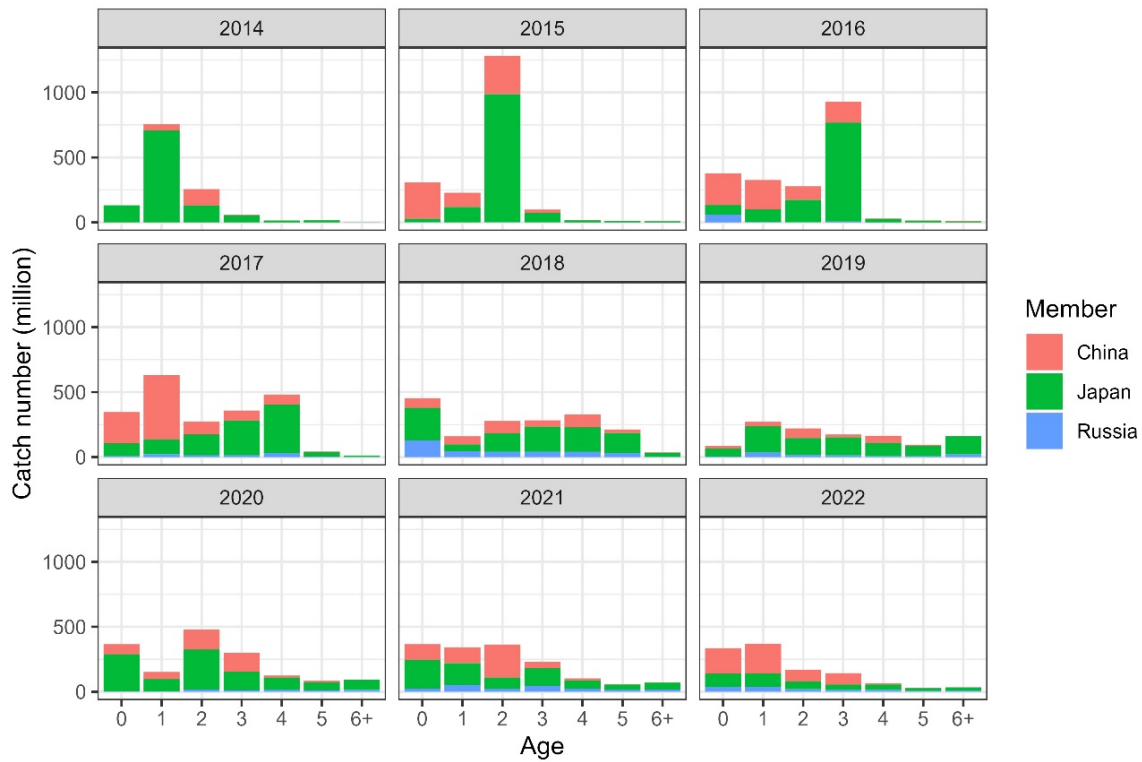
Historical chub mackerel catch in weight by Member. The provisional Chinese catch for CY2023 is estimated using the historical ratio for chub mackerel and blue mackerel. Blue mackerel has been excluded from the catch using the chub-to-blue-mackerel ratio. Catch data for China was obtained from the Annual Summary Footprint, which is available at <https://www.npfc.int/summary-footprint-chub-mackerel-fisheries> and adjusted using this ratio. Russia's catch data is sourced from the Annual Summary Footprint which reflects no blue mackerel catches. Japan's catch data was collected from coastal prefectures along the Pacific Ocean, where chub mackerel are typically captured. The catch data of this figure is different from the catch data described in the data section above.

Figure 5



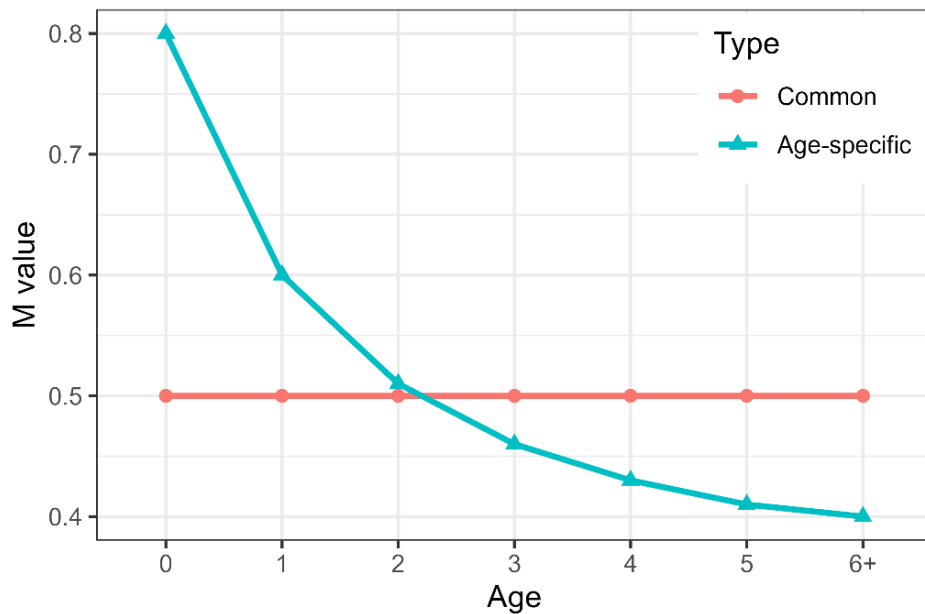
The time series data used for the base case scenario of chub mackerel stock assessment. (a) catch number by age, (b) weight by age, (c) maturity by age, (d) abundance index. Each abundance index is scaled by its mean value for visualization. Note that the five Japanese abundance indices are included through FY2023, but are not used in the base case analysis.

Figure 6



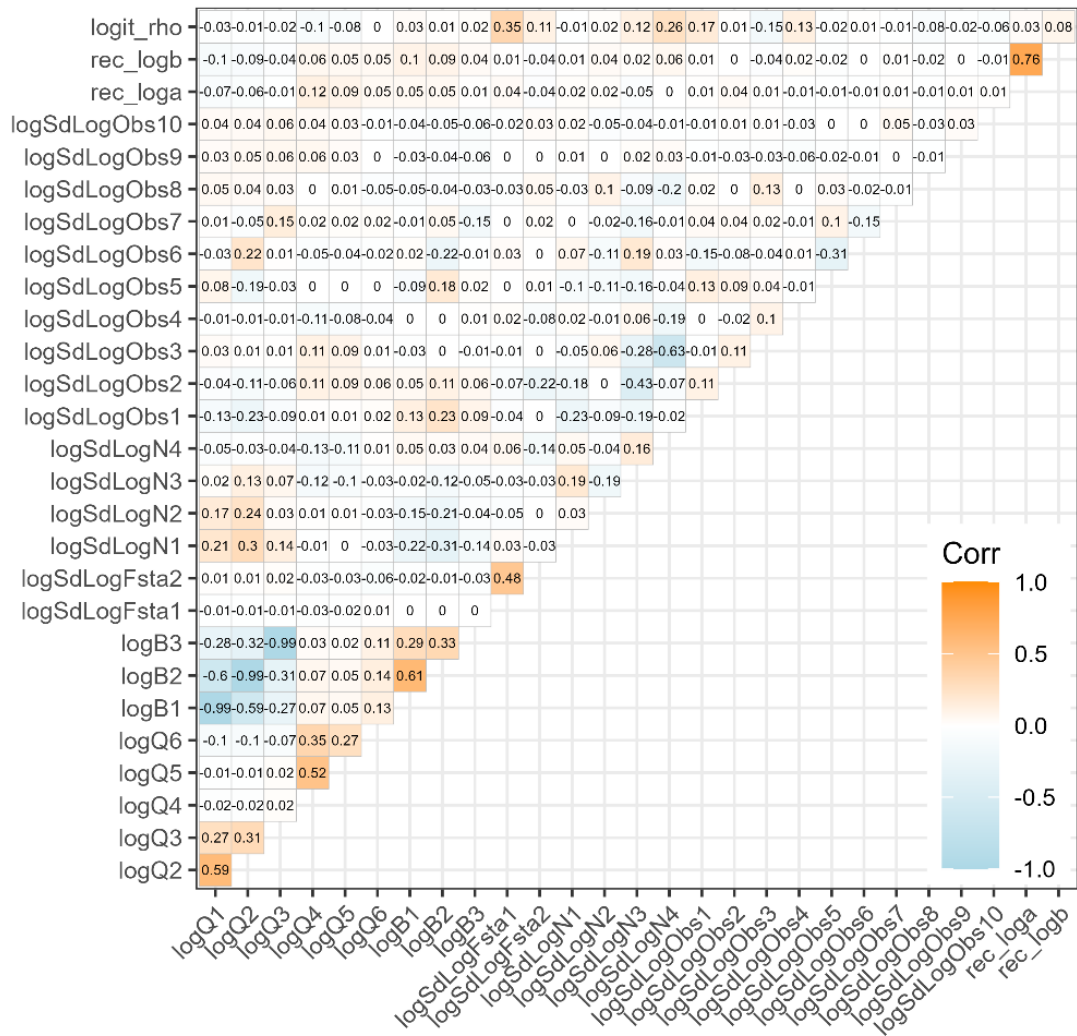
Catch number of chub mackerel by member by age by year from CY2014 to CY2022.

Figure 7



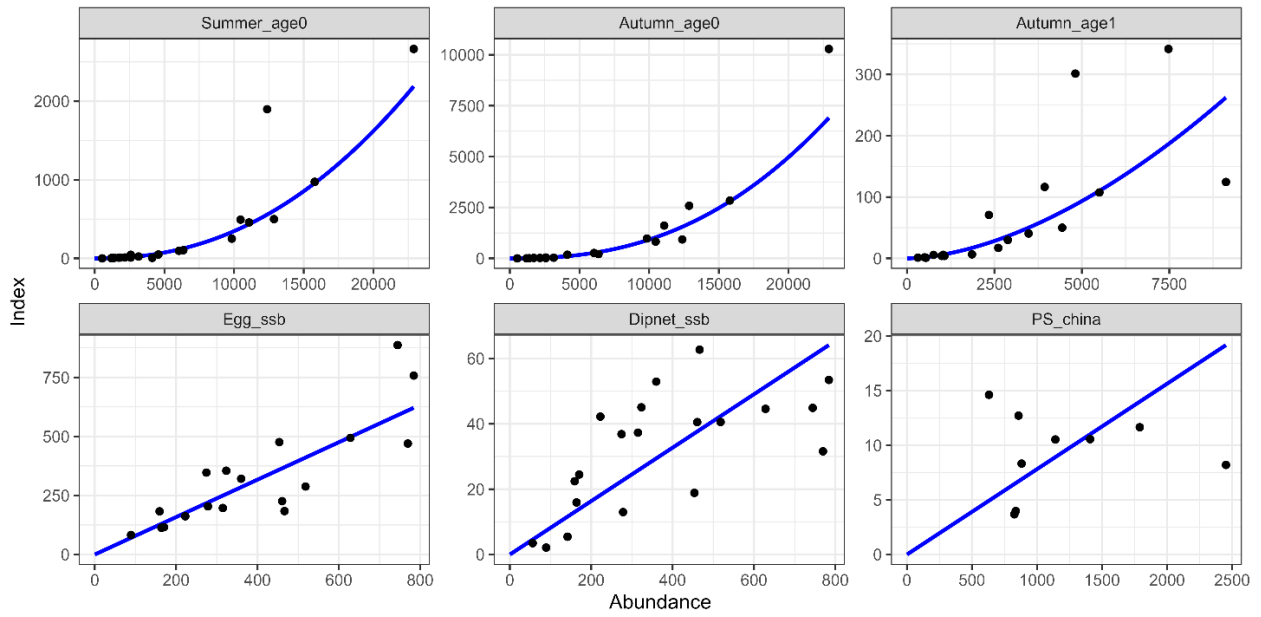
Natural mortality ( $M$ ) values of chub mackerel under the two base case scenarios. The age-specific  $M$  was applied to the base case and representative scenarios.

Figure 8



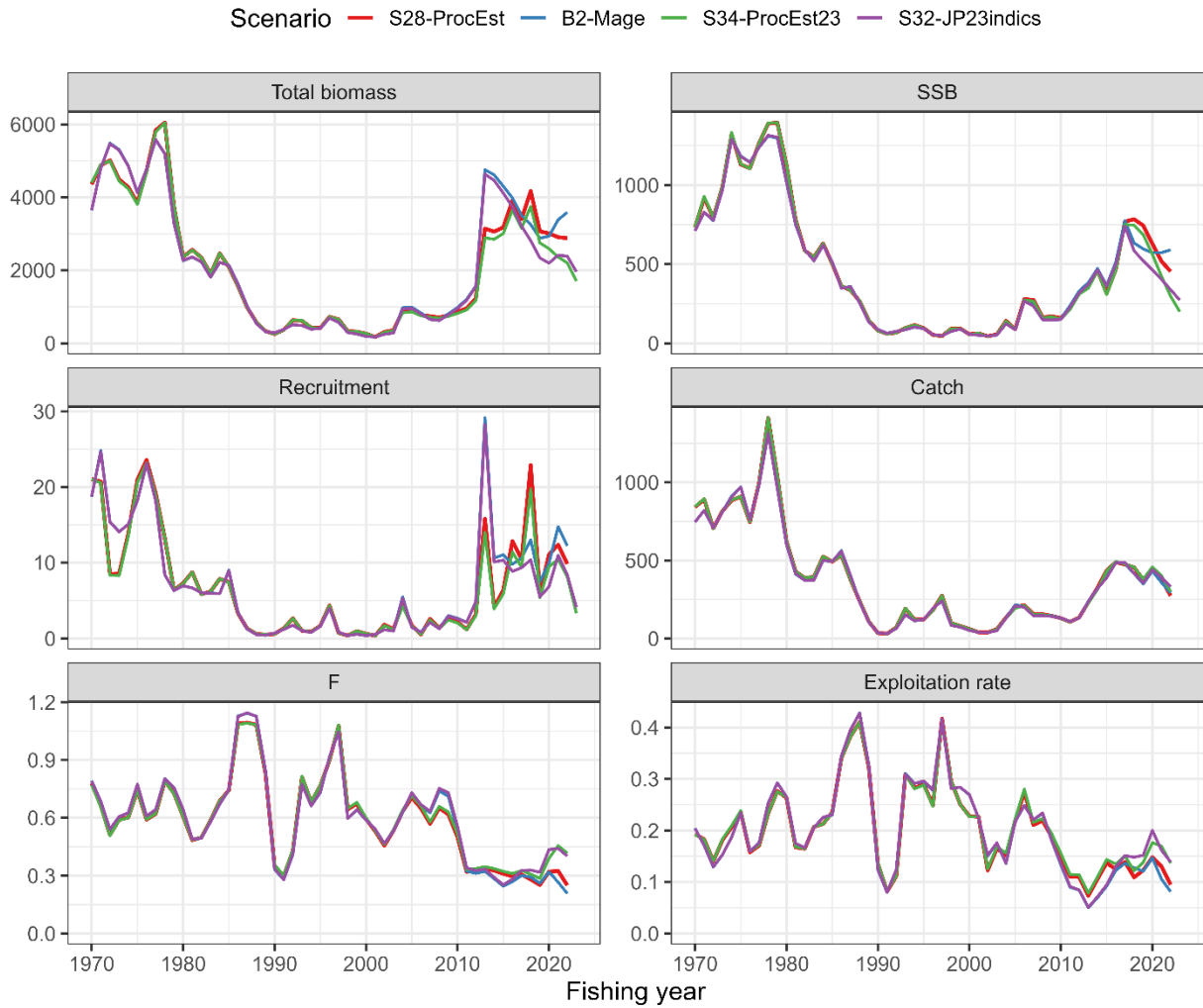
Plot of the correlation matrix obtained from the covariance matrix of the fixed effects parameter estimates, for the base case scenario (S28-ProcEst). Orange colors indicate positive correlation, while light blue indicates negative correlation.

Figure 9



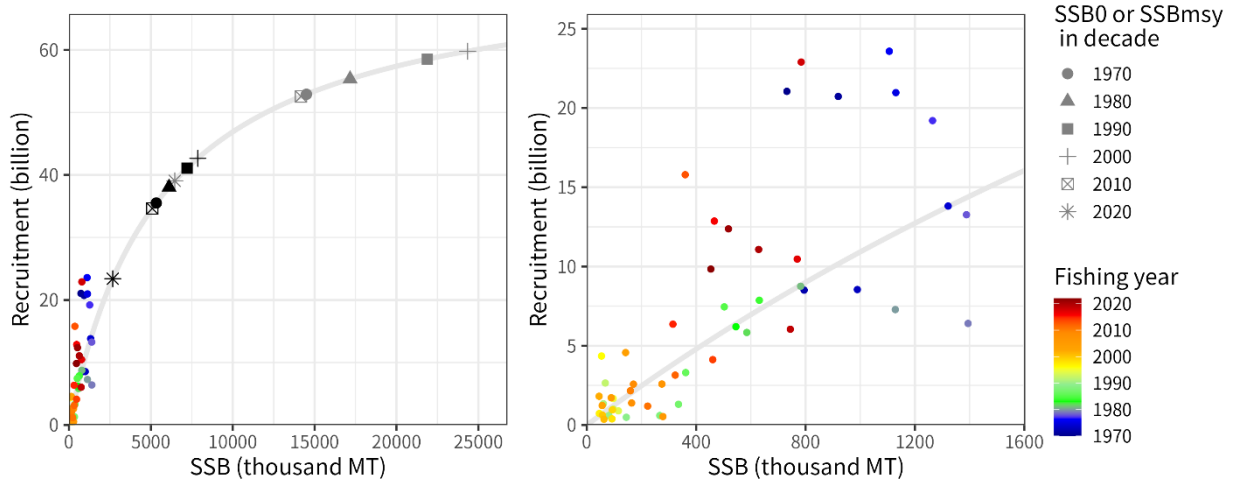
Relationship between six abundance index and their corresponding abundance estimates under the base case scenario (S28-ProcEst). The blue lines indicate the predicted relationships.

Figure 10



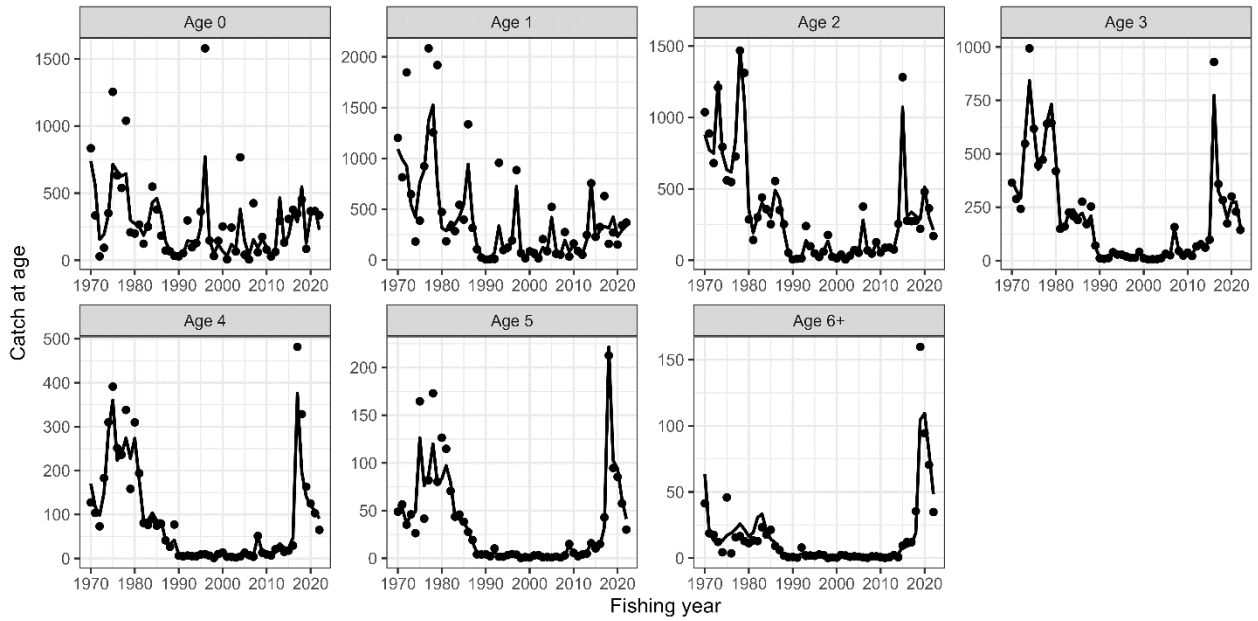
*Time series of estimates of total biomass (1,000 MT), SSB (1,000 MT), recruitment (billion), catch (1,000 MT), mean F, and exploitation rate (catch divided by total biomass) of chub mackerel under the initial base case scenario (B2-Mage), the final base case S28-ProcEst and the representative case scenarios of S32-JP23, and S34-PRocEst23.*

Figure 11



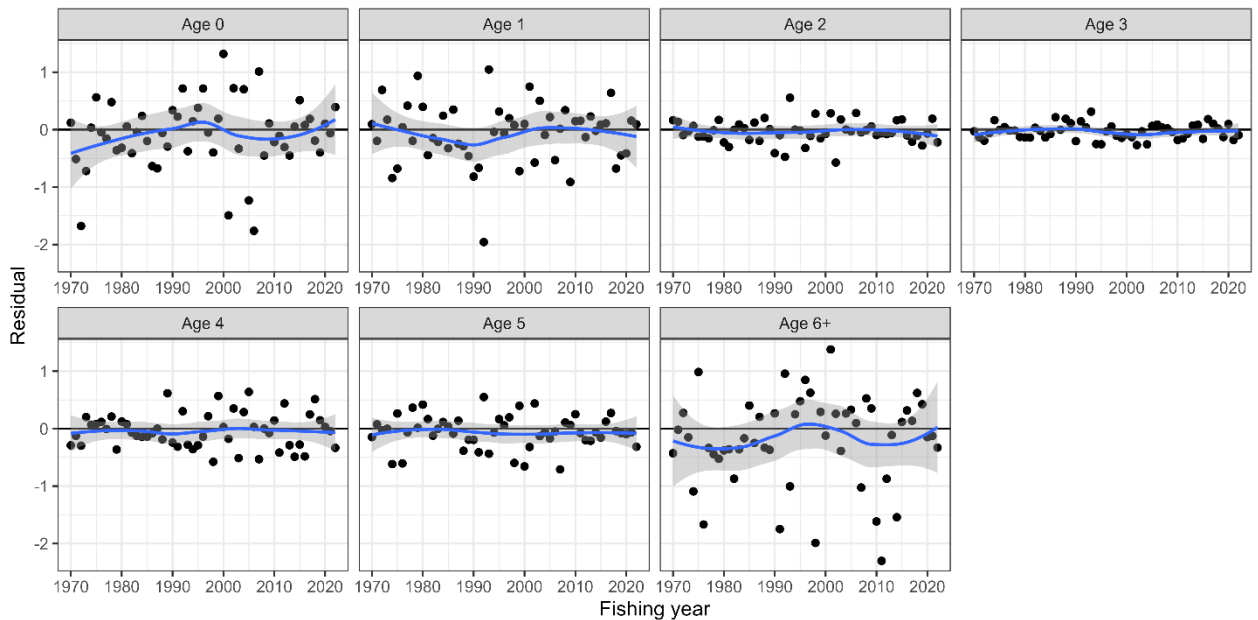
*Estimated Beverton-Holt stock recruitment relationship of chub mackerel under the base case scenario (S28-ProcEst) (gray lines) and estimated past SSB and number of recruits (colored circles) overplotted with estimated SSB0 (equilibrium unexploited spawning biomass, grey symbols) and SSB<sub>MSY</sub> (black symbols). The reference points are calculated using biological parameters averaged during the decades. The unit of SSB on the x-axis is 1000 mt and the unit of subscription on the y-axis is billions.*

Figure 12



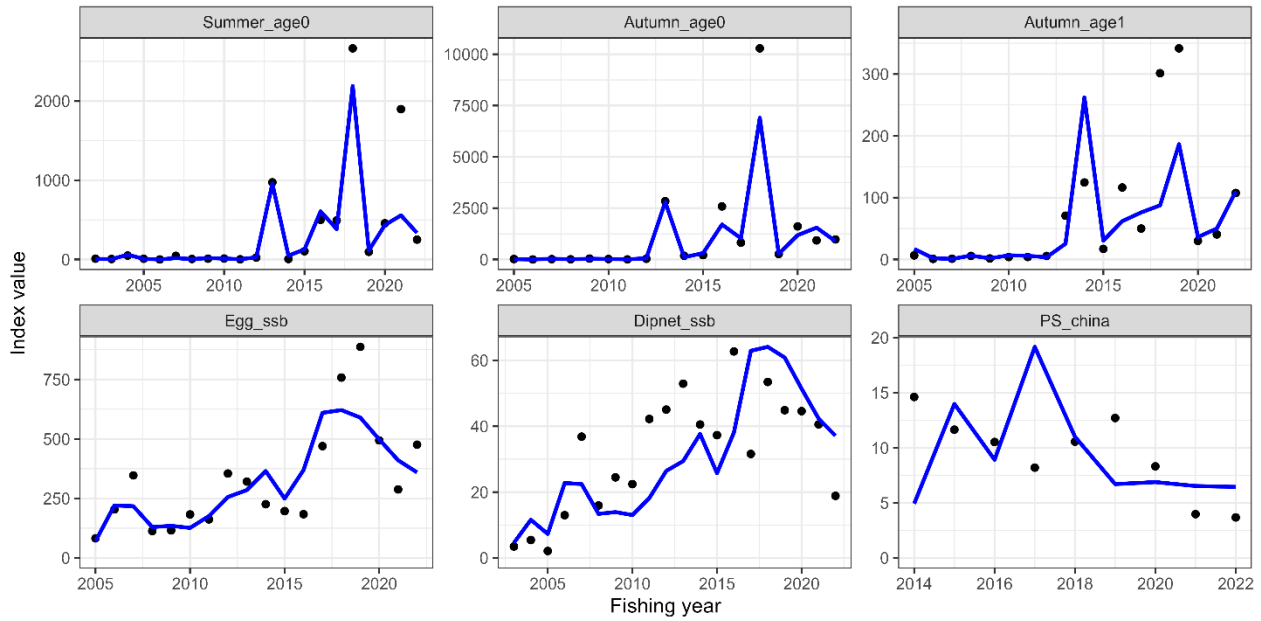
Observed catch numbers by age (dots) and their predicted values (lines) of chub mackerel under the base case scenario of S28-ProcEst.

Figure 13



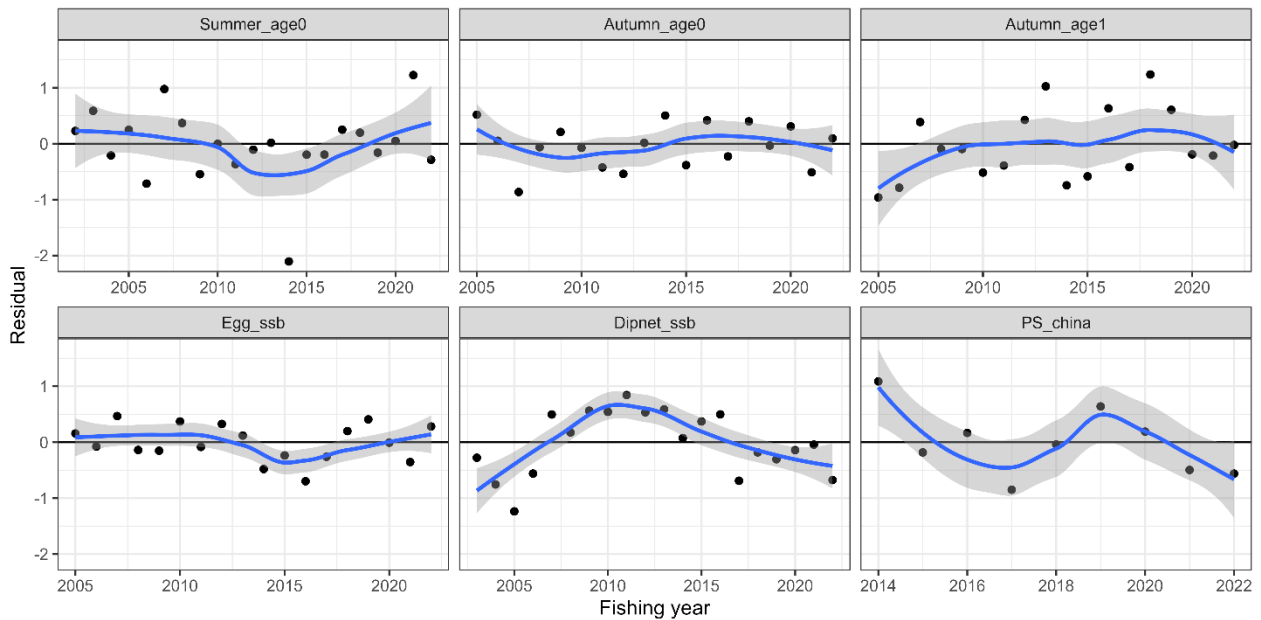
Residual plot for catch numbers of chub mackerel by age under the base case scenario of S28-ProcEst. Blue curves and shaded areas indicate smoothed curves estimated by LOESS and their 95% confidence intervals.

Figure 14



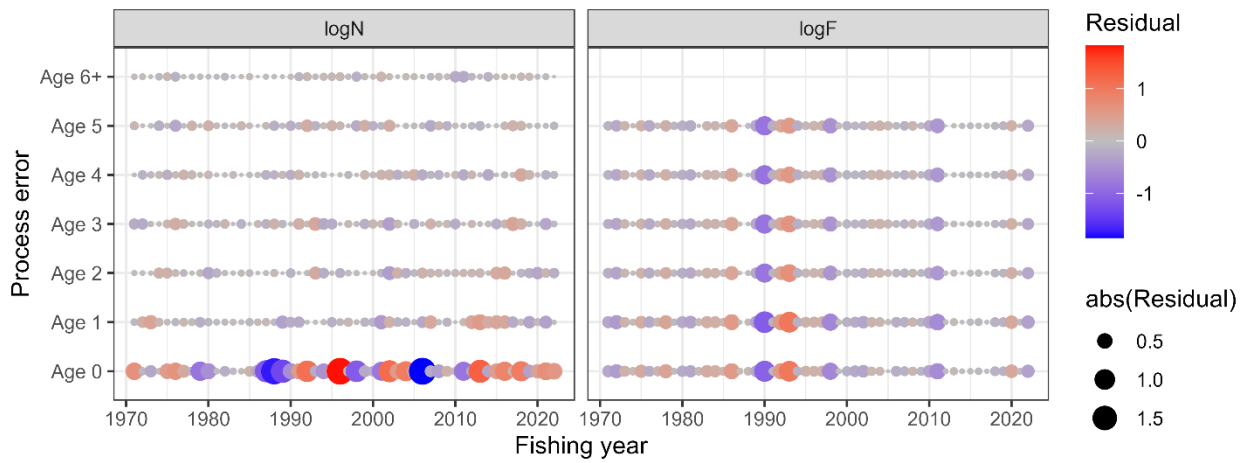
Trends of abundance indices used (dots) and their predicted values (lines) of chub mackerel under the base case scenario of S28-ProcEst.

Figure 15



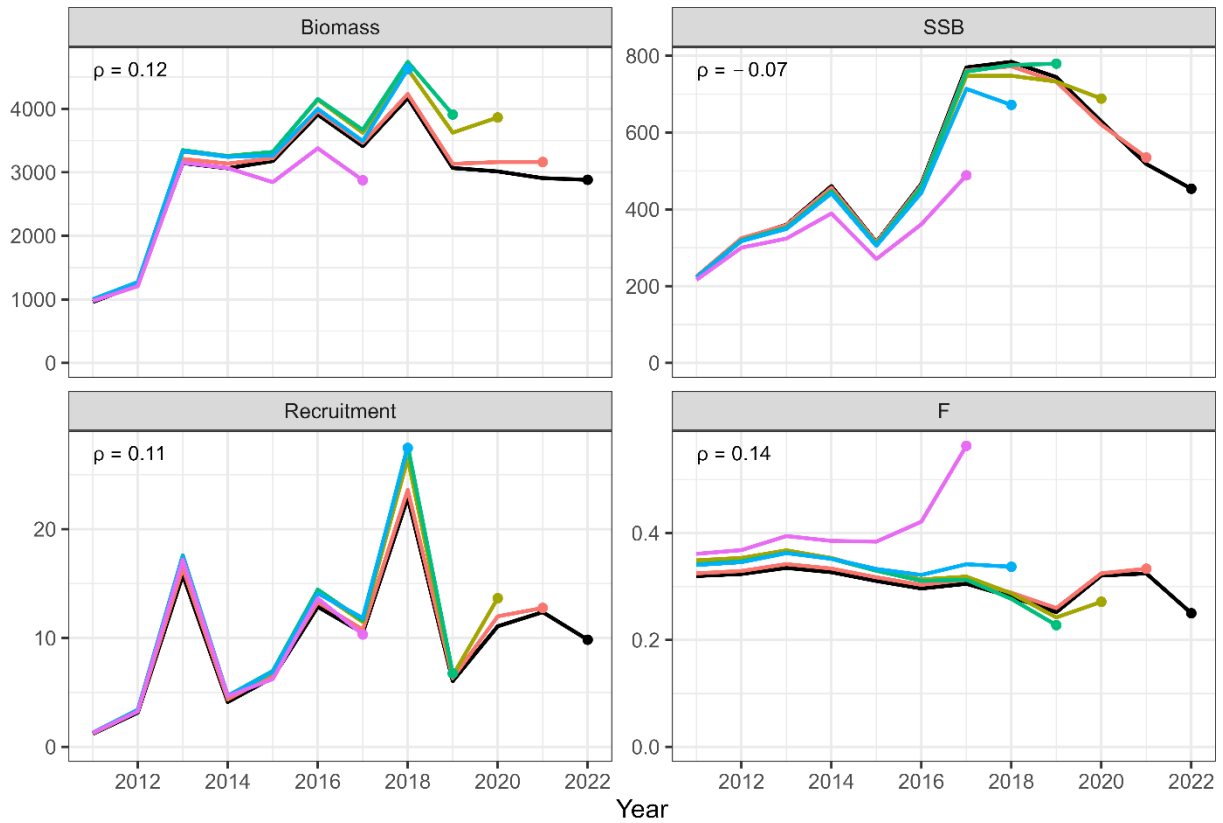
Residual plot for abundance indices of chub mackerel under the base case scenario of S28-ProcEst. Blue curves and shaded areas indicate smoothed curves estimated by LOESS and their 95% confidence intervals.

Figure 16



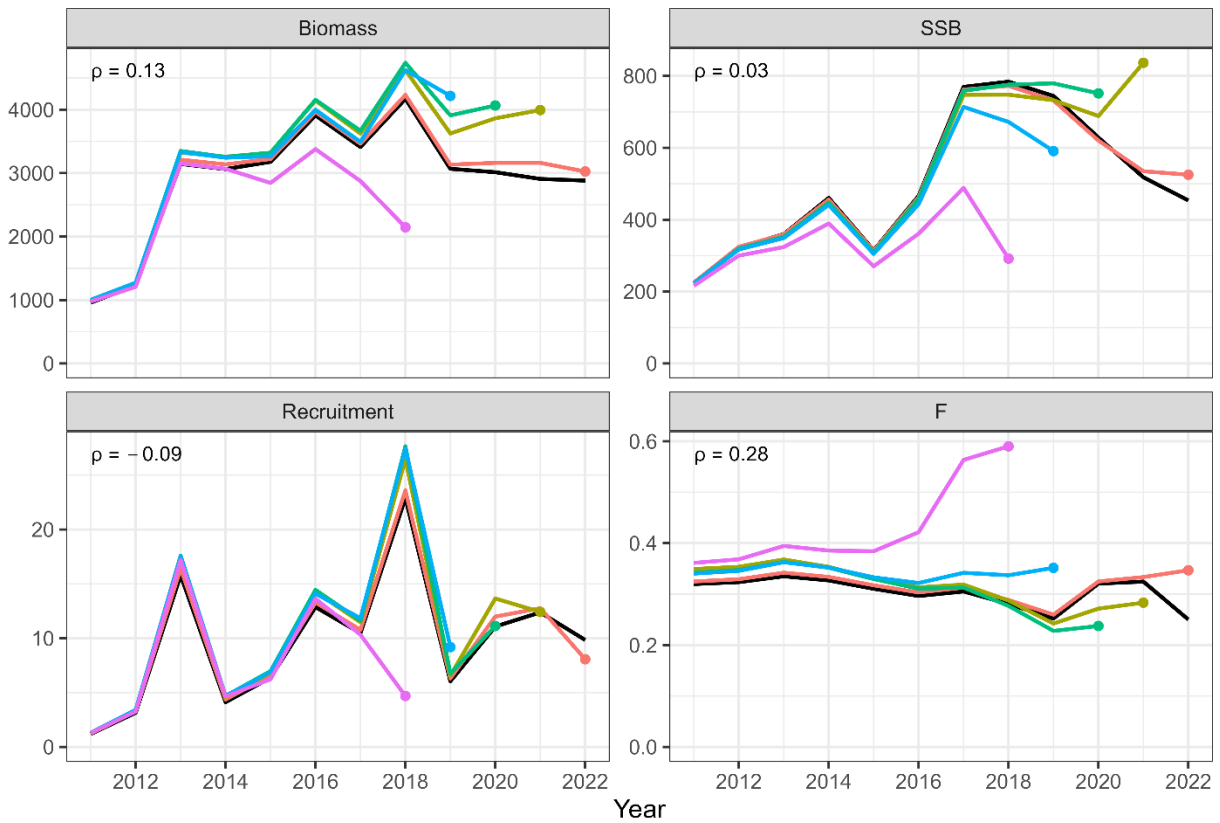
Process errors  $\log(N)$  (left) and  $\log(F)$  (right) of chub mackerel under the base case scenario (S28-ProcEst). Note that the process error in the number of individuals is almost zero, since the number of fish above one year of age is fixed to a small value, and the residuals of zero-year-old recruitment are shown as scattered up and down.

Figure 17



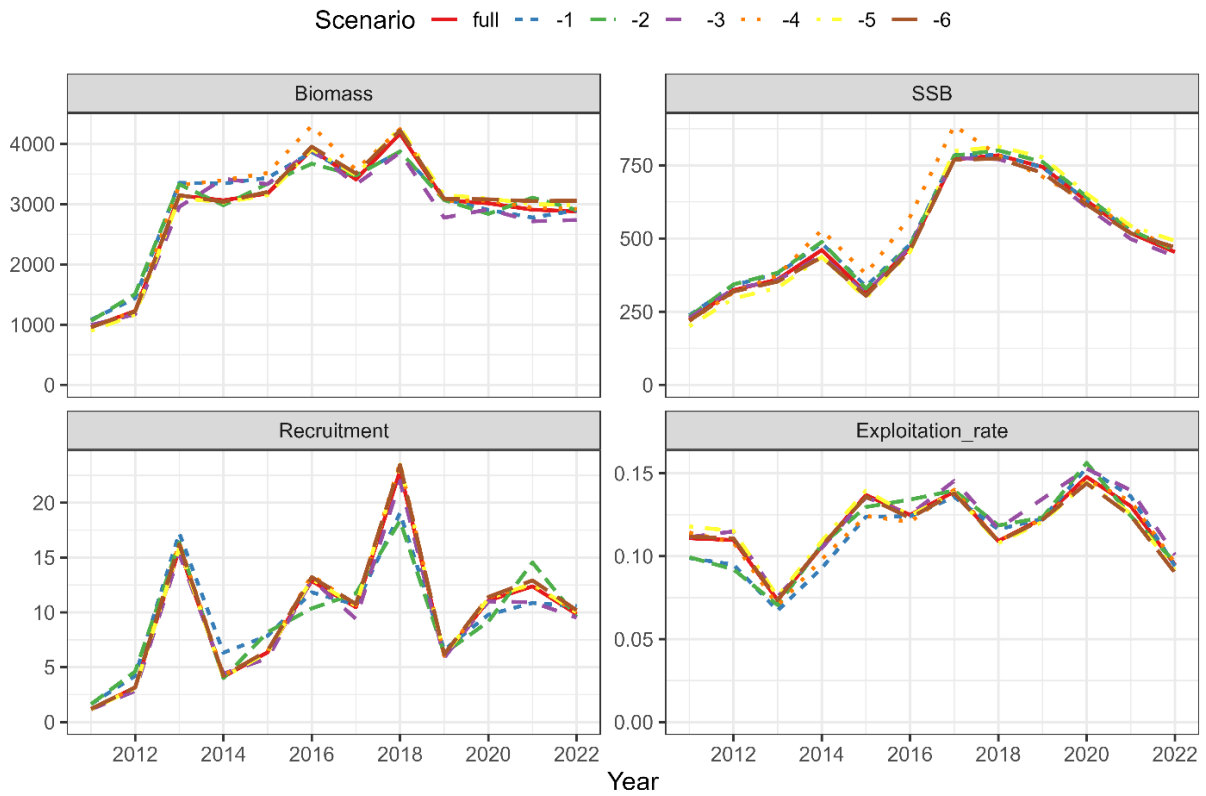
Retrospective patterns for total biomass (top left), SSB (top right), recruitment (bottom left), and mean  $F$  (bottom right) of chub mackerel under the base case scenario of S28-ProcEst. Black Lines represent models with all data, and colored lines represent models with the most recent data trimmed. Mohn's rho is shown in the upper left corner. The dots indicate the terminal year for the calculation of Mohn's rho.

Figure 18



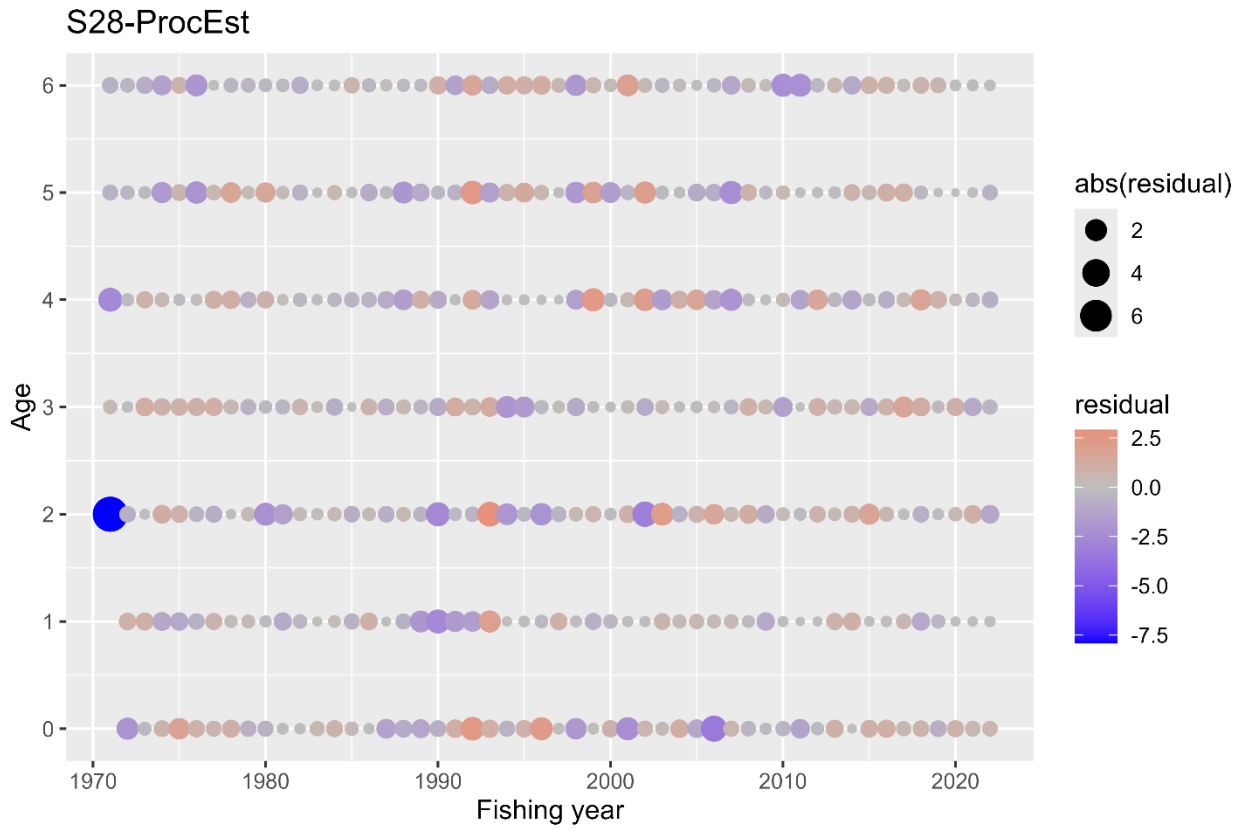
Patterns of retrospective forecasting for total biomass (top left), SSB (top right), recruitment (bottom left), and mean F (bottom right) of chub mackerel under the base case scenario of S28-ProcEst. Black Lines represent models with all data, and colored lines represent models with the most recent data trimmed. Mohn's rho is shown in the upper left corner. The dots indicate the year of one-year-ahead forecasting, used for the calculation of Mohn's rho.

Figure 19



Comparison of the results of the estimates of chub mackerel when all index values are used and when each indicator is excluded for the base case scenario of S28-ProcEst S28-ProcEst. The IDs of the index are as follows: (1) relative stock number of age 0 from the summer survey by Japan, (2) relative stock number of age 0 from the autumn survey by Japan, (3) relative stock number of age 1 from the autumn survey by Japan, (4) relative SSB from the egg survey by Japan, (5) relative SSB from the dip-net fishery by Japan, and (6) relative vulnerable stock biomass from the light purse-seine fishery by China.

Figure 20



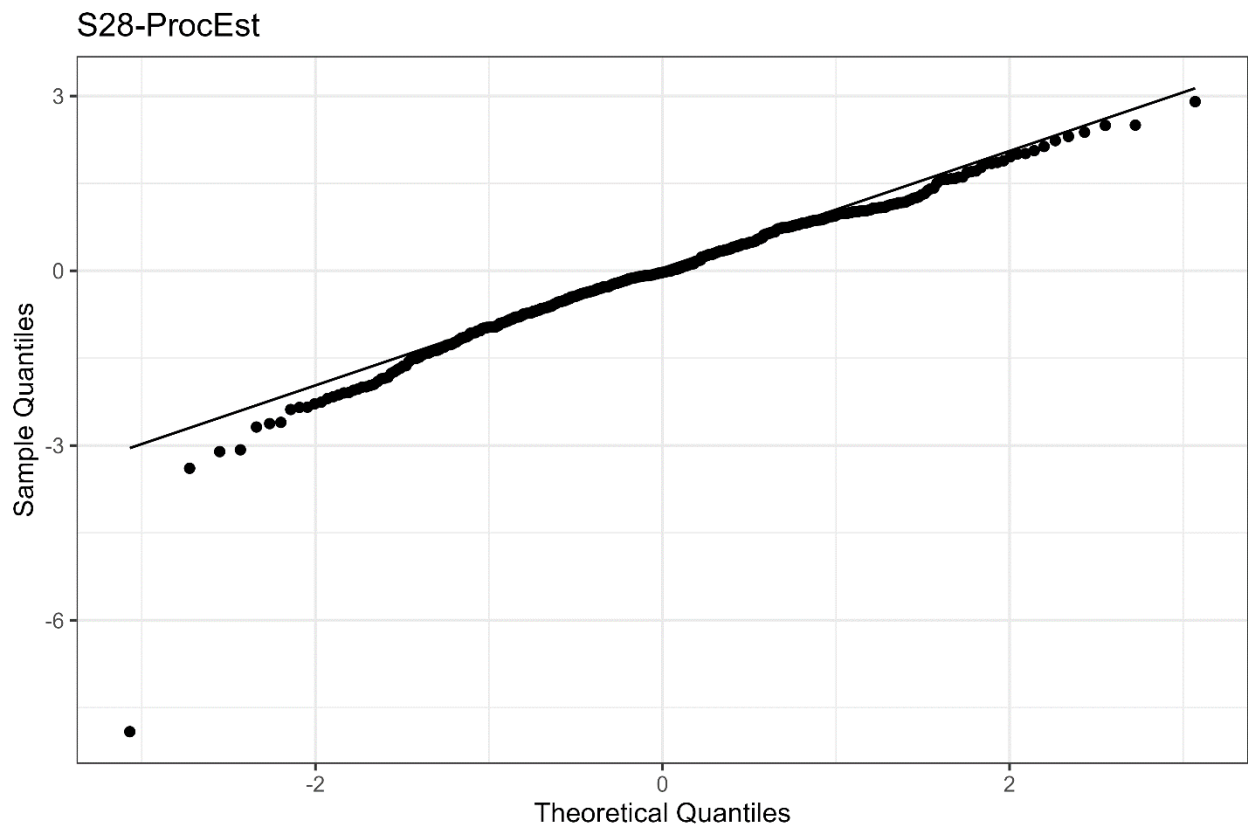
One-Step-Ahead residuals for the age composition for the base case scenario of S28-ProcEst.

Figure 21



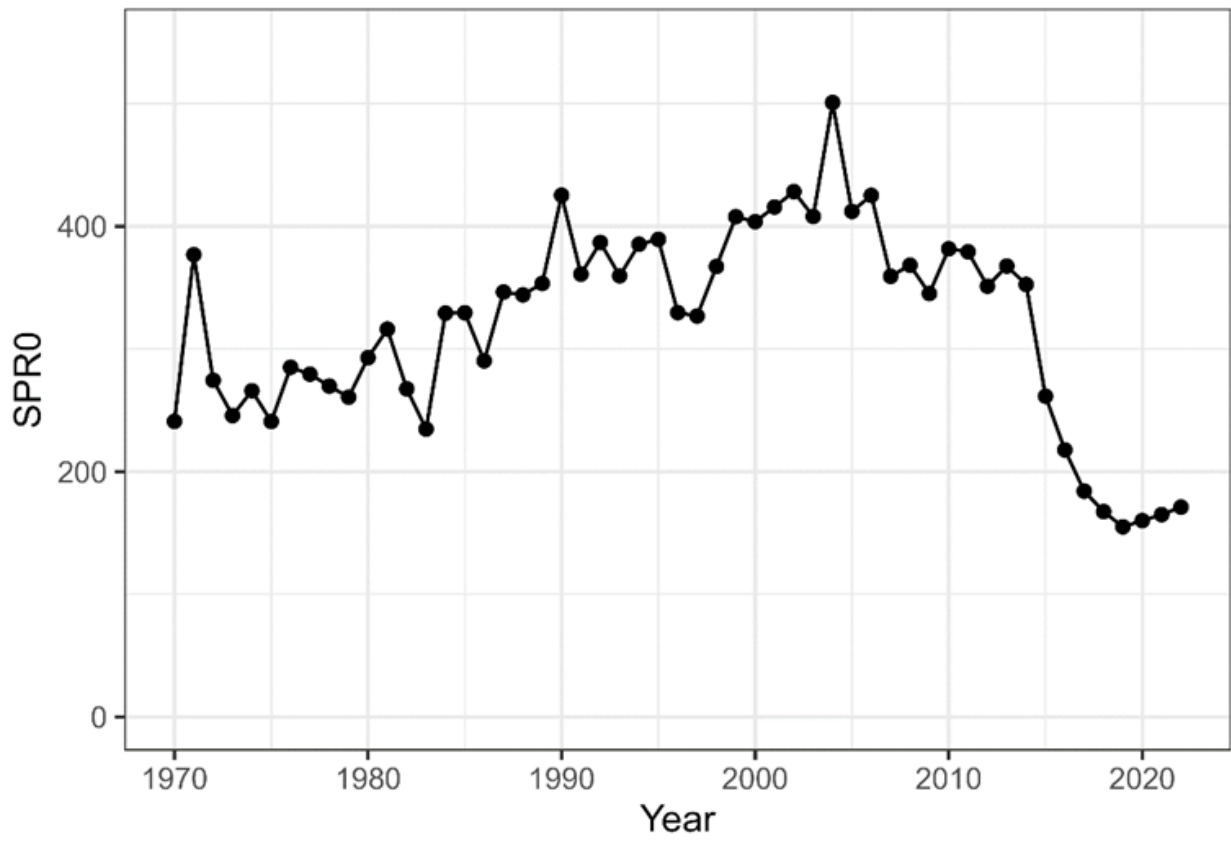
*One-Step-Ahead residuals for the indices of abundance for the base case scenario of S28-ProcEst. The IDs of the index are as follows: (1) relative stock number of age 0 from the summer survey by Japan, (2) relative stock number of age 0 from the autumn survey by Japan, (3) relative stock number of age 1 from the autumn survey by Japan, (4) relative SSB from the egg survey by Japan, (5) relative SSB from the dip-net fishery by Japan, and (6) relative vulnerable stock biomass from the light purse-seine fishery by China.*

Figure 22



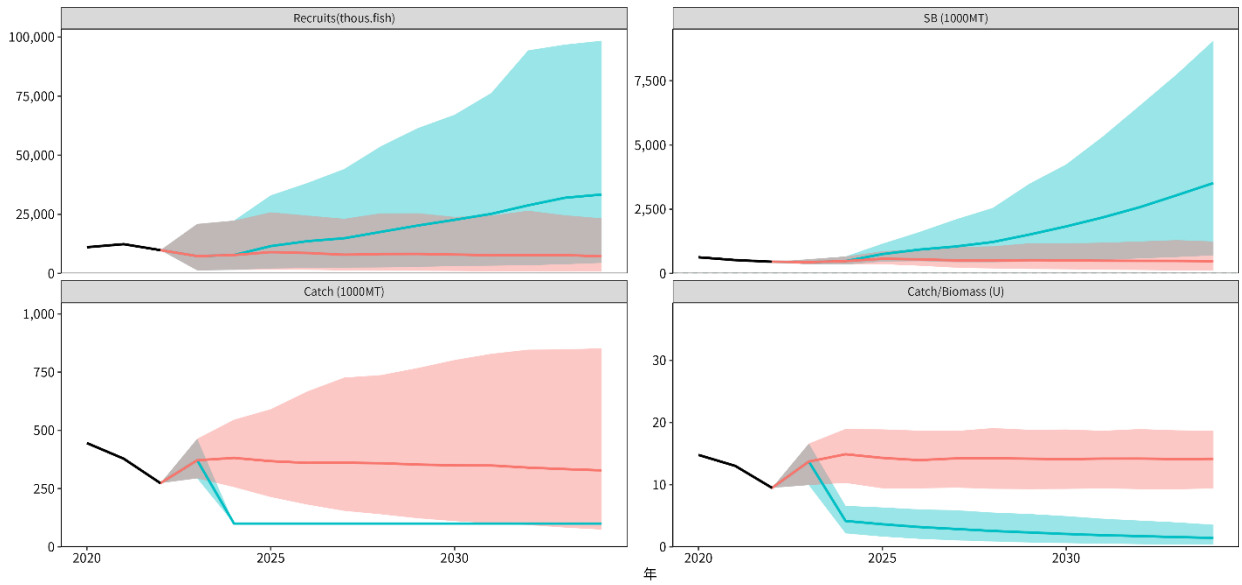
QQplot of the One-Step-Ahead residuals from the indices for the base case scenario of S28-ProcEst .

Figure 23



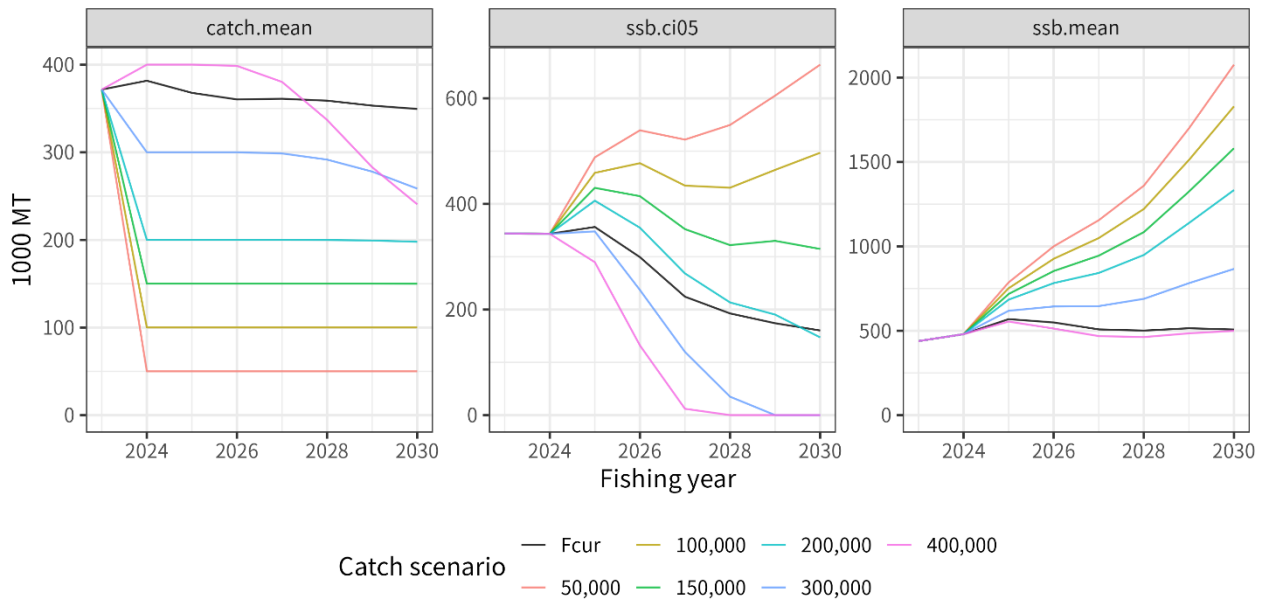
Trajectories of spawners per recruit without fishing (SPR0 in grams).

Figure 24



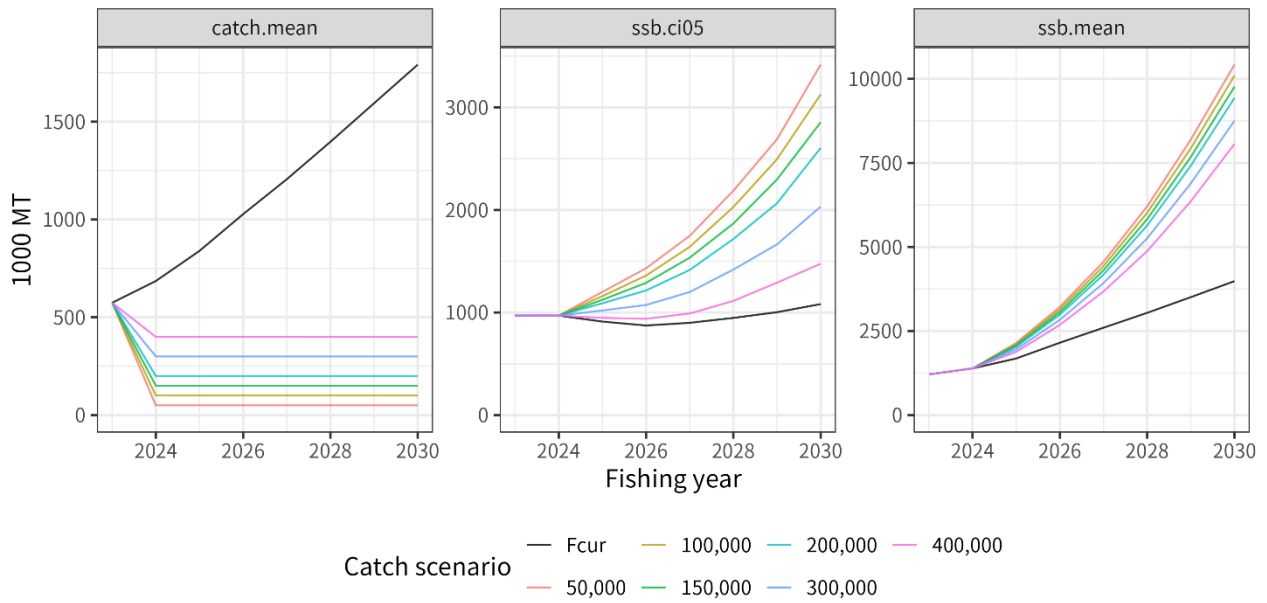
Examples of stochastic future projection results of chub mackerel. In this figure, results based on constant catch=100,000MT (blue) and current  $F$  (red) are compared. The shaded areas represent 90% prediction intervals, black solid lines are estimates by SAM, and colored solid lines are average.

Figure 25



Comparison of future trajectories in different future harvest scenarios (“Catch100” means 100,000MT constant catch) for future average catch (left, catch.mean), lower 5 percentile of spawning biomass (middle, ssb.ci05) and average spawning biomass (right, ssb.mean) of chub mackerel.

Figure 26



Comparison of future trajectories in different future harvest scenarios using all the biological parameter from 1970-2022 (“Catch100” means 100,000MT constant catch) for future average catch (left, catch.mean), lower 5 percentile of spawning biomass (middle, ssb.ci05) and average spawning biomass (right, ssb.mean) of chub mackerel.

## **APPENDIX 1**

Results for representative case runs of B2-Mage (B2), S32-JP23, and S34-PRocEst23

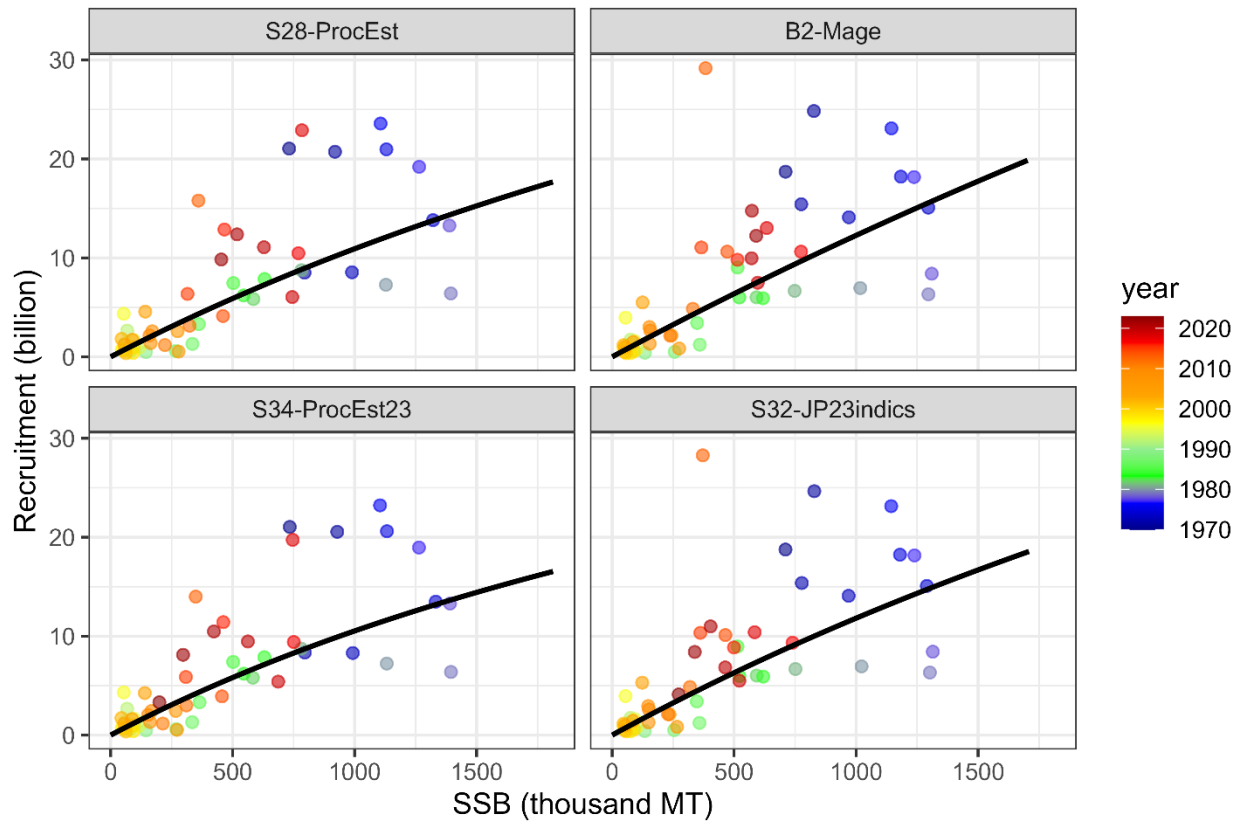
### **Stock assessment scenarios**

In order to improve the SAM fit to abundance indices and retrospective patterns, the TWG CMSA recognized the necessity of introduction of estimation of process error in survival of age groups older than age 0. The TWG CMSA also considered inclusion of FY2023 from the Japanese abundance indices, which had a large impact on the stock status of the most recent years. As a result, the following four scenarios were employed as representative cases:

- 1) B2, Estimate process error for only age 0 (recruitment) ;
- 2) S28-ProcEst, Estimate process error for all age groups;
- 3) S32-JP23, Estimate process error for only age 0 and use Japanese indices up to FY2023;  
and
- 4) S34-ProcEst23, Estimate process error for all age groups and use Japanese indices up to FY2023

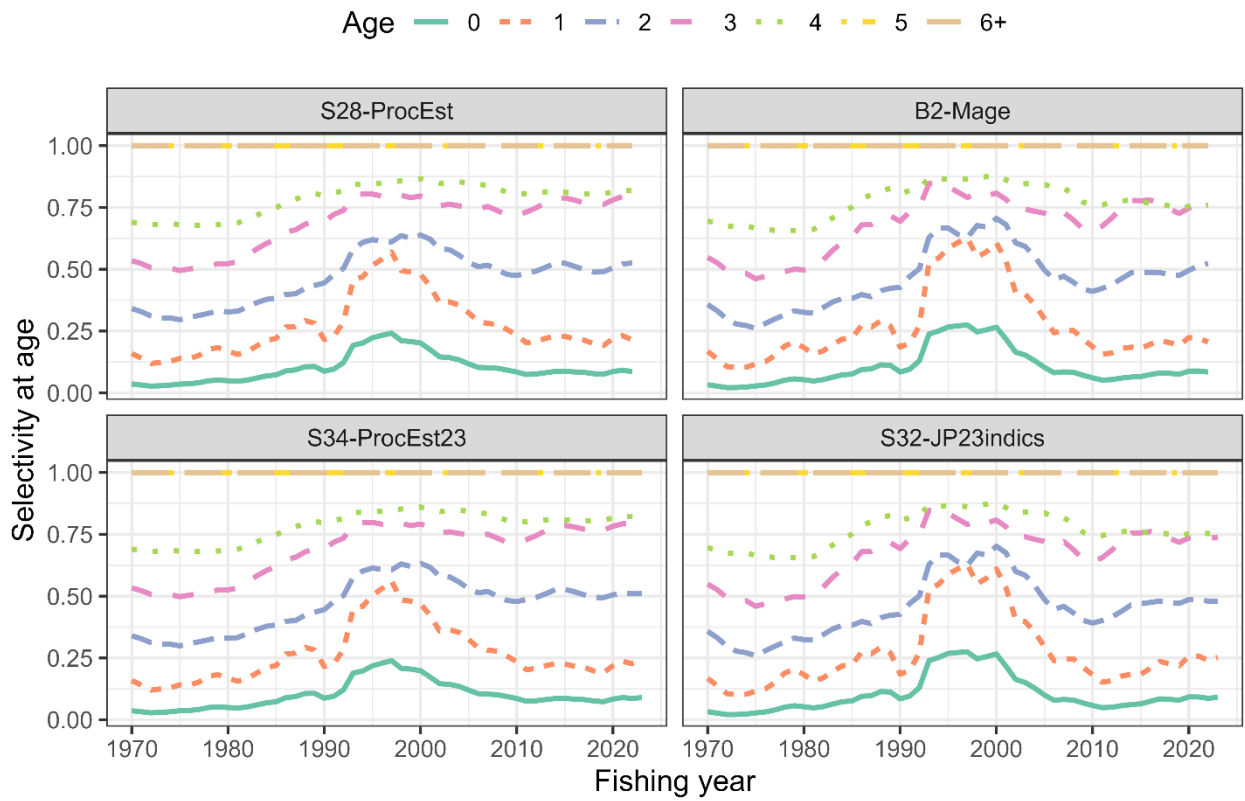
TWG CMSA agreed to select S28-ProcEst as a base case scenario because of the better diagnostics than the model only with recruitment process error and agreement of data usage up to FY2022. This Annex shows the comparison of the above four models along with the following models B1-Mcom, S31-JP23indics,27-ProcEst and S33-ProcEst23.

Figure ANNEX 1



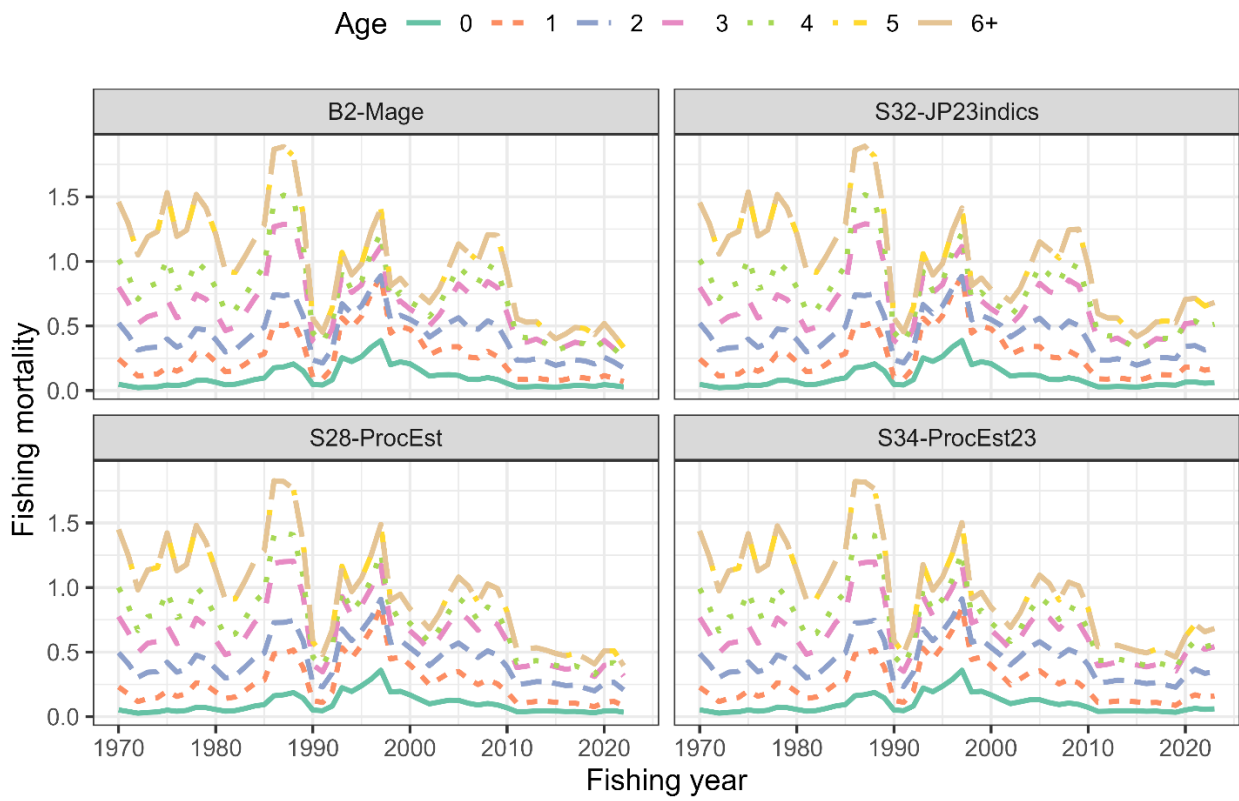
Estimated Beverton-Holt stock recruitment relationship (black lines) and estimated past SSB and number of recruits (colored circles) of chub mackerel under the final base case S28-ProcEst, the initial base case scenario B2-Mage, and other representative cases of S34-ProcEst23 and S32-JP23indics.

Figure ANNEX 2



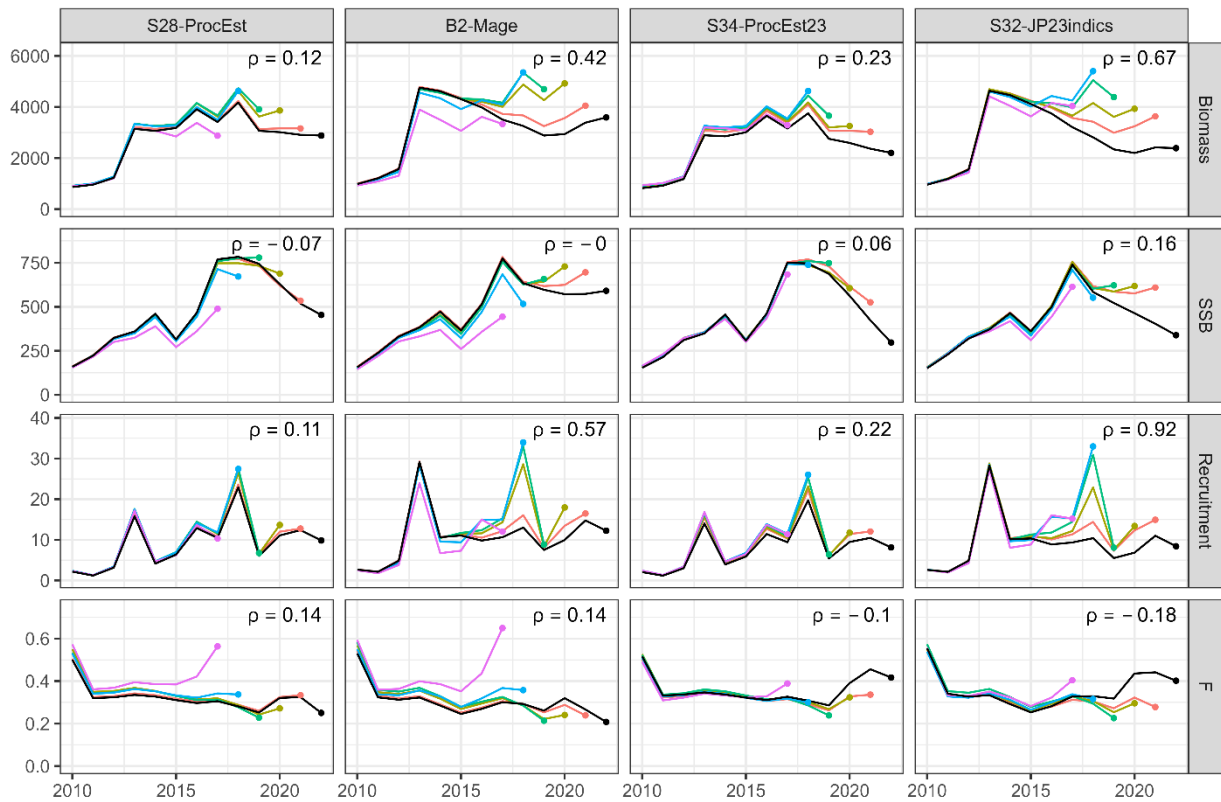
Estimated annual selectivity at age under the final base case S28-ProcEst, the initial base case scenario (B2-Mage), and the other representative cases of S34-ProcEst23 and S32-JP23indics.

Figure ANNEX 3



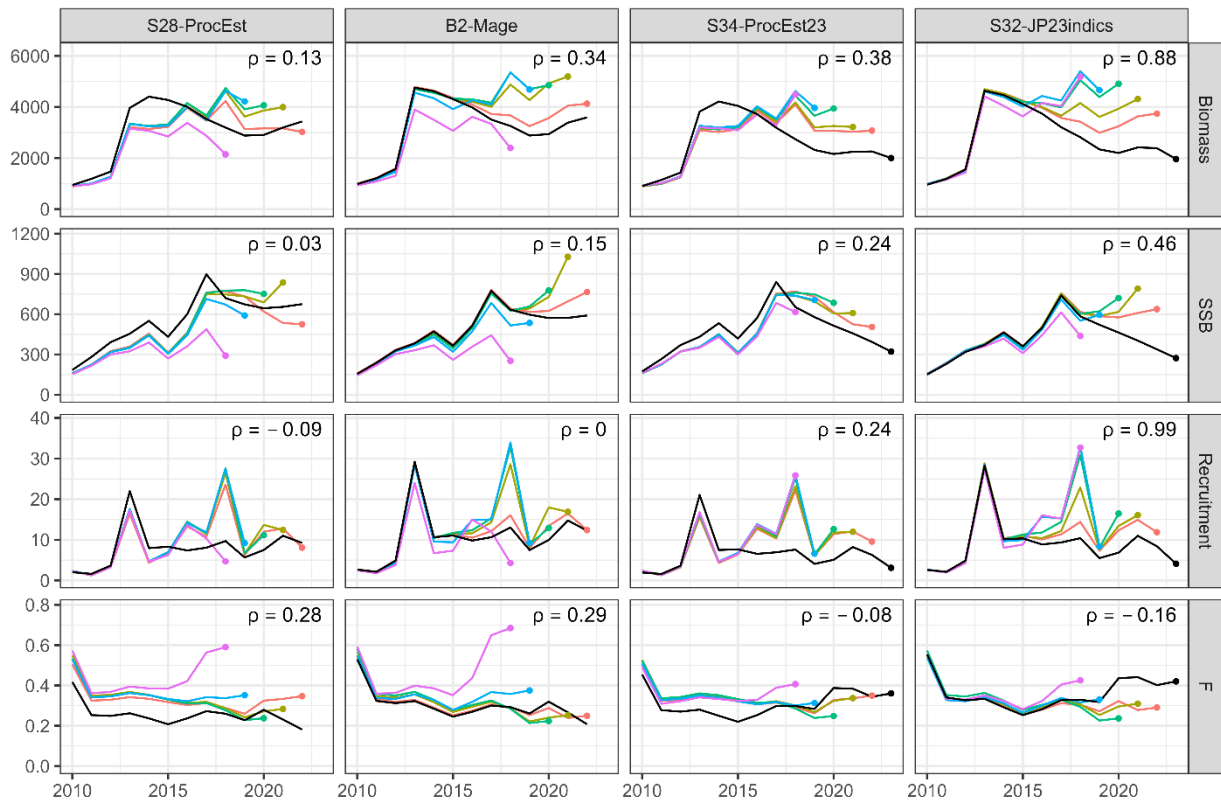
Time series of estimates of  $F$  at age for the final base case S28-ProcEst, the initial base case scenario B2-Mage, and the other representative cases of S34-ProcEst23 and S32-JP23indics.

Figure ANNEX 4



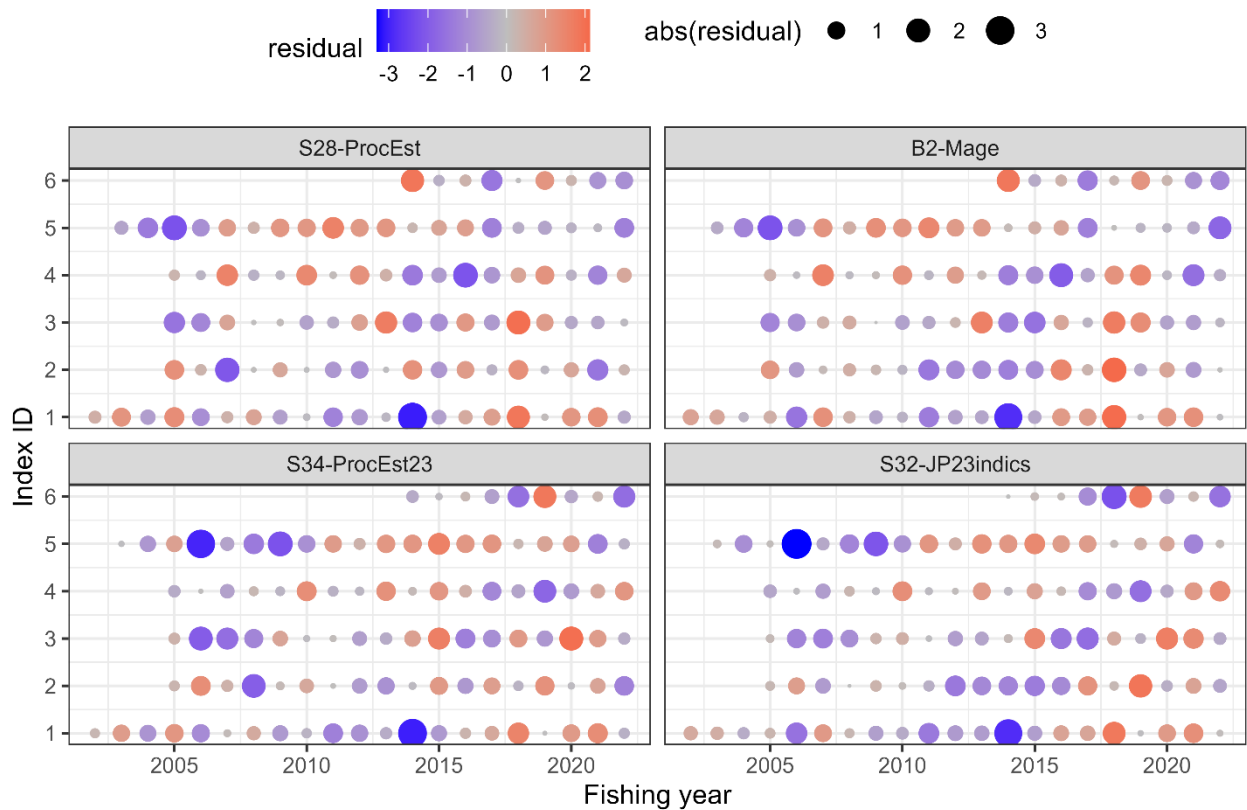
Retrospective patterns for total biomass (top row), SSB (second row), recruitment (third row), and mean  $F$  (bottom) of chub mackerel. Black Lines represent models with all data, and colored lines represent models with the most recent data trimmed. Mohn's rho is shown in the upper right corner. The dots indicate the terminal year for the calculation of Mohn's rho. Scenarios shown here are the final base case S28-ProcEst, the initial base case scenario B2-Mage, the other representative cases of S34-PRocEst23 and S32-JP23indics.

Figure ANNEX 5



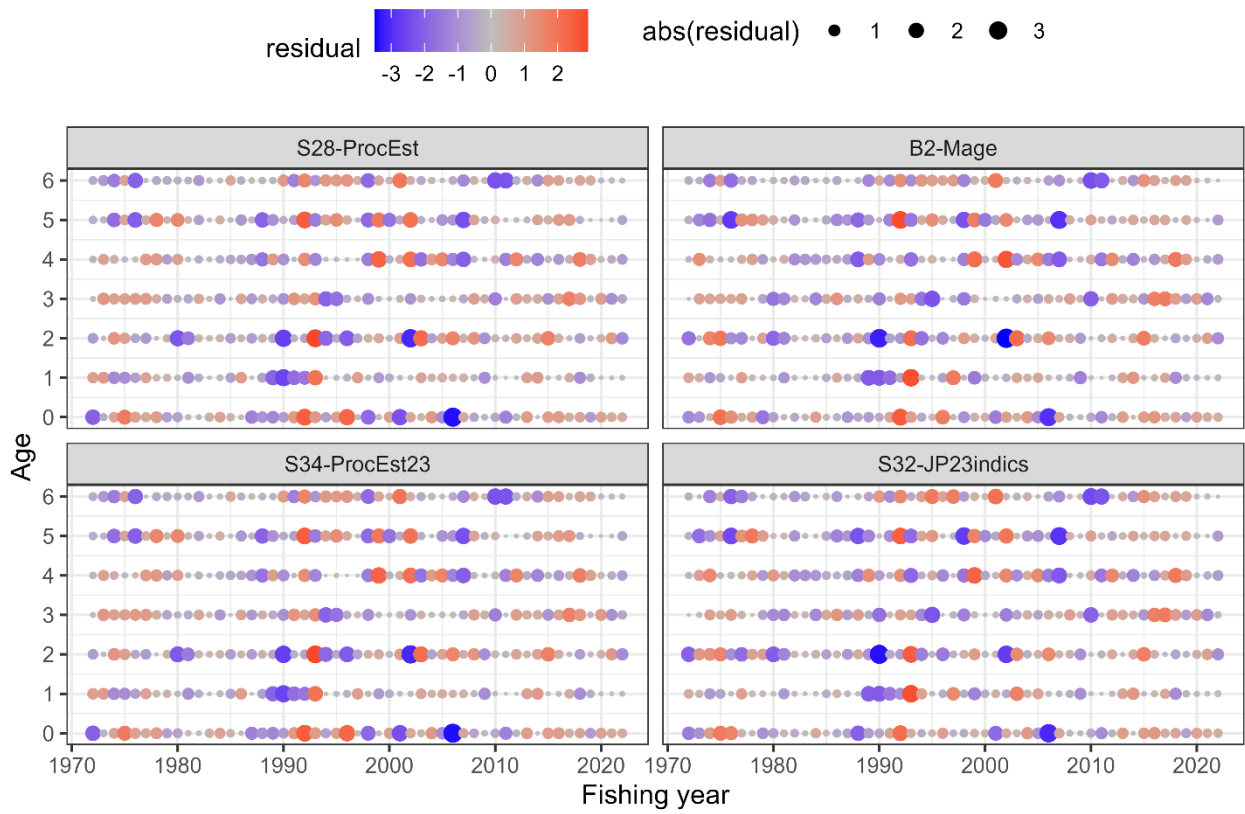
Patterns of retrospective forecasting for total biomass of chub mackerel. Black Lines represent models with all data, and colored lines represent models with the most recent data trimmed. Mohn's rho is shown in the upper right corner. The dots indicate the year of one-year-ahead forecasting, used for the calculation of Mohn's rho. Retrospective patterns for total biomass (top row), SSB (second row), recruitment (third row), and mean  $F$  (bottom). Black Lines represent models with all data, and colored lines represent models with the most recent data trimmed. Mohn's rho is shown in the upper right corner. Scenarios shown here are the final base case S28-ProcEst, the initial base case scenario B2-Mage, and the other representative cases of S34-PRocEst23 and S32-JP23indics.

Figure ANNEX 6



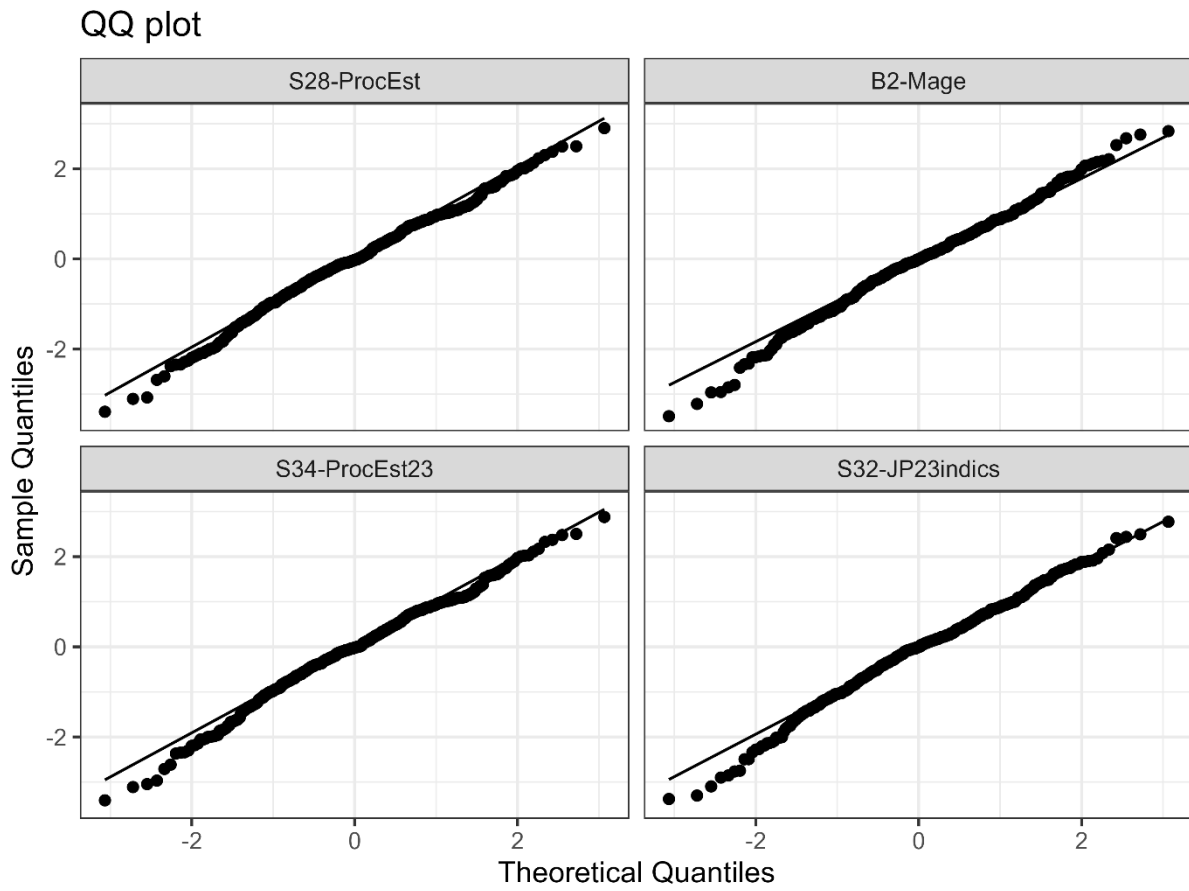
*One-Step-Ahead residuals for the indices of abundance. The IDs of the index are as follows: (1) relative stock number of age 0 from the summer survey by Japan, (2) relative stock number of age 0 from the autumn survey by Japan, (3) relative stock number of age 1 from the autumn survey by Japan, (4) relative SSB from the egg survey by Japan, (5) relative SSB from the dip-net fishery by Japan, and (6) relative vulnerable stock biomass from the light purse-seine fishery by China. Scenarios shown here are the final base case S28-ProcEst, the initial base case scenario B2-Mage, and the other representative cases of S34-PRocEst23 and S32-JP23indics.*

Figure ANNEX 7



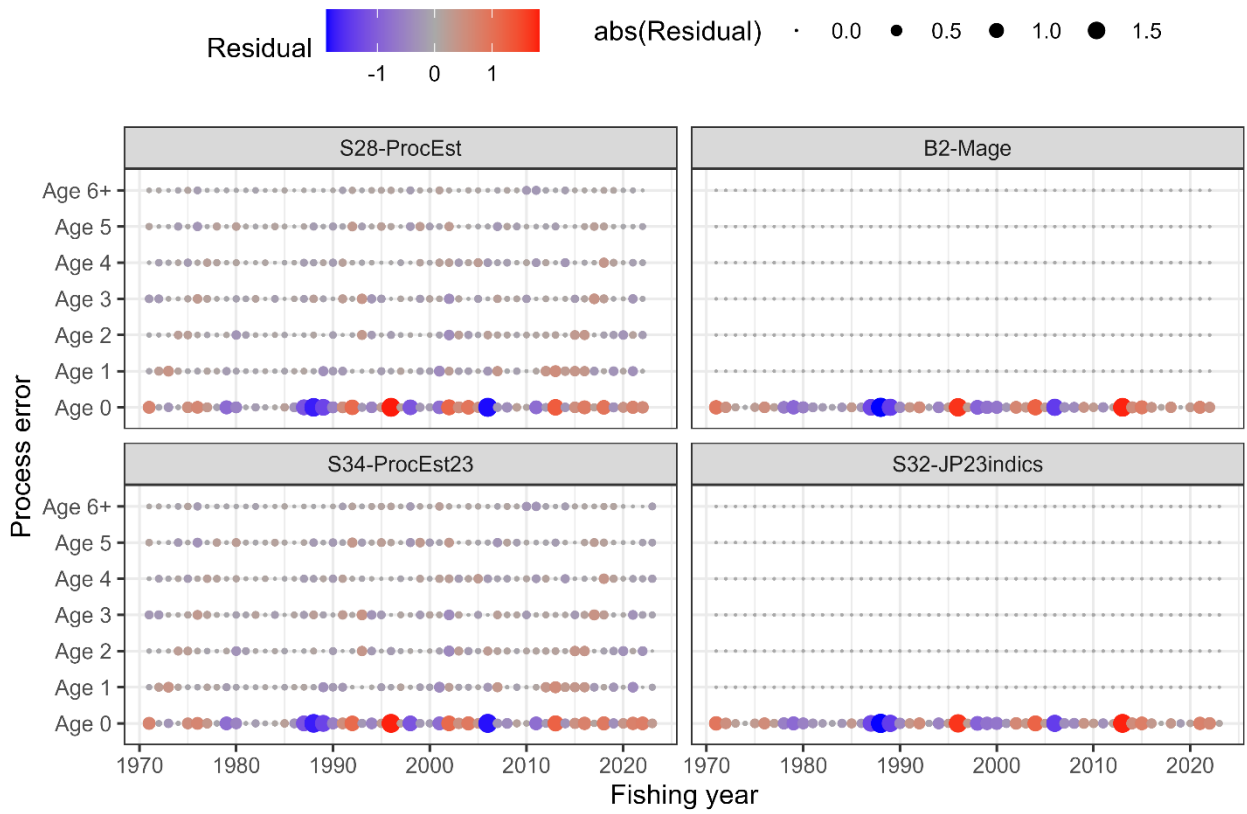
One-Step-Ahead residuals for the Catch at Age data. Scenarios shown here are the final base case S28-ProcEst, the initial base case scenario B2-Mage, and the other representative cases of S34-ProcEst23 and S32-JP23indics.

Figure ANNEX 8



QQ plot of the One-Step-Ahead residuals Scenarios shown here are the final base case S28-ProcEst, the initial base case scenario B2-Mage, and the other representative cases of S34-ProcEst23 and S32-JP23indics.

Figure ANNEX 9



Estimated process error in the numbers at age by year and model. Scenarios shown here are the final base case S28-ProcEst, the initial base case scenario B2-Mage, and the other representative cases S34-ProcEst23 and S32-JP23indics.

Table ANNEX 1

Convergence diagnostics by model. Scenarios shown here are the initial base case scenario B2-Mage, the final base case S28-ProcEst, and the other representative cases of S31-JP23indices and S34-PRocEst23. Bold values indicate the selected base case.

<b>Model</b>	<b>convergence</b>	<b>pdHess</b>	<b>maxGrad</b>
B2-Mage	✓	✓	0.000107
S32- JP23indices	✓	✓	0.001964
<b>S28-ProcEst</b>	✓	✓	<b>0.002456</b>
S34- ProcEst23	✓	✓	0.001749

Table ANNEX 2

Performance measures by model. Scenarios shown here are the initial base case scenario B2-Mage, the final base case S28-ProcEst, and the other representative cases of S31-JP23indics and S34-PRocEst23. Bold values indicate the selected base case.

PM	B2-Mage	S32-JP23indics	S28-ProcEst	S34-ProcEst23
TBy2022	3,591	2,388	<b>2,882</b>	2,204
Sby2022	591	339	<b>454</b>	297
Ry2018	13,019	10,398	<b>22,898</b>	19,737
Ry2019	7,490	5,496	<b>6,043</b>	5,405
Ry2020	9,960	6,840	<b>11,077</b>	9,464
Ry2021	14,760	10,989	<b>12,377</b>	10,479
Ry2022	12,234	8,407	<b>9,839</b>	8,120
AFy2018	0.306	0.344	<b>0.294</b>	0.326
AFy2019	0.274	0.333	<b>0.276</b>	0.315
AFy2020	0.329	0.446	<b>0.342</b>	0.420
AFy2021	0.268	0.427	<b>0.333</b>	0.462
AFy2022	0.202	0.356	<b>0.243</b>	0.376
Ey2018	0.128	0.148	<b>0.109</b>	0.122
Ey2019	0.121	0.152	<b>0.123</b>	0.138
Ey2020	0.147	0.200	<b>0.148</b>	0.176
Ey2021	0.106	0.162	<b>0.130</b>	0.170
Ey2022	0.081	0.139	<b>0.095</b>	0.136
currentSPR	0.319	0.191	<b>0.283</b>	0.193
deple_median_last3	1.609	1.172	<b>1.591</b>	1.382
Fmed/Fcur	0.787	0.490	<b>0.478</b>	0.367
F0.1/Fcur	1.516	0.964	<b>1.344</b>	0.970
FpSPR.30.SPR/Fcur	1.069	0.664	<b>0.942</b>	0.668
FpSPR.40.SPR/Fcur	0.764	0.474	<b>0.673</b>	0.478
FpSPR.50.SPR/Fcur	0.549	0.341	<b>0.484</b>	0.344
FpSPR.60.SPR/Fcur	0.387	0.240	<b>0.342</b>	0.243
FpSPR.70.SPR/Fcur	0.260	0.162	<b>0.230</b>	0.163
Fmsy/Fcur	0.306	0.194	<b>0.258</b>	0.187
Bmsy	21517	12592	<b>9396</b>	7127
SBmsy	6582	3834	<b>2905</b>	2193
h	0.366	0.370	<b>0.358</b>	0.362
SB0	16292	9542	<b>7123</b>	5400
SBmsy/SB0	0.404	0.402	<b>0.408</b>	0.406
FmsySPR	0.662	0.656	<b>0.673</b>	0.668

<b>B/Bmsy</b>	0.167	0.190	<b>0.307</b>	0.309
<b>SB/SBmsy</b>	0.090	0.088	<b>0.156</b>	0.135
<b>SBmsy/SBmax</b>	5.024	2.917	<b>2.083</b>	1.572

---

Table ANNEX 3

Description of performance measures (PM). The most recent three-year averages (FY2020-2022) of F-at-age and the biological parameters (maturity at age and weight at age) are used for PMs related to current F, F reference points, stock-recruitment relationship, and MSY.

PM	Description
TBy2022	Total stock biomass in FY2022 (1,000 MT)
Sby2022	Spawning stock biomass in FY2022 (1,000 MT)
Ry2018	The number of recruits in FY2018 (million)
Ry2019	The number of recruits in FY2019 (million)
Ry2020	The number of recruits in FY2020 (million)
Ry2021	The number of recruits in FY2021 (million)
Ry2022	The number of recruits in FY2022 (million)
AFy2018	Weighted average of F-at-age by estimated catch-at-age in FY2018
AFy2019	Weighted average of F-at-age by estimated catch-at-age in FY2019
AFy2020	Weighted average of F-at-age by estimated catch-at-age in FY2020
AFy2021	Weighted average of F-at-age by estimated catch-at-age in FY2021
AFy2022	Weighted average of F-at-age by estimated catch-at-age in FY2022
Ey2018	Exploitation rate (estimated catch divided by stock biomass) in FY2018
Ey2019	Exploitation rate in FY2019
Ey2020	Exploitation rate in FY2020
Ey2021	Exploitation rate in FY2021
Ey2022	Exploitation rate in FY2022
currentSPR	Spawners per recruit (SPR) in the average of FY2020-2022 (%)
deple_median_last3	Ratio of the average of spawning biomass in FY2020-2022 to its historical median
Fmed/Fcur	Ratio of F median to current F (average F in FY2020-2022)
F0.1/Fcur	Ratio of F0.1 to current F (average F in FY2020-2022)
FpSPR.30.SPR/Fcur	Ratio of F30%SPR to current F (average F in FY2020-2022)
FpSPR.40.SPR/Fcur	Ratio of F40%SPR to current F (average F in FY2020-2022)
FpSPR.50.SPR/Fcur	Ratio of F50%SPR to current F (average F in FY2020-2022)
FpSPR.60.SPR/Fcur	Ratio of F60%SPR to current F (average F in FY2020-2022)
FpSPR.70.SPR/Fcur	Ratio of F70%SPR to current F (average F in FY2020-2022)

Fmsy/Fcur	Ratio of $F_{MSY}$ to current F (average F in FY2020-2022)
Bmsy	Deterministic MSY reference point for total biomass (1,000 MT)
SBmsy	Deterministic MSY reference point for spawning biomass (1,000 MT)
h	Steepness
SB0	Virgin spawning stock biomass (1,000 MT)
SBmsy/SB0	Ratio of $SB_{MSY}$ to SB0
FmsySPR	%SPR for $F_{MSY}$
B/Bmsy	Ratio of total biomass in FY2022 to $B_{MSY}$
SB/SBmsy	Ratio of spawning biomass in FY2022 to $SB_{MSY}$
SBmsy/SBmax	Ratio of $SB_{MSY}$ to the historical maximum of spawning biomass

---